UNIVERSITÀ DEGLI STUDI DI MILANO

Doctorate in Biochemical Sciences
Cycle XXXIII
Department of Pharmacological and Biomolecular Sciences

Study of the role of class I histone deacetylases in differentiation, metabolism and immunophenotype of adipose tissue

BIO/10

Carolina Peri
Matr. R11971

Tutor: Prof. Maurizio Crestani
Coordinator: Prof. Alessandro Prinetti

Academic Year 2019/2020

SUMMARY

1 ABSTRACT

INTRODUCTION Epigenome modifications and metabolic dysregulation have been shown to be connected to disease states like obesity and to the associated comorbidities. Epigenome modifiers such as histone deacetylases are involved in the regulation of adipose tissue pathophysiology. However, their specific role in adipocyte differentiation is still a matter of research. Moreover, in obesity excessive accumulation of fat, especially in visceral depots, triggers a low-grade inflammation that is responsible of metabolic dysfunction. The action of immune cells within adipose tissue affects normal metabolic homeostasis.

PREVIOUS RESULTS Previous *in vitro* results from our group showed that inhibition of class I HDACs with MS-275, during early stage of adipocyte differentiation, leads to reduction of lipid droplets size. This phenomenon was accompanied by increased expression of genes regarding adipocyte functionality, lipolysis and fatty acid β-oxidation. However, these events were not observed in terminally differentiated adipocytes. Moreover, *in vivo* studies showed that HDAC3, a member of class I HDACs, acts as a molecular brake of metabolic rewiring that supports browning in WAT.

AIM of this thesis was to further elucidate how class I HDACs are involved in adipocyte differentiation and in determining the metabolic phenotype of pre-adipocytes. Moreover, we aimed to investigate the changes of immune cell populations at different time points of high fat feeding, to fully characterize the phenotypical consequences of *Hdac3* ablation in mice. In parallel, we wanted to identify key pathways and early events evoked by *Hdac3* gene inactivation through transcriptomic and epigenomic analysis.

RESULTS *In vitro* experiments on adipocytes precursors treated with MS-275 at the beginning of differentiation showed increased expression of genes belonging to mitochondrial activity and browning, which was accompanied by increased H3K27 acetylation of *Pparg* and *Ucp1* gene enhancers. *In vivo* studies in H3atKO mice, exposed to HFD for different periods (4, 9, 16 weeks, respectively), showed changes in immune cell populations. The number of total macrophages significantly increased in epiWAT of H3atKO mice compared to control floxed (FL) mice at all the three periods of treatment. Moreover, H3atKO mice were able to maintain higher ratio of M2 pro-resolving vs M1 pro-inflammatory macrophages from 4 through 16 weeks of HFD feeding. In H3atKO mice fed LFD for 4 weeks we found upregulation of pathways regarding the futile cycle of simultaneous fatty acid synthesis and β-oxidation. Moreover, KO_LFD vs FL_LFD mice shown upregulation of pathways such as ferroptosis, amino acid biosynthesis and valine, leucine and isoleucine degradation pathways, while focal adhesion and extracellular receptor interaction were downregulated. One of the top downregulated gene was neuronatin (*Nnat*); we found a hypoacetylated region upstream the *Nnat* TSS.

CONCLUSIONS *In vitro* results provided evidences regarding the role of class I HDACs in adipocyte differentiation. Their inhibition at the beginning of differentiation promotes an epigenetic imprinting towards oxidative and brown-like phenotype. *In vivo* experiments revealed that mice lacking *Hdac3* were able to maintain a higher ratio of M2 vs M1 macrophages during an inflammatory stimulus such as HFD feeding. Such feature could support a pro-resolving inflammatory process. Omic analysis confirmed the futile cycle of fatty acid metabolism previously observed in our H3atKO model and highlighted interesting new pathways that better characterize H3atKO mice.

2 INTRODUCTION

2.1 Obesity

Data from recent years regarding obesity are dramatic: the World Health Organization (WHO) reported that in 2016 more than 1.9 billion adults were overweight and 650 million were obese. This phenomenon is spreading also in low- and middle-income countries, while once was merely associated in nations with a high standard of living. Each year, at least 2.8 million of people die because they are overweight or obese: from 1975 to nowadays obesity is nearly tripled. (*WHO, 2020*)

Classically, obesity is defined as an excessive fat accumulation that negatively affects health. It is usually diagnosed using body mass index (BMI), expressed as the ratio between a person's weight and his height (BMI= Kg/m^2). When BMI >25 kg/m^2 an individual is considered overweight while BMI >30 kg/m^2 indicates obesity (*WHO, 2020*); healthy BMI ranges between 18.5 and 24.9 of BMI. However, BMI does not take in account adipose locations or sex differences. For this reason, among various methods used to determine obesity, there is waist circumference (useful for measure "abdominal obesity"), bioelectric impedance (BIA), computerized tomography (CT) and magnetic resonance imaging (MRI) (Kim, 2016).

Obesity aetiology derives from a plethora of factors. The main cause is the high energy intake that is unbalanced compared to the energy expenditure; however, we must consider also genetic, environmental, psychological, socio-economic and even political factors. Also, physical activity has changed: more sedentary habits and lifestyles in all ages have promoted obesity development (Wright and Aronne, 2012).

It is now established that obesity is not a pathology limited to increased body weight: in fact, it is a risk factor for many non-communicable diseases like type 2 diabetes, cardiovascular and cerebrovascular diseases and cancer, thus reducing lifespan (Fig. 1) (Haslam and James, 2005). Thus, morbidity and mortality derived from downstream complications of fat accumulation are relevant in obesity and overweight subjects (Kopelman, 2000).

Overweight nowadays is the sixth most relevant worldwide risk factor responsible for diseases development (Haslam and James, 2005). For this reason, finding new intervention strategies and support preventive measures against obesity is a paramount concern.

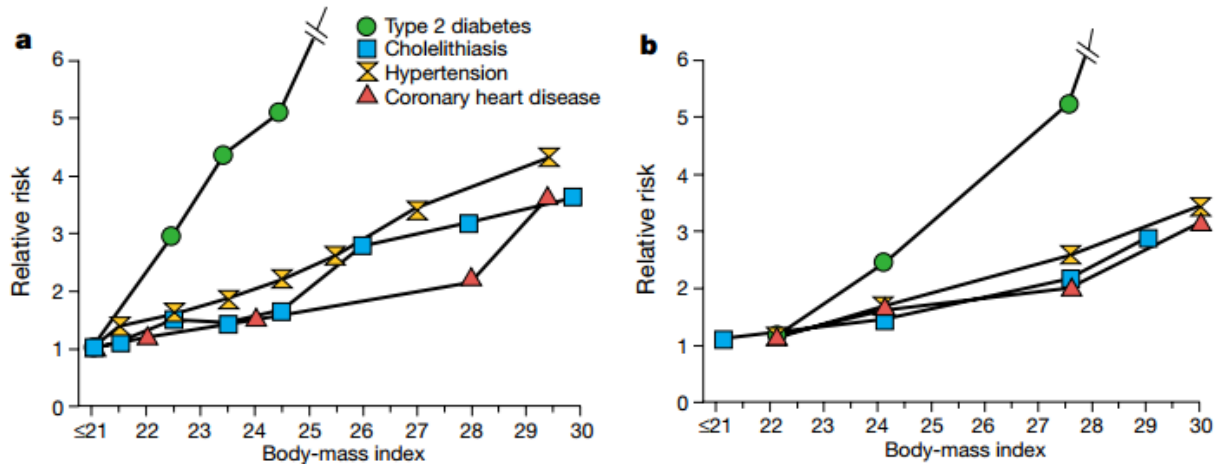

Fig. 1 Relation between BMI up to 30 and the relative risks caused by obesity. A) associations for women, initially 30 to 55 years old, with a follow up for 18 years. B) associations for men, initially 40 to 65 years old, with a follow up to ten years. Adapted from Kopelman, 2000.

2.2 The adipose organ

Although for long time it has been considered merely an inert organ of energy storage, adipose tissue has now been recognized at the centre of the regulation of systemic metabolism and energy homeostasis. It has many functions like cushion of organs and body parts subjected to mechanical stresses and endocrine role in the regulation of hormonal reproductive axis. However, the most important function is to maintain energy balance and nutritional homeostasis (Shapira and Seale, 2016).

Adipose tissue is a very plastic organ and every year, around 10% of adipocytes are renewed at all adult ages (Spalding *et al.*, 2008). Understanding the process of development of new adipocytes is fundamental to fight obesity: adipogenesis depends on a multistep process that is finely regulated by a network of transcriptional factors (TFs) and cell cycle regulators (Fig. 2). It acts through at least two principal waves of pro-adipogenic TFs: the first step arises after 4 hours from induction of differentiation and involves the CCAATenhancer-binding proteins C/EBPβ and -δ, the cAMP response element binding protein (CREB), the sterol regulatory element-binding protein 1c (SREBP-1c) and the signal transducer and activator of transcription 5A (STAT5A). Within two days from induction, this process activates a second wave including two main factors, PPARγ and C/EBPα, which are considered master regulators of adipogenesis: they induce the expression of genes that lead to changes in cell morphology from a fibroblast-like shape to mature rounded adipocytes (Siersbæk, Nielsen and Mandrup, 2012).

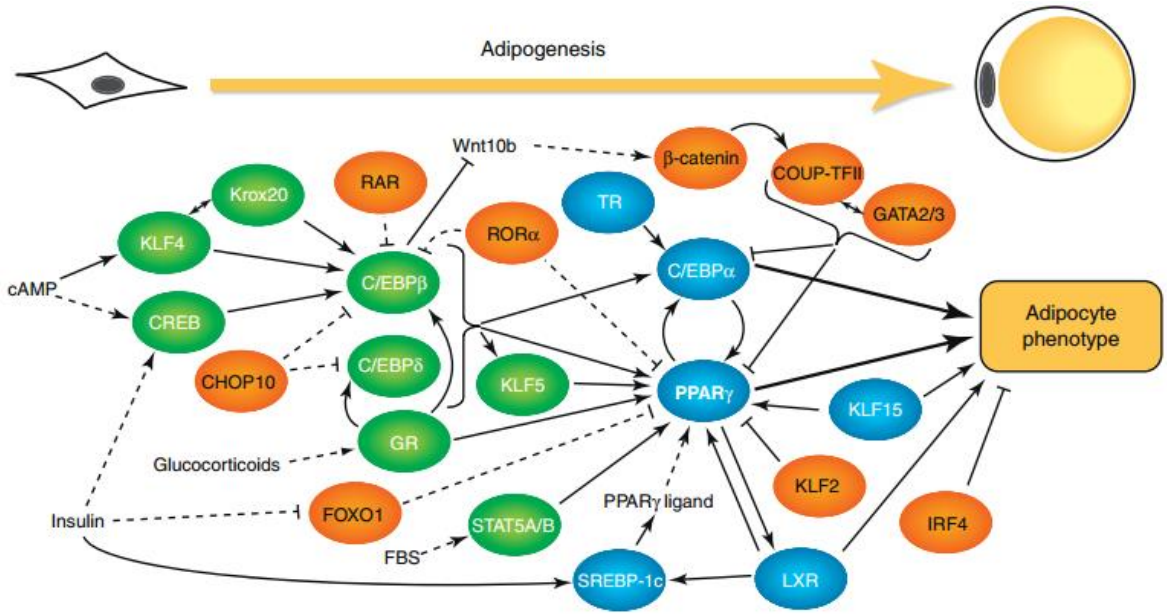

Fig. 2: Transcriptional actors of adipocyte differentiation. Green parts represent transcription factors belonging to the first adipogenic wave that, in turn, induces the second wave factors (in blue). In orange anti-adipogenic factors. Adapted from Siersbæk, Nielsen and Mandrup, 2012.

Tipically, adipocytes have been classified by morphology in white and brown; a third type of so-called beige or brite adipocytes has been recognized both in humans and rodents.

Even though they share several characteristics, they derive from different precursors; brown adipocytes develop from Pax7+/Myf5+ lineage, the same precursors that also give rise to skeletal myogenic cells.

White and beige adipocytes, on the other hand, do not express Myf5 and Pax7 and their origin is different from brown adipocytes. There are two main accredited theories regarding development of beige adipocytes in WAT: one embraces the transdifferentiation model from white adipocytes, under specific stimuli. The other one hypothesizes the existence of different progenitors for white and beige adipocytes. Rosen and Spiegelman suggest a unifying model whereby, under specific conditions (i.e. cold exposure) a committed precursor differentiate into beige adipocytes that, in turn, activate its own thermogenic capacity. When the system returns to normal condition, beige adipocytes assume white characteristics, thus adopting energy storage behaviour. This theory underlines the great plasticity of adipose tissue, that can adapt to different physiological conditions.

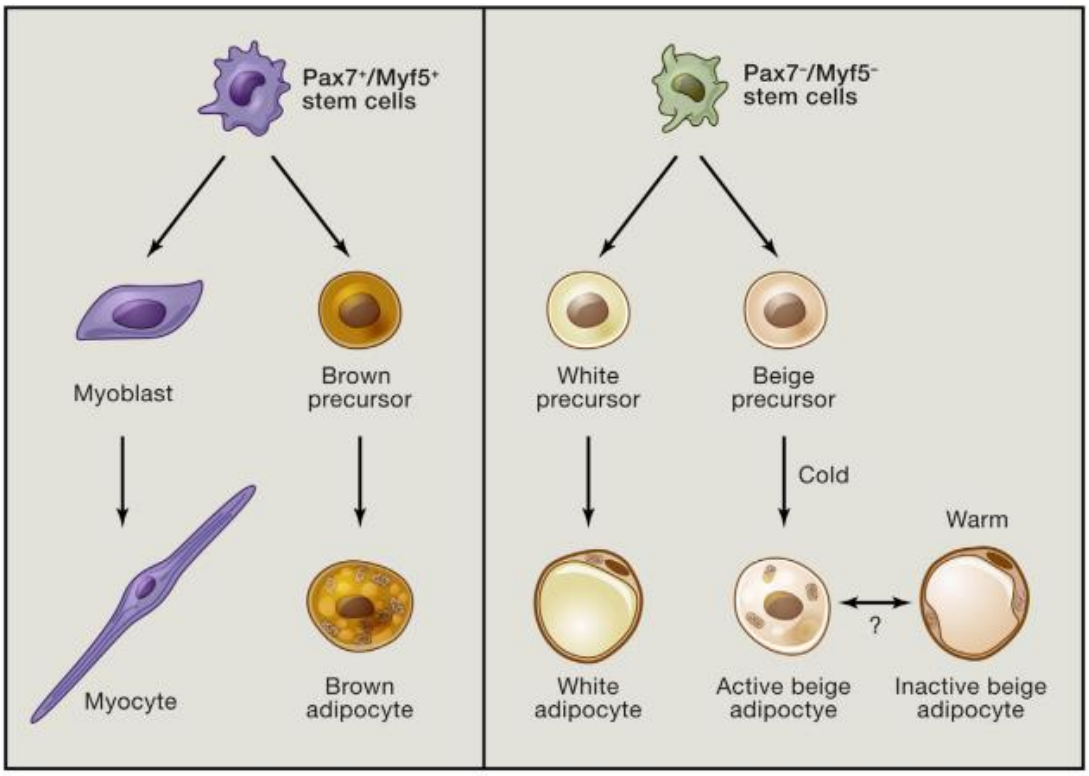

Fig. 3: Origins of adipose tissue: a clear distinction between brown Pax7+/Myf5+ precursors cells and white/beige lineage. Adapted from Rosen and Spiegelman, 2014.

2.2.1 White adipose tissue

Mature white adipose tissue (WAT) is made up of unilocular adipocytes, the most abundant type: the cytoplasm is mainly occupied by a large lipid droplet to store energy as triglycerides, while nucleus and other organelles are confined in the periphery of the cell.

Anatomically, there is a simplified distinction of WAT in two main depots differing for location and properties: one of them is subcutaneous fat (scWAT) that provides insulation from heat/cold and mechanical stresses. It is located underneath the skin, particularly in the interscapular, and posterior inguinal (IngWAT) region in mice. In humans, scWAT is typically distributed around the hips, thighs, and buttocks. On the other hand, visceral fat (ViscWAT) is linked to metabolic diseases and it is located inside the peritoneum, distributed around internal organs. In mice it is found in the perigonadal (epididymal in males), mesenteric, and retroperitoneal WATs. These depots correspond to omental area in humans (Park, Won and Bae, 2014).

The large lipid droplet typical of the adipocyte is a dynamic organelle designated to energy storage and release: it contains triacylglycerols (TGs) derived from the condensation of three molecules of free fatty acids (FFAs) with glycerol. When energy deprivation occurs, triglycerides undergo lipolysis that

releases free fatty acids and glycerol. TGs hydrolyse through the serial action of three enzymes: adipose triglyceride lipase (ATGL), hormone-sensitive lipase (HSL) and monoacylglycerol lipase (MGL). FFAs are released in the bloodstream and used by other tissues, where they can undergo fatty acid oxidation and produce energy.

Adipose tissue is also a complex and dynamic endocrine organ: it secretes a variety of bioactive molecules, defined adipokines, that are important in maintaining metabolic homeostasis and their disfunction can be linked to metabolic diseases. They mediate a crosstalk between adipose tissue and many other organs like muscle, brain, liver and pancreas. Leptin, one of the most reviewed adipokines, is involved in the regulation of appetite: it exerts potent anorexic effects by reducing food intake stimulating satiety and by increasing energy expenditure through its action on the hypothalamus. Adiponectin is another adipokine abundant in the blood: it has a role in improving insulin resistance and obesity by stimulating lipid oxidation and anti-inflammatory response (Cao, 2014). Finally, under particular conditions like obesity, the adipose organ can also secrete inflammatory cytokines such as TNF-α (Tumor necrosis factor α) and IL-6 (Interleukin-6) with concurrent infiltration of immune cells into adipose tissue, leading to chronic low-grade inflammation and insulin resistance (Cao, 2014). Therefore, white adipose tissue beside its main role in lipid storage/release has an important capacity to communicate with other organs within the body.

2.2.2 Brown adipose tissue

Brown adipocytes contain multilocular lipid droplets and large number of mitochondria and contribute to thermogenesis via the expression of uncoupling protein 1 (UCP1).

The major BAT depots in mice are in the interscapular and perirenal regions. In humans BAT is typical of infants since it is crucial in maintaining body temperature through non-shivering thermogenesis after birth. It is located in the interscapular region in newborns and it was thought to gradually disappears with aging, while in rodents it remains through life. However, thanks to images studies, it was possible to identify BAT depots also in adult humans. These depots are present in cervical, supraclavicular, and paravertebral regions (Fig. 4) (Sidossis and Kajimura, 2015).

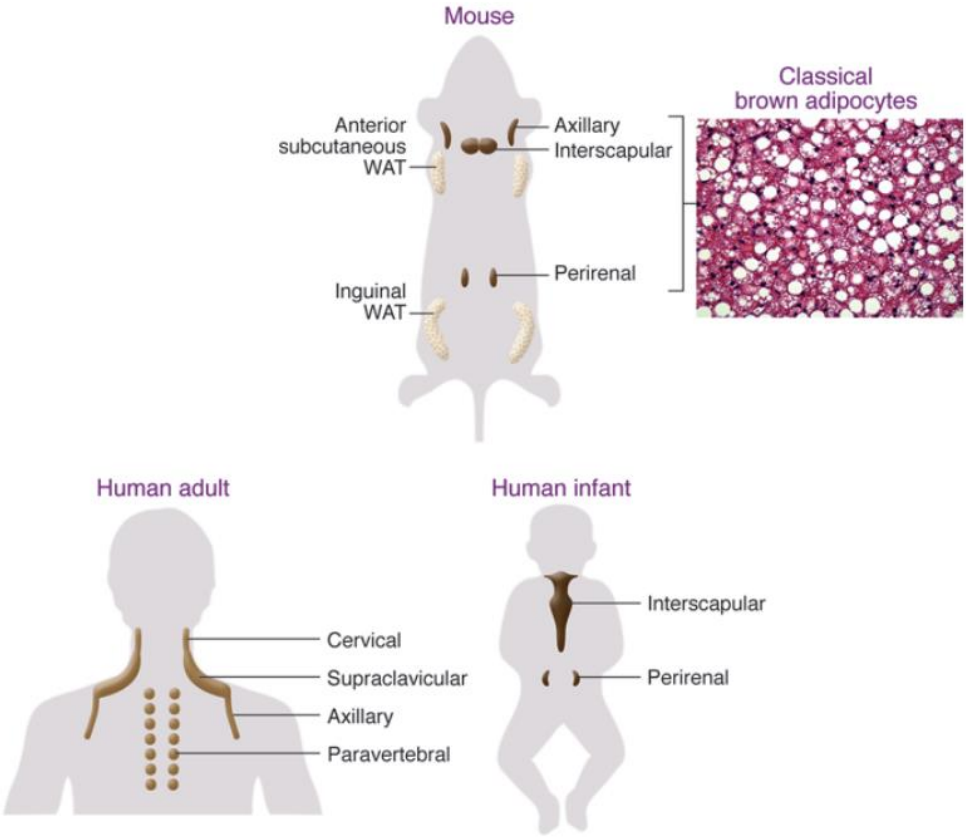

Fig. 4 Localization of brown fat in mouse and in human adult or infant. Adapted from Sidossis and Kajimura, 2015

The main function of BAT is non-shivering thermogenesis, a system based upon the uncoupling of oxidative phosphorylation from electron transport chain made possible by the mitochondrial uncoupling protein 1 (UCP1).

The most accredited model/theory regarding the control of UCP1 activity is fatty acids-mediated control: long chain free fatty acids (LCFAs) activate UCP1 functioning as a LCFA-/H+ symporter where LCFA anion is bounded to the protein. On the other hand, cytosolic purine nucleotides like ATP, GTP and ADP inhibit UCP1 activity (Fedorenko, Lishko and Kirichok, 2012). Upon external stimuli like cold, norephinephrine is released by the sympathetic nerves and acts through β3-adrenoceptors triggering the activation of cAMP-dependent protein kinase (PKA). PKA phosphorilates HSL (hormone sensitive lipase) and perilipin leading to lypolisis of triglicerides. LCFAs coming either from lypolisis of BAT lipid droplets or from the blood undergo to β-oxidation thus contributing to the creation of the proton gradient in the mitochondria. UCP1 acts as transmembrane protein allowing the proton to re-entry in the mitochondrial matrix, leading to the generation of heat rather than ATP, thanks to the dissipation of the electrochemical gradient (Fig. 5) (Fenzl and Kiefer, 2014).

Several investigations have reported that UCP1 is fundamental for thermogenesis in BAT: in fact, mice lacking *Ucp1* when exposed to acute low temperature developed hypothermia and are not able to maintain an appropriate body temperature. Moreover, transgenic mice with BAT deficiency developed obesity and diabetes under normal environment temperature (Ikeda and Yamada, 2020).

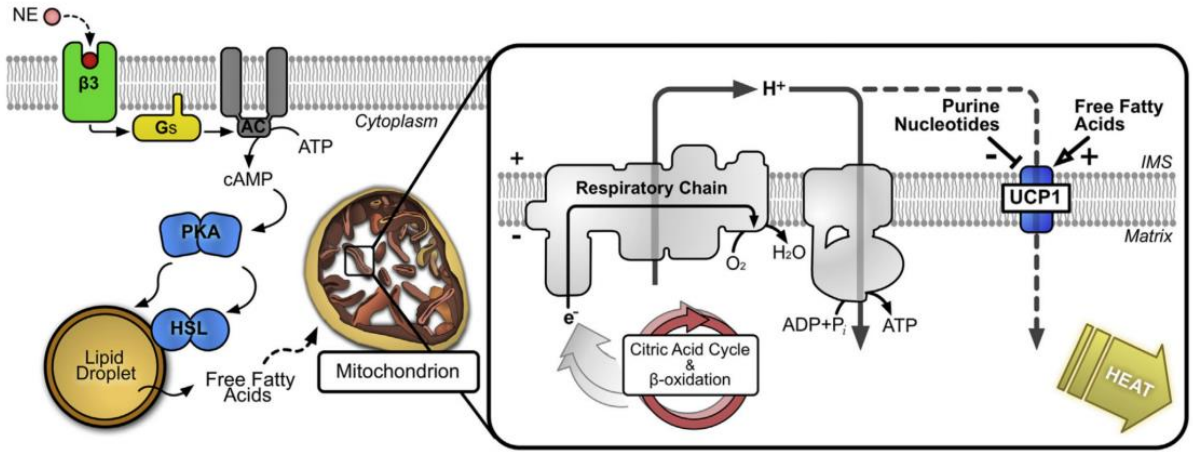

Fig. 5 Activation of UCP1 in brown adipose tissue.
From the left: after stimuli such as cold, norepinephrine (NE) is released from sympathetic system: it turns on a molecular cascade that activates cAMP-dependent pathway leading lipolysis and release of FFAs. Those activates UCP1 in the mitochondria with proton gradient dissipation. As a result, energy is dissipated as heat. Adapted from Crichton, Lee and Kunji, 2017.

2.2.3 Beige adipose tissue

Within white adipose tissue, there is a population of adipocytes that upon certain stimuli undergoes a process called “beiging or browning”, whereby it assumes intermediate characteristics between white and brown phenotype. Similarly to brown adipocytes, beige adipocytes are described as multilocular with numerous mitochondria (Harms and Seale, 2013). However, they are considered different and independent cell types for many reasons: they derive from different precursors, as already mentioned, and they express adipogenic genes like *Ucp1* and *Pgc1-α* under specific stimuli. Cold, adrenergic activation, exercise and microbiota modifications induce a brown-like functionality and thermogenesis in beige adipocytes (Corrêa, Heyn and Magalhaes, 2019). This phenomenon is largely studied because it is associated with ability to counteract metabolic diseases like obesity and type 2 diabetes.

Several studies have reported the increasingly important role of beige adipose tissue in thermogenesis through pathways that deviate from the classical UCP1-driven thermogenesis. Ikeda et al demonstrated the existence of an UCP1-indipendent mechanism that requires ATP-dependent Ca2+ cycling by SERCA2b (sarco/endoplasmic reticulum Ca^{2+}-ATPase2b) and ryanodine receptor 2 (RyR2). More in details, they generated a mouse model with high level of beige fat (*Prdm16* Tg mice) and they crossed them with *Ucp1*−/− mice, thus obtaining *Prdm16*Tg x *Ucp1*−/− animals. Interestingly, they

found that *Prdm16* Tg mice were able to maintain a proper body temperature even in absence of Ucp1, thus suggesting the existence of an alternative thermogenic pathway, independent from UCP1. Moreover, both *Prdm16* Tg and *Prdm16*Tg x *Ucp1*−/− mice showed a better tolerance to HFD challenge. They also noticed that *Prdm16*Tg x *Ucp1*−/− animals used glucose as energy source rather than fatty acids that are the primary substrates utilized by UCP1-dependant thermogenesis in brown and beige adipocytes. This metabolic switching depends on SERCA2b-RyR2 mechanism whereby adrenergic stimulus increases Ca^{2+} flux in the cytoplasm and mitochondria. In turn, Ca^{2+} in mitochondria activates PDH phosphatases and ATP synthesis. UCP1-indipendent thermogenesis take place through uncoupling of Ca^{2+} transport and ATP hydrolysis by SERCA2b (Ikeda *et al.*, 2018). Therefore, trying to activate Ca^{2+} cycling selectively in beige adipocytes might be a promising therapeutic intervention to counteract obesity: a recent paper proposed an optogenetical device that triggers Ca^{2+} cycling specifically in subcutaneous adipocytes of mice thus paving the way to future treatments of obesity through non-canonical thermogenesis (Tajima *et al.*, 2020).

2.3 Immune cells in adipose tissue

Adipocytes are not the only cell population of the adipose organ: it is estimated that adipocytes are one third of the total population, while the rest is composed of pre-adipocytes, stromal cells, fibroblasts, endothelial and immune cells (Chait and den Hartigh, 2020).
Indeed, adipose tissue is plastic and its composition and morphology can vary under certain conditions like obesity. In particular, cells of both innate and adaptive immunity that are already present in non-pathological conditions, can change during the onset of obesity, leading to inflammation, insulin resistance and metabolic disfunctions.

2.3.1 Innate immunity cell populations

Obesity leads to adipose tissue remodelling with changes in the number (hyperplasia) and size (hypertrophy) of adipocytes. Hypertrophic adipocyte leads to harmful disfunctions like increased hypoxia and fibrosis, necrotic abnormalities, elevated cytokines secretion followed by increased inflammation. Moreover, increased release of free fatty acids from adipose tissue leads to accumulation in ectopic organs such as muscle and liver, thus contributing to lipotoxicity (Choe *et al.*, 2016). When the adipocytes size reaches the critical threshold, it starts the recruitment of precursors in order to expand the cells number through hyperplasia. This process is considered a “buffer

mechanism" of the body to respond to excess energy intake and metabolic alterations (Longo *et al.*, 2019).

Adipose tissue expansion is followed by infiltration of inflammatory cells, most of which are represented by macrophages (Fig. 6). Under normal conditions, they constitute around 5–10% of cells but, with the onset of obesity, they can reach 50% (Weisberg *et al.*, 2003).

Macrophages derive from both local proliferation or recruitment of circulating monocytes and several chemokines are involved in this process (Zheng *et al.*, 2016). It has been shown that more than 90% of macrophages are found surrounding dying adipocytes. They bind adipose cells, forming syncytia and scavenging adipocyte residuals thus developing multinuclear giant cells. These peculiar structures of necrotic-adipocytes surrounded by macrophages are defined as crown-like structures (CLS) (Cinti *et al.*, 2005). Adipocyte death is mostly associated both to obese mice and humans. By quantifying the CLS in different WAT depots, it has been shown that visceral WAT is more prone to acquire CLS compared to subcutaneous site. These two fat depots differ for cell size since visceral fat has smaller cells. In both depots, adipocyte size is positively correlated to CLS density, indicating that macrophage infiltration is connected to hypertrophic adipocyte. However, the expansion threshold of visceral adipocytes is lower compared the corresponding subcutaneous cells, as they are more prone to recruit macrophages and form CLS. On the other hand, subcutaneous adipocytes are larger and they can reach higher critical size than visceral adipocytes. For this reason, visceral fat is considered a fat depot more susceptible to trigger macrophage-driven inflammation, thus leading to systemic metabolic disorders (Murano *et al.*, 2008)

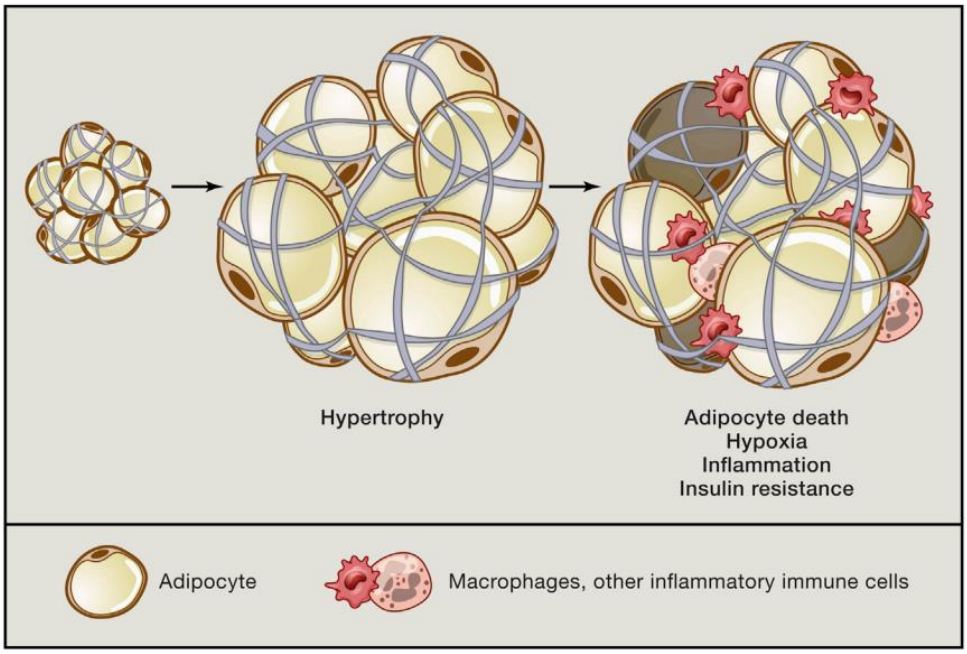

Fig. 6: Adipose tissue hypertrophy and consequent macrophages accumulation. Adapted from Rosen and Spiegelman, 2014.

The canonical subdivision of adipose tissue macrophages (ATMs) includes M1 or "classically-activated" macrophages and "alternative-activated" M2 macrophages. M1 type is predominant in the obese state and they depend on glycolysis for their metabolic necessities. M2 macrophages, on the other hand, are the most abundant in lean mice and they rely on oxidative phosphorylation (OXPHOS) metabolism: their characteristic is the expression of the surface marker CD206 (also known as mannose receptor C type 1, MCR1), the macrophage galactose C-Type Lectin/CD301a/CLEC10A (MGL1), and arginase-1 (ARG1). They release anti-inflammatory cytokines such as IL-10 and TGF-β, thus contributing in maintaining the metabolic homeostasis in lean state. However, in obese subjects M1 macrophages contribute to the inflammation process. M1 type is defined as F4/80+/CD11c+ cell; they surround the dying adipocyte forming the so-called crown-like structures (CLS). They secrete proinflammatory cytokines like TNF-α, IL-6 and IL-1β (Chung et al., 2018).

However, the classical subdivision M1/M2 is not exhaustive: evidences regarding macrophages in the adipose tissue, identified multiple populations that do not conform to the characteristics typical of M1/M2 paradigm. Particularly, obese ATMs show a metabolically activated phenotype (MMe) when they participate in the clearance of dead adipocytes. They express specific markers including ABCA1, CD36 and PLIN2 and their activation is influenced by different external stimuli like FFAs, increased insulin or glucose (Li, Yun and Mu, 2020). MMe macrophages clearance activity is driven by NADPH oxidase 2 (NOX2). Localized within crown-like structures, we find also CD9 macrophages that contain high level of lipids and have pro-inflammatory characteristics: transfer of CD9 in lean mice led to development of obesity-associated inflammation in the adipose tissue. On the contrary Ly6c macrophages are found outside the CLS and express genes related to angiogenesis and tissue organization. They sustain normal adipose physiology as they induce genes belonging to cholesterol and lipid biosynthesis (Hill *et al.*, 2018).

ATMs found close to crown-like structures promote the clearance of death adipocytes that are produced with the onset of obesity; this process might promote AT remodelling and resolve inflammation. Moreover, inflammation coming directly from adipocytes is not necessarily detrimental for the adipose tissue functionality; on the contrary, it can be important for adipocytes renewal since proinflammatory signaling in the adipocyte is required for proper adipose tissue remodeling and expansion (Asterholm *et al.*, 2014). Asterholm et al, generated three complementary mouse models with a reduction of pro-inflammatory capacity, specifically in the adipose tissue. When mice were exposed to HFD, they were not able to proper expand adipose tissue, due to their inability to generate an adequate local pro-inflammatory response. This phenomenon led to ectopic lipid deposition and, consequently, to metabolic disfunctions. So, they speculated that an acute inflammatory response is

fundamental for healthy remodeling and for maintaining an adequate metabolic functionality in expanding adipose tissue (Asterholm *et al.*, 2014).

Another recent study investigated the role of adipocyte inflammation in insulin sensitivity. The investigators generated two mouse models in which they blocked inflammatory pathways of adipocytes and macrophages (RIDad and RIDmac mice, respectively). RIDad mice, already on chow-diet, showed glucose intolerance and impaired insulin sensitivity; this trend worsened when mice were exposed to HFD. On the contrary, RIDmac mice on HFD displayed no significant changes regarding insulin tolerance. This demonstrated that adipose tissue inflammation is important for maintaining adipose tissue functionality and systemic insulin sensitivity (Zhu *et al.*, 2020).

Upon onset of inflammation, neutrophils (Ly6G+) are the first immune cells to be engaged. In turn, they promote the immune response by recruiting other cells like macrophages, dendritic cells and lymphocytes. It has been shown that in mice fed HFD, neutrophils infiltrate adipose tissue as early as day 3 of diet and their content remains continuous for the following 90 days of HFD (Talukdar *et al.*, 2012). Adipose tissue neutrophils produce chemokines and cytokines thus contributing to the chronic low-grade inflammation that is typical of insulin resistance caused by obesity. They are members of granulocytes and they present intracellular vesicles containing lysozymes, neutrophils elastase (NE) and myeloperoxidase (MPO). The expression of NE, a proinflammatory proteinase, increased when mice were exposed to HFD: pharmacological inhibition or genetic deletion of NE improved glucose tolerance, insulin sensitivity and diminished weight gain in mice (Talukdar *et al.*, 2012).

Another member of granulocytes are eosinophils which contribute in the anti-inflammatory immune response (Fig. 7). They secrete many cytokines such as IL-4, IL-10, IL-13 and TGF-β contributing to adipose tissue homeostasis and anti-inflammatory immune response (Lee, 2014).

Finally, dendritic cells (DCs) are specialized antigen presenting cells with important role in linking innate and adaptive immunity. There are two main types of DC: conventional cDCs (identified by the expression of MHCII and CD11c+) and plasmacytoid pDCs (Macdougall and Longhi, 2019). Although their role in obesity-induced inflammation in still not clear, it seems that DCs are prone to adopt a pro-inflammatory state in obesity (Patsouris *et al.*, 2009).

2.3.2 Adaptive immune cell populations

Adaptive immunity also plays an important role in pathophysiology of adipose tissue; around 10% of cells in AT are constituted by lymphocytes including T and B cells, natural killer cells (NK) and innate lymphoid cells (ILCs).

T and B cells were found surrounding the dying adipocytes in crown-like structures together with macrophages (Fig. 7) (Mclaughlin *et al.*, 2017).

It has been shown that $CD8^+$ effector T cells infiltrate during the early stages of inflammation in diet induced obesity. Immunological and genetic depletion of $CD8^+$ T lymphocytes showed less infiltration of M1 macrophages thus ameliorating adipose tissue inflammation. On the same line, *in vitro* studies showed that activation of $CD8^+$ T cells by adipocytes, contributes to recruitment of macrophages, thus indicating the key role of $CD8^+$ T cells in the development of obesity-induced inflammation (Nishimura *et al.*, 2009).

$CD4^+$ T lymphocytes comprise some sublineages considered proinflammatory like Th1 and Th17 cells and others anti-inflammatory like T regulatory cells (Treg) and Th2. Deng et al. reported a disbalance of $CD4^+$ T lineages in obesity. The production of INFγ changes the ratio of Th1/Treg and leads to the reduction Treg cells, thus impairing inflammation and systemic insulin resistance. Manipulation of Treg cells with loss-of-function and gain-of-function experiments revealed their importance in protecting against excessive adipose tissue inflammation and in downstream metabolic complication like insulin resistance (Feuerer *et al.*, 2009).

Not only T lymphocytes but also B cells are involved in inflammation and in the pathogenesis of obesity-induced insulin resistance. Genetic depletion of B cells or specific treatment with antibodies improved glucose tolerance and inflammation in DIO mice. B cells support the activation of M1 macrophages, $CD8^+$ and Th1 cells and produce pathogenic IgG antibodies thus contributing to disease development (Winer *et al.*, 2011).

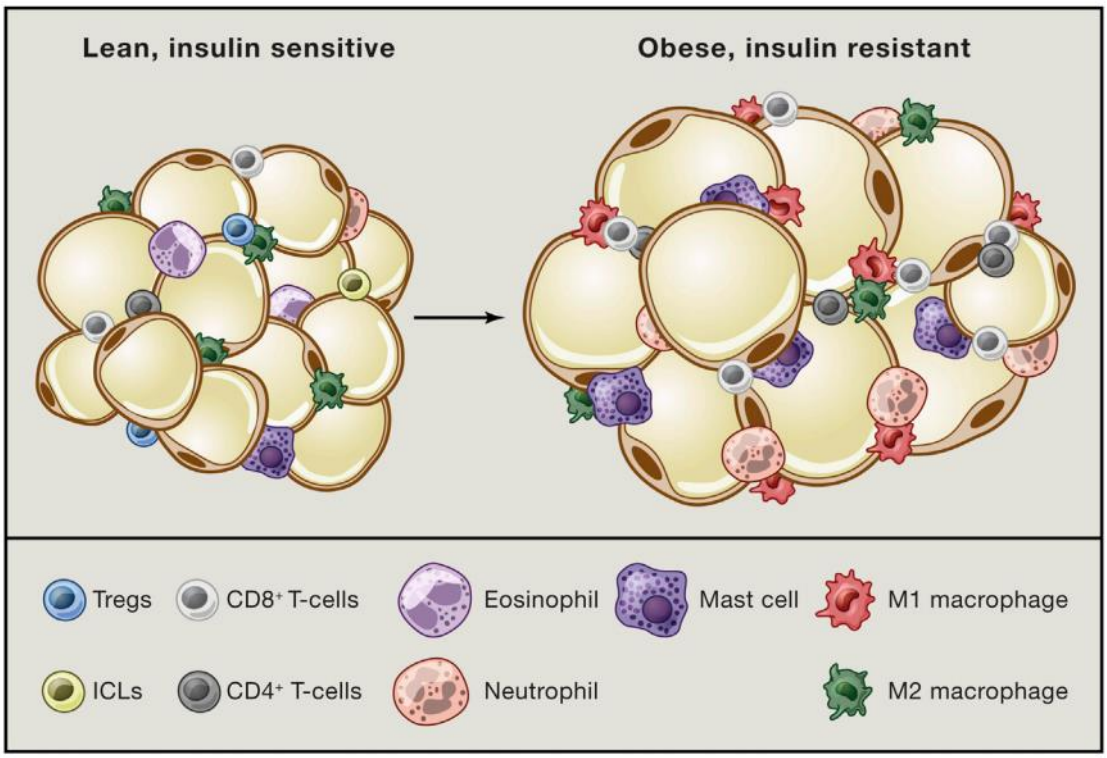

Fig. 7 From lean to obese status immune cells can change. In lean fat eosinophils, M2 macrophages and Tregs cells are predominant. When obesity occurs, there is a switch to M1 phenotype with accumulation of mast cells and T lymphocytes. Adapted from Rosen and Spiegelman, 2014.

2.4 Epigenetics

We are all influenced by the environmental cues and cells have developed molecular mechanisms that allow adaptation: in this process the epigenome is fundamental, acting as an interface between genes and environment that contributes to the regulation of genome functions.

Epigenetics studies heritable and dynamic changes that affects gene expression without altering the DNA sequence (Kaushik and Anderson, 2016). Epigenetics allow to understand how the environment, lifestyle, external stimuli and nutrients influence the phenotype.

Epigenome modifications occur through different mechanism, mostly at DNA or histone levels, bringing to chromatin remodelling. Euchromatin comprises chromatin regions more “open” and accessible to transcriptional factors, where gene transcription is more active. On the contrary, heterochromatin includes “close” chromatin regions, where gene transcription is reduced. Chemical modifications of DNA and histone proteins, made possible by chromatin modifiers, are mainly responsible of such dynamic changes of chromatin structure (Ferrari *et al.*, 2018). However, this definition might be simplistic, given that chromatin is a dynamic and constantly evolving system, where

different factors participate in its modifications. In fact, a single epigenetic modification mostly does not work by itself but it is often the result of a synergic modifications (Strahl and Allis, 2000).

DNA methylation is one of the modifications that the epigenetic machinery can bring: it entails the covalent attachment of a methyl group to the C5 position of cytosine through DNA methyltransferase enzymes (DNMT) (Sadakierska-Chudy, Kostrzewa and Filip, 2015). Methyl groups derive from S-adenosylmethionine (SAMe) that, after demethylation, yields S-adenosyl homocysteine (SAH) as a product (Ferrari *et al.*, 2018).

Methylation also occurs at the histone levels together with other modifications such as acetylation, phosphorylation, ADP-rybosilation, sumoylation, biotinylation, ubiquitinylation and others.

Mono-, di- and tri-methylation or acetylation can affect lysine on histone tails, while arginine is interested only by mono or di-methylation. Studies regarding global mapping of histone modifications (i.e. ChIP-seq) spotted specific modifications and associate them with peculiar class of *cis*-regulatory elements (Zentner and Henikoff, 2013). H3K4me3 is a marker of active promoters, while enhancers are marked with H3K4me1/me2, H3K27ac. H3K36me3 and H3K79me3 are related to ongoing transcription. On the other hand, inactive chromatin, is characterized by histone marks such as H3K9me3 (lysine 9 tri-methylation), H3K27me2/me3 (histone 3 lysine 27 di- and trimethylation), and H4K20me3 (histone 4 lysine 20 trimethylation) (Longo *et al.*, 2017).

It is known that there is a connection between epigenetics and metabolism both in physiological and pathological conditions. Epigenome signatures mirror the extracellular stimuli surrounding environment. The levels of metabolic intermediates and cofactors affect epigenome modifiers and their enzymatic activities and, consequently, chromatin structure and genome function. For example, intermediates like acetyl-CoA, ATP, SAMe and methyl donors deriving from nutrients are fundamental for enzymatic reactions and any chromatin changes might have consequences on the epigenetic remodelling of chromatin (Keating and El-Osta, 2015).

One of the epigenetic mechanisms influenced by metabolism is methylation of both DNA and histones (Fig. 8). Main actors of this process are the intermediate metabolites S-adenosyl methionine (SAMe), which is necessary for transfer of methyl groups, and the product of methylation reactions (SAH): such metabolites belong to the so called “one carbon metabolism”. From diet intake, also folic acid, B12 and B6 vitamins and choline participate in one carbon metabolism, hence in methylation reactions. On the other hand, histone demethylation is catalysed by lysine-specific histone demethylases (LSDs) and Jumonji-C domain containing histone demethylases (JHDM). They use FAD and α-ketoglutarate converted to succinate as cofactor, respectively. DNA demethylation probably takes place through the conversion of methyl-cytosine residues to hydroxy-methyl-cytosine by Ten-eleven Translocation (TET) enzyme. Furthermore, succinate and fumarate inhibit TET and JHDM by competing with α-ketoglutarate (Fig. 8).

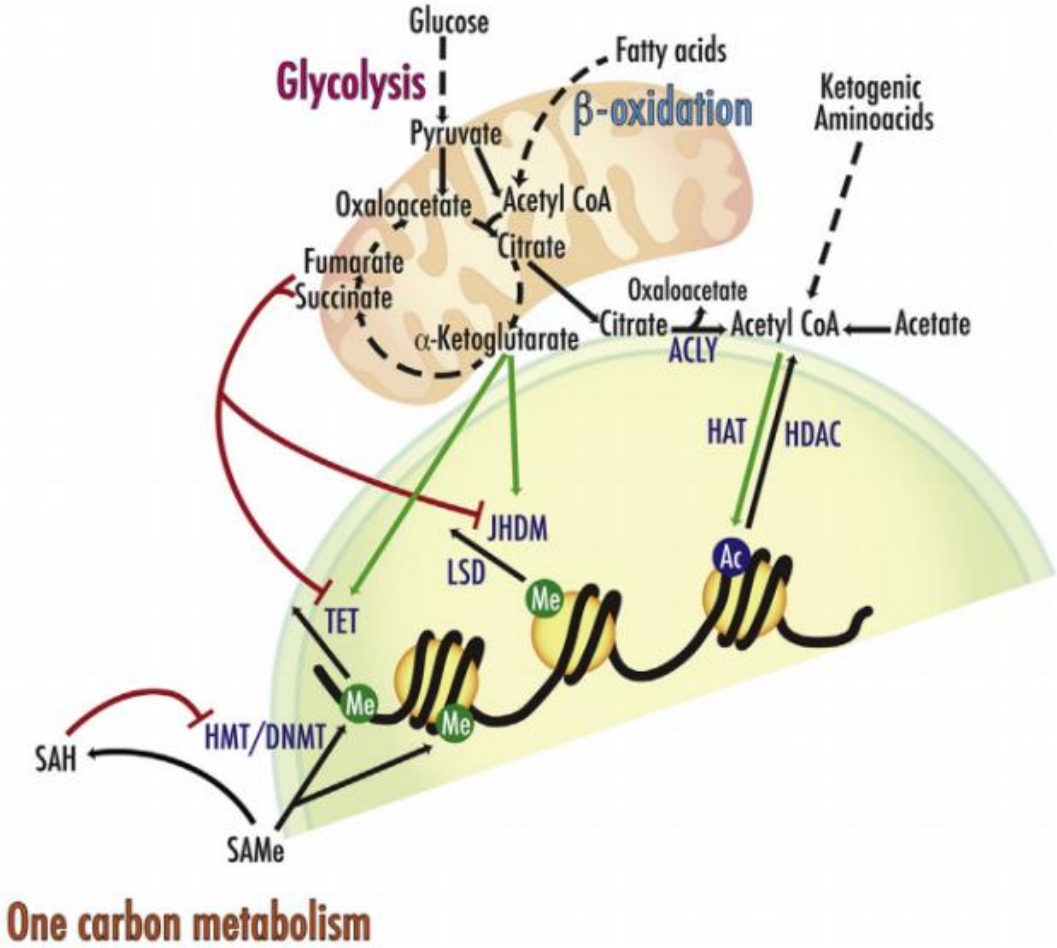

Fig. 8 Summary of some metabolic intermediates involved in chromatin modification. Adapted from Ferrari et al., 2018.

Finally, among metabolites that are important for epigenetic enzymes, acetyl-CoA is used as a substrate for histone acetylation through the action of histone acetyl transferases (HAT). Glucose availability and free fatty acids are the main source for histone acetylation; also, it has been shown that the lipogenic enzyme ATP-citrate lyase (ACLY) produces nuclear acetyl-CoA and oxaloacetate from citrate. Nuclear acetyl-CoA is then used for acetylation of histone tails (Fig. 8).
All together, these observations support the concept that different metabolites influence the activity of epigenomic enzymes.

2.4.1 Epigenetic and diseases

Epigenome modifications are involved in many disease states and there are evidences that they could be relevant also for obesity. However, the causality correlating epigenome modifications and the onset of obesity is still matter of study. Dietary habits and lifestyle have a role in epigenome modifications:

in recent years, advances in genomic technologies and epigenome-wide association studies (EWAS) made it possible to better study the link between epigenome and metabolic diseases. EWAS attempted to identify potential epigenetic biomarkers associated to the pathology. Some of these studies (reviewed by Dijk *et al.*, 2015) showed altered methylation pattern in site on PGC1A, HIF3A, ABCG1, CPT1A and the RXRA that are associated with increased BMI.

Other studies focused on epigenetic signature present in early stages of life, that might affect the health of the individual throughout life. At this regard it was shown that maternal nutrition and environment during pregnancy profoundly influence the possibility to develop disease like obesity during adulthood. Epigenomic studies on people conceived during period of food deprivation, like the Dutch Hunger Winter in 1944 and the Great Chinese Famine from 1958 to 1961, revealed a transgenerational connection between nutrients and genes. These tragic events allowed to investigate how maternal malnutrition can affect the risk for the offspring to develop diseases during life; in fact, it was found that maternal exposure to famine led to increase BMI in middle aged women offspring (Stein *et al.*, 2007). Also, 6 decades later, Heijmans et al. extracted DNA from people prenatally exposed to the Dutch famine: they found decrease methylation of the insulin-like growth factor II (IGF2), a maternally imprinted gene important for growth and development. This trend was observed in individuals whose mothers suffered hunger during the first period of pregnancy. All together these findings indicate early life events are crucial for the establishment of epigenetic signature, whose effects reflect through life (Heijmans *et al.*, 2008).

2.4.2 Histone deacetylases

Histone acetylation/deacetylation are among the first described histone modifications. Histone deacetylases (HDACs) reverse lysine acetylation from histone tails thus compacting chromatin that becomes less accessible for the transcription machinery. They are also involved in the deacetylation of many non-histone proteins. In opposition, HATs catalyzes the transfer of acetyl groups to the ε- amino group on lysine residues, neutralizing positive charges and making local chromatin regions transcriptionally active (Bannister and Kouzarides, 2011). Eighteen known mammalian HDAC enzymes have been categorized in different families. Classical HDACs includes class I, IIa, IIb and IV that have a zinc-dependent mechanism for lysine deacetylation and class III HDACs, often referred as sirtuins. HDAC1, 2, 3 and 8 belong to class I: they are largely expressed and localize predominantly in the nucleus where they exert their deacetylase activity. Class IIa comprises HDAC4, 5, 7 and 9 that, depending on their phosphorylation status, can be found both in cytoplasm and nucleus; they show a low deacetylases activity. HDAC6, that is largely localized in the cytoplasm, and HDAC10 are included in the class IIb. Little is known about HDAC11, the only component of class IV. Sirtuins are NAD^+-

dependent deacetylases sensitive to changes in NAD^+/NADH ratio: they have been involved in different biological processes such as glucose and lipid metabolism as well as aging (Haberland, Montgomery and Olson, 2009).

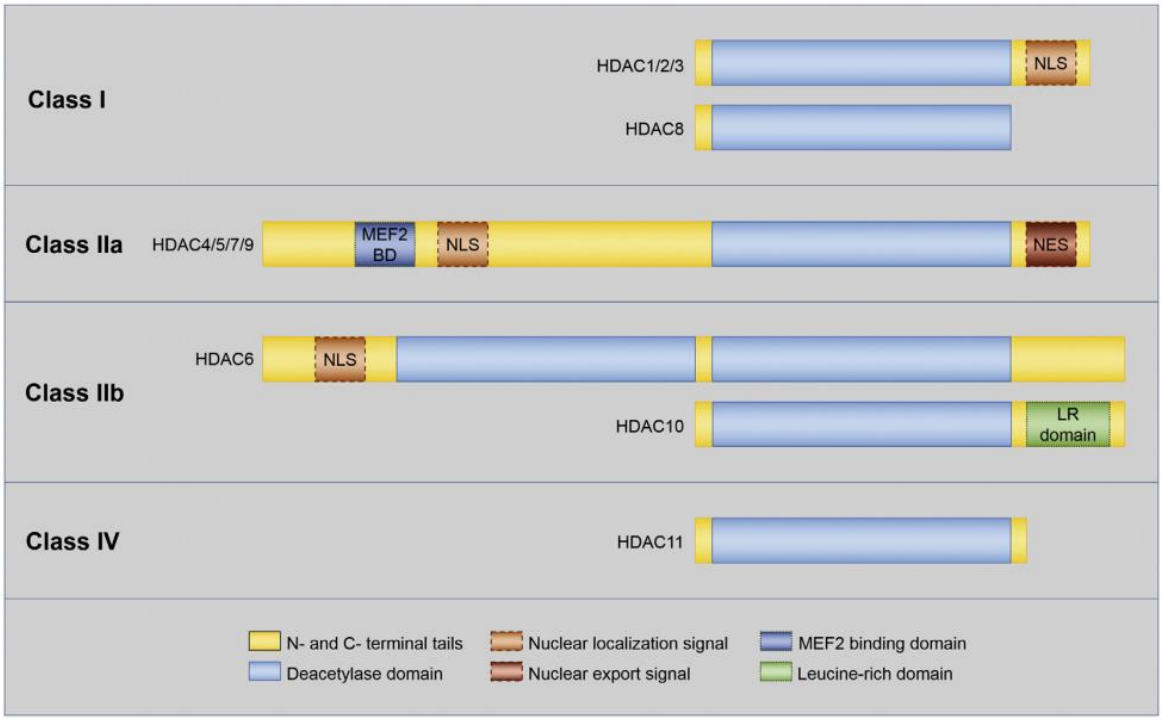

Fig. 9 : Summary of the HDACs superfamily. Adapted from (Bagchi and Weeks, 2019).

Histone deacetylases are involved both in physiological and pathological conditions. They are required for regular development and abnormalities in their function may lead to health problems. HDACs are relevant in many pathologies like cancer, metabolic disorders and inflammatory, neurological and cardiac diseases (Seto and Yoshida, 2014).

There are plenty of evidences that testify the involvement of HDACs in metabolism, and in some metabolic organs such as adipose tissue, skeletal muscle and liver(Ferrari *et al.*, 2012). For instance, treatment of obese mice with Scriptaid, a molecule targeting the class IIa HDAC-corepressor complex, promotes the expression of oxidative genes, thus increasing fatty acids β-oxidation and decreasing triglycerides in skeletal muscle (Gaur *et al.*, 2017).

Other authors showed that genetic deletion of *Hdac9* in obese mice, ameliorated body weight, glucose and insulin sensitivity. Moreover, *in vitro* overexpression of *Hdac9* in adipocytes reduced lipid storage capacity and expression of adipogenic genes like *Pparg*, *C/EBPα* and *Fabp4*, thus highlighting the critical role of HDAC9 in adipocyte differentiation (Chatterjee *et al.*, 2011).

Another study demonstrated the involvement of HDACs in metabolism: the authors showed that HDAC3, 1 and particularly HDAC7 synergistically with corepressors SMRT and NCoR1 leads to inhibition of *Cyp7a1*, a key gene involved in bile acids biosynthesis in the liver (Mitro *et al.*, 2007).

Focusing on inflammation, a study showed the role of HDACs in myocardial infarction in mice. Following the cardiac event, HDACs inhibition promoted polarization of inflammatory M1 to M2 pro-resolving macrophages. M2 macrophages recruitment ameliorated ventricular functions and remodelling, thus highlighting the importance of HDAC inhibition as a promising target in macrophage phenotype handling (Kimbrough *et al.*, 2018).
Another study, regarding specifically HDAC3, highlighted its role in inflammation: mice lacking *Hdac3* in macrophages showed to preferentially adopt IL-4 induced alternative M2 phenotype. ChIP-seq analysis demonstrated that HDAC3 leads to decreased acetylation nearby enhancers on genes related to the IL-4 induced alternative activation, thus limiting gene expression and a pro-resolving inflammation. This fact suggested that the removal of the HDAC3 brake drives macrophages to alternative, pro-resolving activation (Mullican *et al.*, 2011).

Given the involvement of HDACs in many pathologies, efforts have been made to synthetize HDACs inhibitors. Those currently available act through coordination of the zinc ion or by impeding substrate binding. Some of them, like Tricostatin (TSA) and suberoylanilide hydroxamic acid (SAHA), that is used for cancer therapies, are pan-inhibitors that block class I, IIa, IIb and IV. Others, like MS-275, also known as Entinostat, are more specific. MS-275 is a benzamide that selectively inhibits class I enzymes except HDAC8 (Seto and Yoshida, 2014).

2.4.3 HDAC3

HDAC3 belongs to class I HDACs that usually functions together to protein complexes whereas, when alone, their enzyme activity is reduced. HDAC3 is found in the SMRT (silencing mediator of retinoic acid) complex or the homologous NCoR1 (nuclear receptor or co-repressor complex), interacting with a conserved deacetylase activation domain (DAD). Watson et al showed the structure and the mechanism whereby HDAC3/SMRT-DAD interact: they identified inositol (1,2,5,6)-tetraphosphate within HDAC3 and SMRT complex, sticking together the two proteins (Fig. 10). Its presence has proven fundamental for HDAC3/SMRT-DAD mechanism since it promotes the interaction between the two proteins.

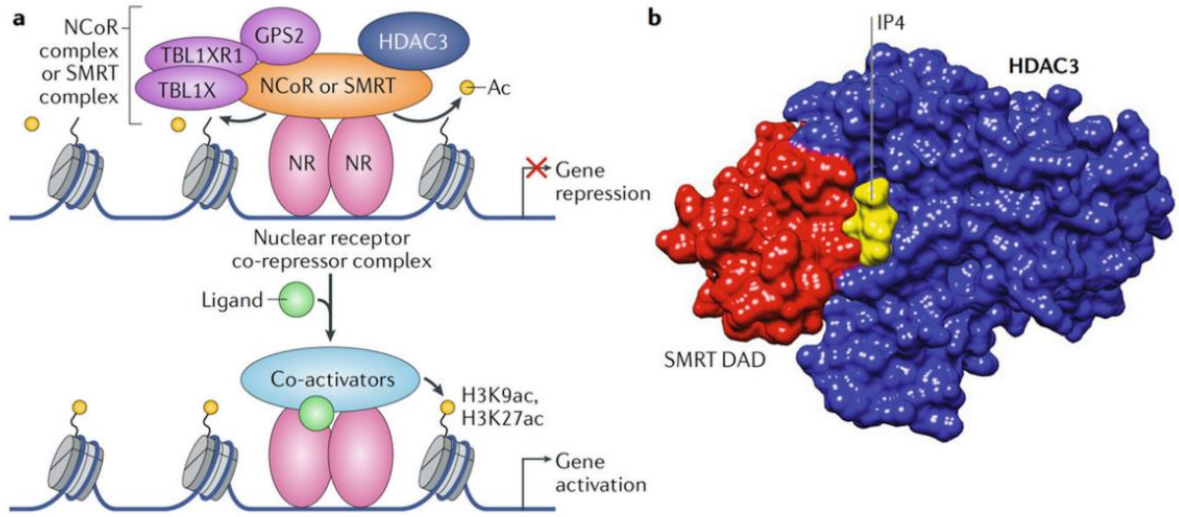

Fig. 10 a) Mechanism of activation/repression of gene transcription through the HDAC3 co-repressor complex. b) Crystal structure of HDAC3 complex: in blue HDAC3, yellow the inositol (1,2,5,6)-tetraphosphate and red the SMRT-DAD complex. Taken from Emmett and Lazar, 2019.

Several studies reported the involvement of HDAC3 in many pathologies such as metabolic disorders, inflammation, cancer and neurodegenerative diseases (Emmett and Lazar, 2019).

Studies in genetically modified mice revealed the importance of HDAC3 in liver metabolism. Liver specific *Hdac3*-null mice showed hepatomegaly and alterations of lipid, cholesterol and carbohydrate metabolism as well as variation in the expression of some gene like *Pparg* (Knutson *et al.*, 2008). However, despite hepatosteatosis, mice lacking *Hdac3* showed better insulin sensitivity and glucose tolerance compared to their control littermates. The hepatic inactivation of *Hdac3* reroutes metabolic precursors from gluconeogenesis toward lipid synthesis, thus avoiding exogenous lipid accumulation and lipotoxicity. In fact, perilipin 2 (*Plin*2) that is involved in the formation of lipid droplets is highly upregulated after *Hdac3* ablation and it participates in both hepatic steatosis and improvement in glucose tolerance (Sun *et al.*, 2012).

HDAC3 is involved also in the regulation of heart metabolism. Post-natal gene inactivation of *Hdac3* in heart and skeletal muscle did not cause lethality in mice fed at chow diet. However, when fed high fat diet, mice developed cardiac disfunction as hypertrophic cardiomyopathy and heart failure. In fact, decreased expression of mitochondrial genes, especially those related to lipid metabolism, led to failure in response to high fat diet overload. These evidences highlight the importance of HDAC3 in cardiac metabolism and that its ablation weakens the capacity of cardiac mitochondria to react to dietary challenge (Sun *et al.*, 2011).

In brown adipose tissue, HDAC3 is fundamental for non-shivering thermogenesis. Mice lacking *Hdac3* in BAT do not survive when exposed to very cold temperatures; this was mirrored by downregulation of gene regarding oxidative phosphorylation with reduction in mitochondrial respiration. Motif analysis revealed that HDAC3 is a coactivator of Estrogen-Related Receptors α (ERRα): this coactivation occurs through deacetylation of PGC-1α (PPARγ coactivator 1 α), leading to increased expression of genes like *Ucp1*. These data suggested that HDAC3 is fundamental in preparing BAT to respond to cold via non-shivering thermogenesis (Emmett, Lim, Jager, Richter, Adlanmerini and Lazar, 2017).
Finally, recent evidences showed that HDAC3 is important in lipid metabolism in intestinal epithelium: deletion of *Hdac3* in intestine reduced diet-induced obesity in mice that maintained the phenotype through life. Intestinal cells coming from KO mice showed increased expression of genes related to FAs oxidation and lipidome remodelling with reduction in triglycerides content. In accordance, pharmacological inhibition of HDAC3 *in vivo* increased the expression of genes for FA β-oxidation in the intestine, thus highlighting the role HDAC3 as possible target for preventing obesity (Dávalos-Salas *et al.*, 2019).

Altogether these evidences emphasize the important role of HDACs and particularly HDAC3 in metabolism of many organs. A better understanding of its involvement in metabolic disorders is fundamental to probe the potential of targeting HDAC3 in obesity and the related complication.

3 AIM

This thesis focuses on the study of the pathophysiology of adipose tissue, with emphasis on epigenetic modifications regulating the function of fat tissue.

Obesity and its plethora of comorbidities have become a serious health problem on which the scientific community is focusing its efforts. Connections between epigenetics, metabolism and related diseases like obesity have been reported and epigenome modifiers such as histone deacetylases (HDACs) are involved in the regulation of adipose tissue metabolism (Herrera, Keildson and Lindgren, 2011).

Scientific literature describes "*browning*" as a phenomenon occurring in adipocytes interspersed within WAT, which acquire characteristics typical of brown adipose tissue. The resulting "*beige*" or "*brite*" adipocytes within WAT develop thermogenic abilities, whereby fatty acids are burnt and energy is dissipated as heat (Rosen and Spiegelman, 2014). Browning in mouse models has been shown to improve body weight and metabolic dysfunctions thus suggesting that its induction could be a promising therapeutic approach to counteract metabolic diseases (Harms and Seale, 2013). Furthermore, different studies showed that HDACs are involved in regulating metabolism of different organs such as liver (Knutson *et al.*, 2008) (Sun *et al.*, 2012), skeletal muscle and heart (Sun *et al.*, 2011). These observations imply that modulation of HDACs activities could be involved in metabolic dysfunctions in different organs and more in-depth investigations are needed to fully evaluate their implications in diseases state and possible therapeutic applications.

In our laboratory we previously demonstrated that inhibition of class I HDACs enhanced oxidative metabolism and promoted the switch of white adipocytes to brown-like phenotype in diet-induced obese (DIO) and *db/db* mice. Particularly, the treatment with MS-275, a chemical inhibitor of class I HDACs, decreased body weight and improved glucose tolerance. Fatty acid β-oxidation and thermogenic capacity increased in mice treated with MS-275, thus ameliorating the metabolic profile of obese mice (data not shown) (Galmozzi *et al.*, 2013) (A. Ferrari *et al.*, 2017). These evidences highlighted the importance of HDACs in regulating energy metabolism and prompted us to investigate the role of HDACs in adipocyte differentiation and functionality. *In vitro* experiments on C3H/10T1/2 preadipocytes highlighted that, when inhibition of class I HDACs with MS-275 occurred in early differentiating adipocytes, there was an influence on adipocyte morphology as shown by the reduction in lipid droplet size (Fig. 11A). Moreover, there was increased expression of markers belonging to adipocytes differentiation and functionality (Fig. 11D); also, genes involved in lipolysis and β-oxidation were upregulated (Fig. 11B and C) indicating that class I HDAC inhibitor MS-275 promotes oxidative metabolism in adipocytes precursors cells. On terminally differentiated adipocytes, the above described phenomena did not occur (data not shown). Kinetic experiments showed that C3H/10T1/2 cells exposed to MS-275 for the first 72 hours from induction of differentiation, maintained upregulation of genes belonging to adipocyte functionality, even after inhibitor removal (Fig. 12).

These results suggested that class I HDACs impacts adipogenesis program during early crucial phases at the beginning of differentiation.

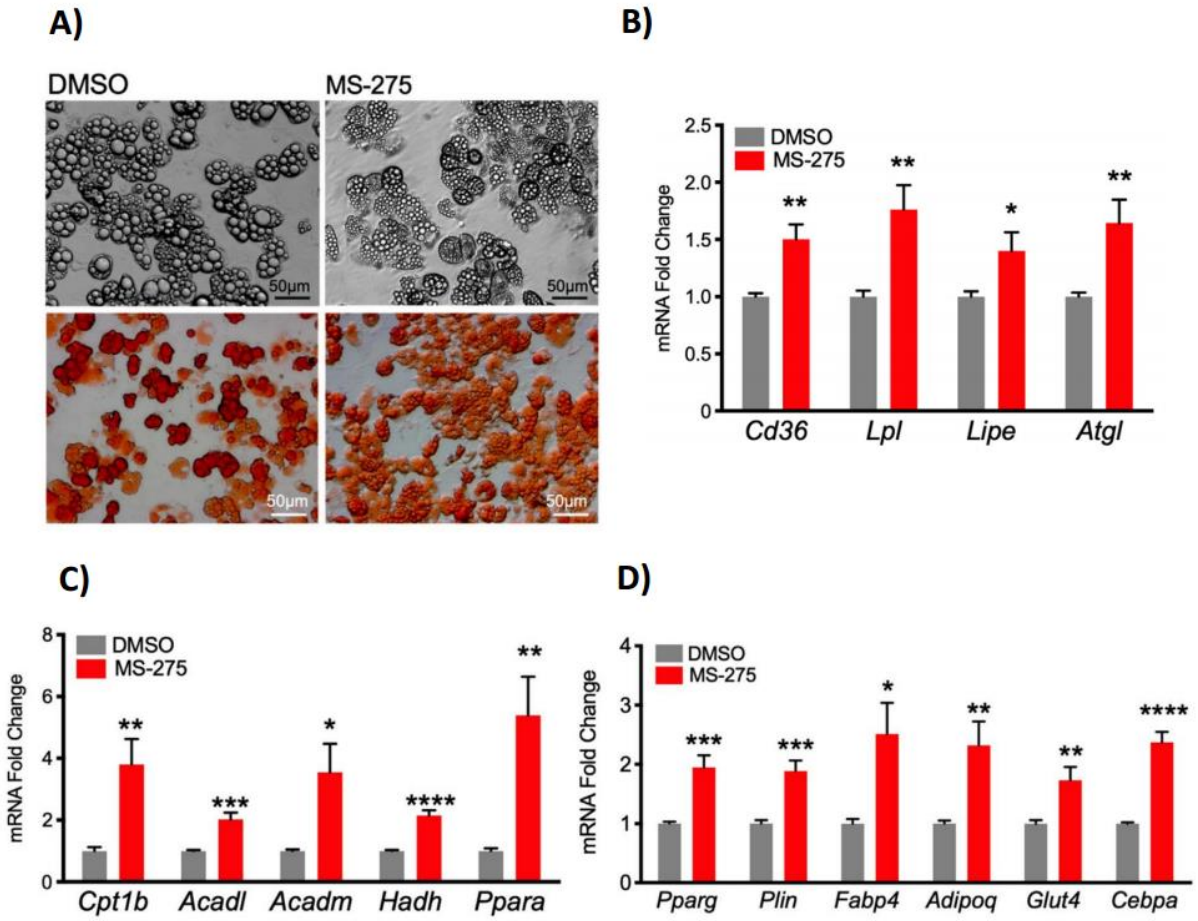

*Fig. 11 Effects of class I inhibition at the beginning of differentiation. A) Cells morphology and ORO staining at day 9 from differentiation in presence of DMSO or MS-275. B), C) and D) Gene expression of C3H/10T1/2 cells at day 9 of differentiation exposed to DMSO/MS-275. Student's t test; *p<0.05; **p<0.01; ****p<0.0001. Adapted from* (Ferrari *et al.*, 2020).

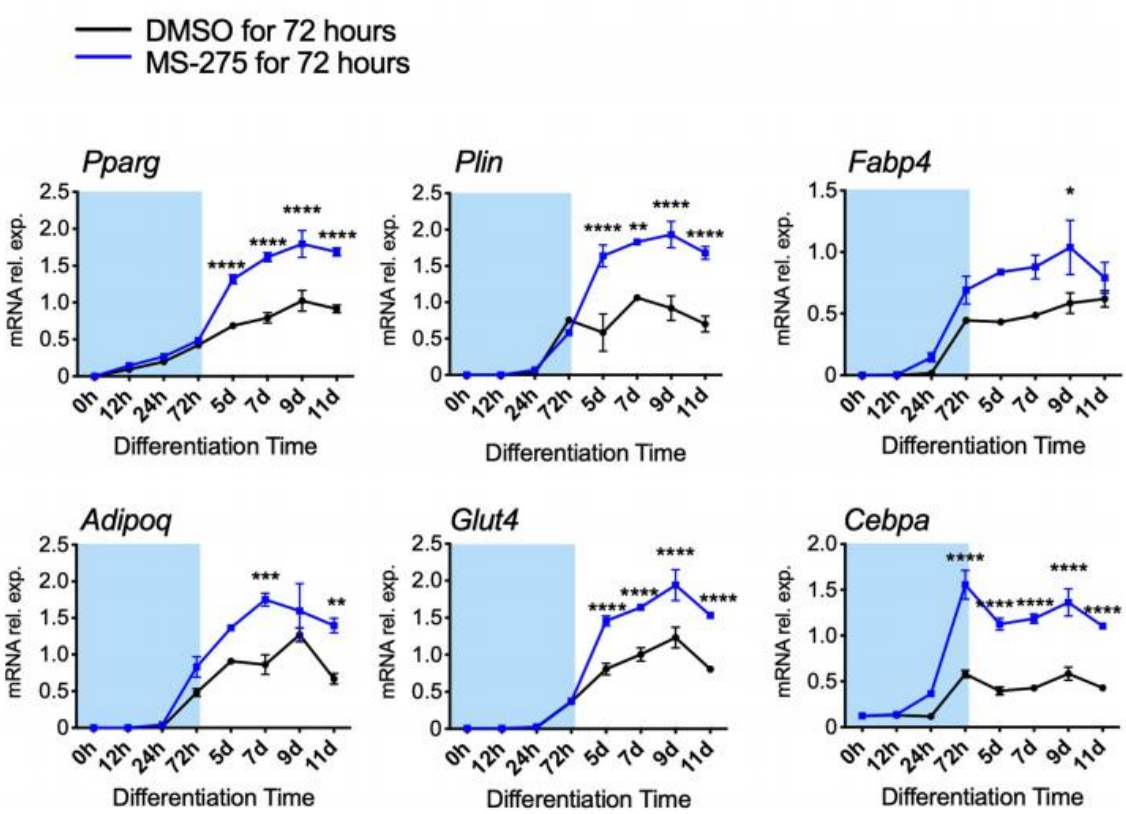

*Fig. 12 Kinetic experiments on gene expression during the first 3 days of differentiation program on C3H/10T1/2 cells exposed to DMSO/MS-275. Statistical analysis: Two-way ANOVA with Tukey's as post hoc test, *p< 0.05, **p< 0.01, ***p< 0.001, ****p< 0.0001. Adapted from* (Ferrari *et al.*, 2020).

We furthermore demonstrated that fat specific genetic inactivation of *Hdac3* in mice remodelled white adipose tissue phenotype and induced browning (Ferrari *et al.*, 2017); inguinal WAT from H3atKO mice appeared reddish (Fig. 13a) with multilocular adipocytes and reduced cells size with a strong increase of *Ucp1* expression (Fig. 13b, c, d and e). Moreover, cold challenge revealed a better tolerance to cold in Hdac3 KO as compared to control mice, thus demonstrating that *Hdac3* ablation promotes browning (Fig. 13f). Transcriptomic analysis showed upregulation of genes forming part of lipid and oxidative metabolism; these data were confirmed by qPCR analysis revealing increased expression of genes belonging to adipocyte functionality, oxidative metabolism and browning (data not shown).

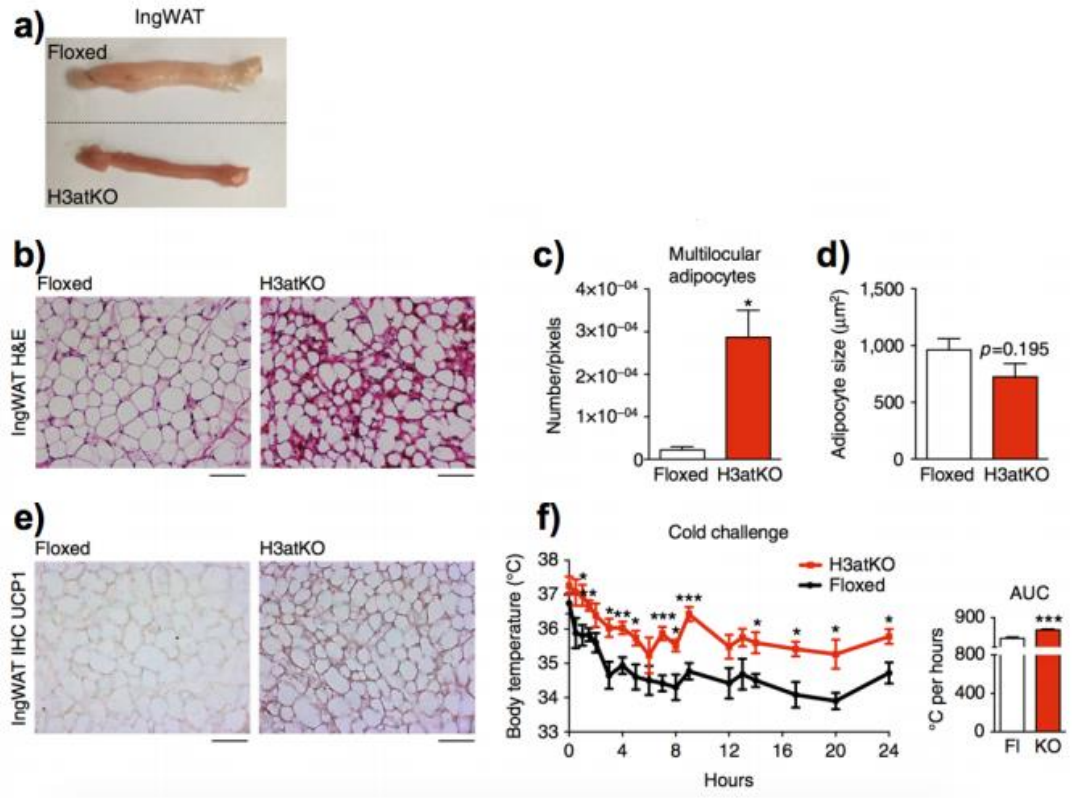

*Fig. 13: H3atKO mice show increased browning of WAT on LFD. a) IngWAT from H3atKO and flowed mice, b) Hematoxylin–eosin staining of IngWAT c) quantification of multilocular adipocytes and d) adipocytes size e) immunohistochemical analysis of UCP1 of floxed and H3atKO mice f) cold-challenge test on mice exposed at 4°C for 24h (n=6 per groups). Statistical analysis: Student'st-test, *p<0.05, **p<0.01, and ***p<0.001. Adapted from* Ferrari *et al.*, 2017.

On this line, we discovered that ablation of *Hdac3* (H3atKO mice) rewires metabolism towards a futile cycle of fatty acid β-oxidation and synthesis, a process that supports thermogenic capacity and browning. We noticed a global reduction of metabolites, particularly citrate, intermediates of glycolysis and TCA cycle, saturated and unsaturated fatty acids. Pyruvate was preferentially converted to anaplerotic oxalaceate and addressed to refill the TCA cycle, as indicated by the increased expression of pyruvate kinase (*Pkm)* and pyruvate dehydrogenase kinase 4 (*Pdk4)* genes. At the molecular level, *Hdac3* ablation led to a transcriptional reprogramming increasing acetylation of lysine 27 of histone H3 (H3K27ac) in specific chromatin regions including *Pparg* and *Ucp1* enhancers and putative regulatory regions of *Pparα* gene. Increased expression of these genes resulted in simultaneous activation of lipolysis and fatty acid synthesis, a process sustaining futile cycle and browning. Within this frame ATP-citrate lyase (ACLY), which converts cytosolic citrate into acetyl-CoA and oxaloacetate, plays a dual role in providing the substrate for *de* novo fatty acid synthesis and for histone acetylation of "hot chromatin regions". Moreover, *de* novo synthesized free fatty acids activate UCP1 thus sustaining thermogenesis in beige adipocytes of WAT.

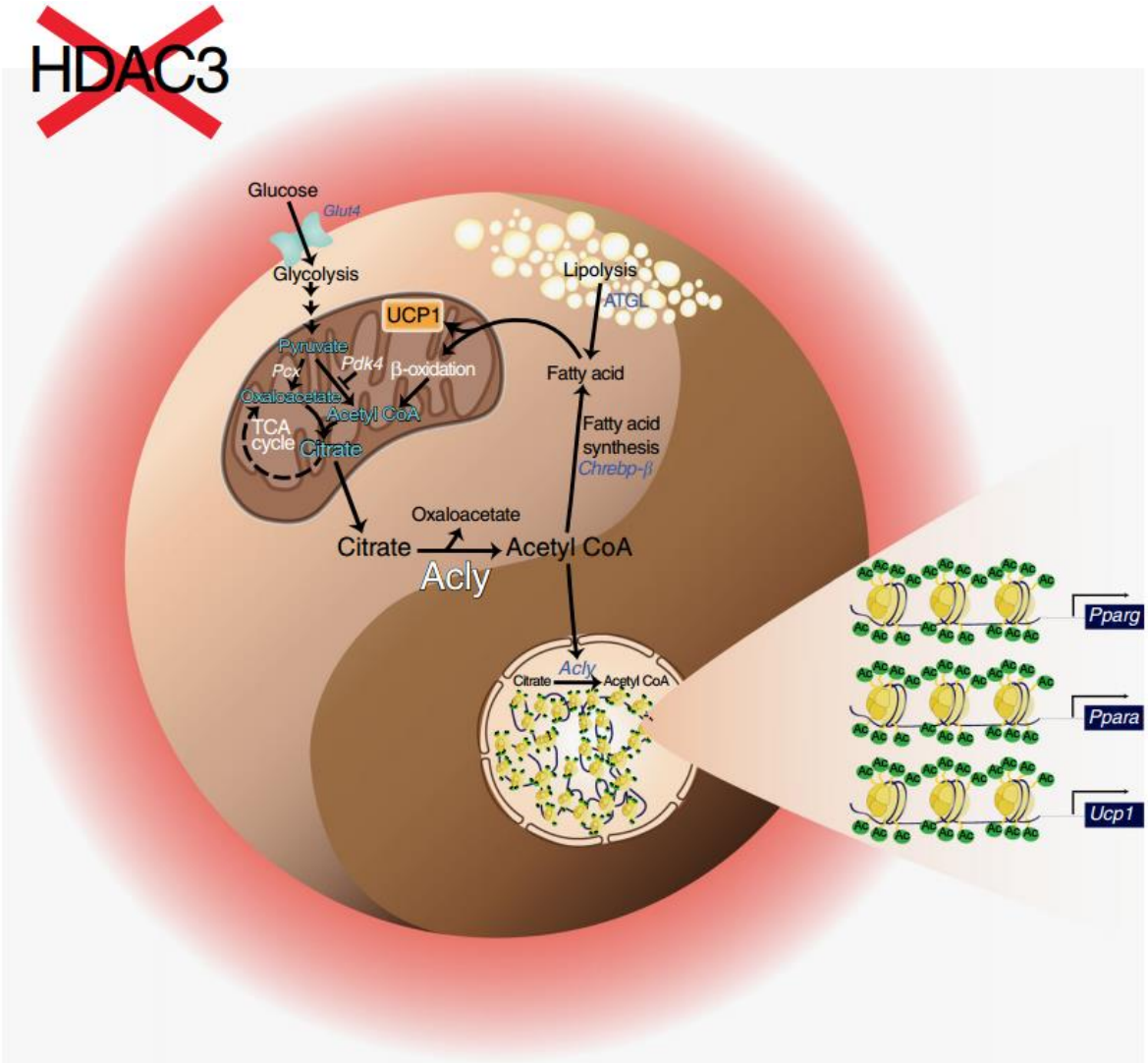

Fig. 14: a representative image reassuming the transcriptional and metabolic rewiring in WAT of H3atKO mice (Ferrari et al. 2017)

Finally, immune cells play a considerable role in pathophysiology of adipose tissue, promoting inflammation and obesity related diseases.

Based on the previous findings and on the above considerations, my PhD project was aimed to further shed light on how class I HDACs regulate adipocyte differentiation and metabolic phenotype and to investigate how immune cell populations change through different times of high fat diet feeding, in order to fully characterize the phenotypical consequences of *Hdac3* ablation in mice. We focused on visceral fat of H3atKO mice since it is more prone to undergo inflammation thus worsening systemic metabolism in obesity.

In parallel, by using omic approaches and bioinformatic analysis, we investigated key genes and regulatory pathways evoked by *Hdac3* ablation. We performed RNA and ChIP sequencing at the beginning of the exposure to diet (4 weeks). The rational was to identify early events resulting from

Hdac3 knock out at transcriptomic and epigenomic level. Early modifications could be fundamental to understand the trigger regulating downstream changes and events.

By integrating RNA-seq and ChIP-seq analysis we investigated possible correlations between differentially expressed genes and the acetylation state of nearby chromatin regions; the focus was on H3K27ac enriched regions of key genes resulting from *Hdac3* ablation.

Finally, we aimed to identify possible pathways, emerging from omic data, related to immunophenotyping.

4 MATERIALS AND METHODS

4.1 *In vitro* experiments

4.1.1 Cell cultures

C3H/10T1/2 cells, Clone 8 (ATCC® CCL-226™) were maintained in culturing Dulbecco's modified Eagle's medium supplemented with 10% Fetal Bovine Serum (FBS, Euroclone), 1% glutamine (Life Technologies) and 1% penicillin/streptomycin (Pen/Strep, Life Technologies). Differentiation to adipocytes was performed according to the scheme below. Differentiation medium was additioned with 5 µg/ml insulin (Sigma-Aldrich), 0.5 mM 3-isobutyl-1-methylxanthine, 2 µg/ml dexamethasone (Sigma-Aldrich) and 5 µM rosiglitazone (Cayman Chemicals). During maintenance culturing medium was supplemented with 5 µg/ml insulin (Sigma-Aldrich). Three days after induction of differentiation cells were switched to maintenance medium supplemented with 5µg/ml insulin for 6 additional days. DMSO, 1µM MS-275 or 10µM garcinol (Cayman Chemicals) was added during differentiation or in the last 24 hours of differentiation as indicated.

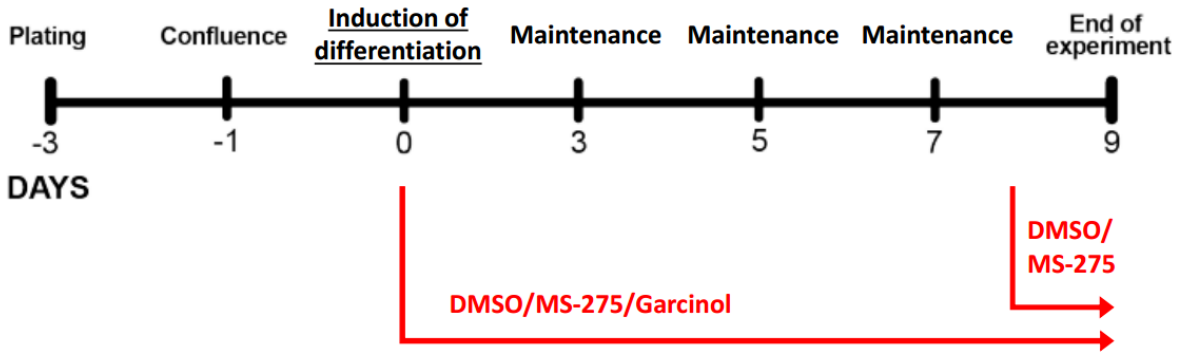

4.1.2 Quantification of lipid content

Quantification of lipid content was performed with Oil Red O (ORO) staining. Cell were differentiated in 12 well plate and fixed in 10% formalin in PBS and then washed with 60% isopropanol. Staining was eluted from wells with 1.5 ml of 100% isopropanol (10 min incubation) and absorbance was measured (516 nm, 0.5 second reading). ORO staining quantification was normalized for total RNA or protein content.

4.1.3 Gene expression

Cells were lysed using TRIzol (Invitrogen) or RA1 lysis buffer (Macherey-Nagel) supplemented with β-mercaptoethanol and RNA was purified using the Nucleospin RNA II kit (Macherey-Nagel). Adipose

tissues were isolated with Qiazol reagent (Qiagen) and purified with commercial kit (RNeasy Lipid Tissue Mini kit, Qiagen). RNA was quantified with Nanodrop (Thermo Scientific, Wilmington, DE) and then amplified by real time PCR, using iScript™One Step RT PCR for Probes (Bio-Rad Laboratories). Data were normalized to 36b4 mRNA and quantified by setting up a standard curve. Specific primers and probes were designed using Realtime PCR Tool (Integrated DNA Technologies) and synthesized by Eurofins Genomics.

4.1.4 Protein analysis

C3H/10T1/2 cells were lysed with SDS sample buffer (20% glycerol, 4% SDS, 100 mM Tris-HCl pH 6.8, 100 mM dithiothreitol, 0.002% bromophenol blue), 1 mM protease inhibitors (Sigma), and homogenized with TissueLyser (Qiagen). Samples were separated by SDS-page and transferred to nitrocellulose membranes: the correct transfer of proteins on the membranes was examined by Ponceau staining. Membranes were incubated for 1 hour with blocking buffer (5% non-fat dry milk in 1X TBS-t or 5% BSA in 1X TBS-t) on shaking. The adopted primary antibodies were: PPARγ antibody (sc7273, Santa Cruz Biotechnology), ATGL antibody (#2138 s, Cell Signaling), HSP90α/β antibody (sc-69703, Santa Cruz) and β-actin antibody (A5441, Sigma). After an overnight incubation with primary antibodies, membranes were incubated with HRP-conjugated goat anti-mouse (SigmaAldrich), HRP-conjugated IgG goat anti-rabbit #7074 (Cell Signaling) secondary antibodies. Detection were performed with with chemiluminescence (ECL, Pierce).

4.1.5 Chromatin Immunoprecipitation

C3H/10T1/2 cells were cross-linked with 1% formaldehyde after differentiation in presence of DMSO or MS-275 for 12 h or 9 days. Chromatin was sonicated using SLPe sonicator, Branson. The adopted antibody for chromatin immunoprecipitation was H3K27ac antibody (ab4729, Abcam). After cross-link reversion, DNA was purified with QIAquick gel extraction kit columns (QIAGEN).

4.1.6 Statistical analysis

Analysis were performed using the unpaired two-tailed Student t-test or One-way ANOVA with Tukey as post hoc test or Two-way ANOVA with Tukey as post hoc test with GraphPad PRISM software (San Diego, CA).

4.2 *In vivo* experiments

4.2.1 Mouse model

In order to obtain a specific deletion of *Hdac3* in adipose tissues *Hdac3* floxed mice in C57Bl/6J background (provided by Dr. Scott W. Hiebert laboratory, Vanderbilt University) were crossed with B6; FVBTg (Adipoq-Cre)1Evdr/J mice (The Jackson Laboratory). Mice were fed until 8 weeks age with standard diet (4rf21 GLP certificate, Mucedola) and then with LFD (LFD, D12450H, Research Diet) or HFD (HFD, D12451, Research Diet) for 4, 9 or 16 weeks. The body weight was monitored before and during diet. At the end of the treatment blood, brown and white adipose tissue were collected from individual animals; the retrieved brown and white adipose tissues (the latter one including subcutaneous inguinal adipose tissue, subWAT, and visceral epididymal adipose tissue, epiWAT) were snap frozen in liquid nitrogen and then stored at -80°C. Blood samples were centrifuged at 4°C, 8000g for 10 minutes in order to obtain plasma.

4.2.2 Chromatin Immunoprecipitation and sequencing (ChIP-seq)

Subcutaneous inguinal WAT collected from mice exposed to LFD or HFD for 4 weeks was combined in 12 pools. However, we discarded pool 12 due to quality issues. Below the experimental scheme:

Group 1: Floxed + LFD 4 wks			Group 2: KO + LFD 4 wks			Group 3: Floxed + HFD 4 wks			Group4: KO+HFD 4wks	
POOL NUMBER			POOL NUMBER			POOL NUMBER			POOL NUMBER	
1	2	3	4	5	6	7	8	9	10	11

Tissues were cross-linked with 1% formaldehyde for 10 minutes at RT with moderate shaking. Cross-linking was stopped by adding 125 mM glycine (final concentration). Samples were homogenized using a dounce homogenizer and then sonicated (15 pulses, 15 seconds with SLPe sonicator, Branson). Each IP was settled using 8µg of sheared chromatin and 2µg of antibody H3k27ac (ab4729, Abcam): Ab and chromatin were incubated at 4°C o/n on a shaking platform. Meanwhile, Protein A Sepharose beads (GE Healthcare) were prepared, according to the manufacturer instructions. Beads were added and samples were incubated for 2 hours at 4°C on a rotating platform. After cross-link reversion, immunoprecipitated DNA and input were purified with QIAquick gel extraction kit columns (QIAGEN).

4.2.3 RNA-sequencing (RNA-seq)

Library preparation was performed using the Illumina TruSeq reagents (TruSeq STR-RNA Zero) and samples were sequenced on the Illumina HiSeq 4000 SR 150.
Purity-filtered reads were adapted and quality trimmed with Cutadapt (v. 1.8). Reads matching to ribosomal RNA sequences were removed with fastq_screen (v. 0.11.1). Remaining reads were further filtered for low complexity with reaper (v. 15-065). Reads were aligned against *Mus musculus* (GRCm38.92) genome using STAR (v. 2.5.3a). The number of read counts per gene locus was summarized with htseq-count (v. 0.9.1) using *Mus musculus* (GRCm38.92) gene annotation. Quality of the RNA-seq data alignment was assessed using RSeQC (v. 2.3.7).
Statistical analysis was performed for genes independently in R (R version 3.5.2). Genes with low counts were filtered out according to the rule of 1 count(s) per million (cpm) in at least 1 sample. Library sizes were scaled using TMM normalization. Subsequently, the normalized counts were transformed to cpm values, and a log2 transformation was applied, by means of the function cpm with the parameter setting prior.counts = 1 (EdgeR v 3.24.3). As a final step, the log-CPM data were quantile normalized.

Transcriptomic and epigenomic analysis were carried out in collaboration with the laboratory headed by professor Béatrice Desvergne, at the Centre Integratif de Genomique, and professor Nicolas Guex, Centre de Bioinformatique, University of Lausanne.

Following bioinformatic analysis were performed using several software such as GSEA (Gene Set Enrichment Analysis), KEGG Pathway database, iDEP.91 (Integrated Differential Expression and Pathway analysis) and IGV (Integrative Genomics Viewer).

4.2.4 Immunophenotyping

Floxed and H3atKO mice at 9 weeks of age were fed with LFD and HFD for the following 4, 9 or 16 weeks. During the diet exposure body weight was monitored. At the end of the diet feeding, mice were euthanized, and blood and tissues were collected. Freshly collected blood was stained after lysis of red blood cells with ACK solution (KHCO3 10mM, NH4Cl 150 mM, EDTA 0.1 mM) for 10 minutes at RT.
Spleen was isolated and weighted. A uniform cell suspension was prepared by washing in 2% FBS, 2µM EDTA PBS (MACS buffer) and by mashing the spleen through a 70 µm cell strainer followed by centrifugation. The supernatant was aspirated and 5mL (per mice) of Red Cell Blood Lysis Buffer were

added for 5 minutes at 4°C. After washing step, samples were centrifuged and cells were suspended in 10 mL of MACS buffer; cells were then counted and stained with antibody mix.

Visceral epididymal adipose tissue (epiWAT) was collected in PBS containing 5% BSA and then added with collagenase (200 mg/ml final concentration, NB4 standard grade, Serva) and $CaCl_2$ (5 mM final concentration). After incubation at 37°C for 40 minutes under agitation, samples were topped up with MACS (PBS, 2% FCS, 2 mM EDTA) and then filtered with 100 µm and 70 µm cell strainers. After lysis of red blood cells with ACK, samples were resuspended in antibody mix. Optimal antibody concentrations for staining were calculated based on manufacturer instructions. For immunophenotyping, a cell suspension containing $1x10^6$ cells or 50 µL of blood were acquired with or Novocyte 3000 (ACEA Biosciences) and LSR-II (BD Biosciences).

Immunophenotyping experiments were conducted at the Department of Pharmacological and Biomolecular Sciences, in collaboration with Dr. Fabrizia Bonacina in the Laboratory of Lipoproteins, Immunity and Atherosclerosis headed by professor Alberico Catapano and Danilo Norata.

4.2.5 Ethical permits for animal experiments

Animal experiments were conducted strictly following the Italian law (d.lgs. 26/2014) and the EU directive 2010/63, permit 898-2015-PR.

5 RESULTS

5.1 Inhibition of class I HDACs stimulates oxidative metabolism and browning of differentiating adipocytes

Results previously obtained in our laboratory, demonstrated that the inhibition of class I HDACs with a specific molecule, MS-275, ameliorated metabolic profile and induced browning in mouse model of obesity (DIO and *db/db* mice). *In vitro* preliminary experiments in C3H/10T1/2 preadipocytes showed that class I HDACs inhibition stimulated the adipogenic potential and promoted oxidative metabolism in differentiating adipocytes (Fig. 11). Moreover, those experiments highlighted that class I HDACs impacts adipogenesis program during early crucial phases at the beginning of differentiation (Fig. 12). On this line, we further investigated the role of HDACs in adipocyte differentiation and functionality and we asked whether the inhibition of HDAC influenced additionally metabolic genes.

To this end, we exposed C3H/10T1/2 mesenchymal stem cells to MS-275 either at beginning or at the end of the differentiation process. We chose C3H/10T1/2 cells since they are a model of early adipocytes precursors. Cells were treated with DMSO (vehicle) or with 1µM MS-275 from the induction of differentiation (day 0, Fig. 15A)

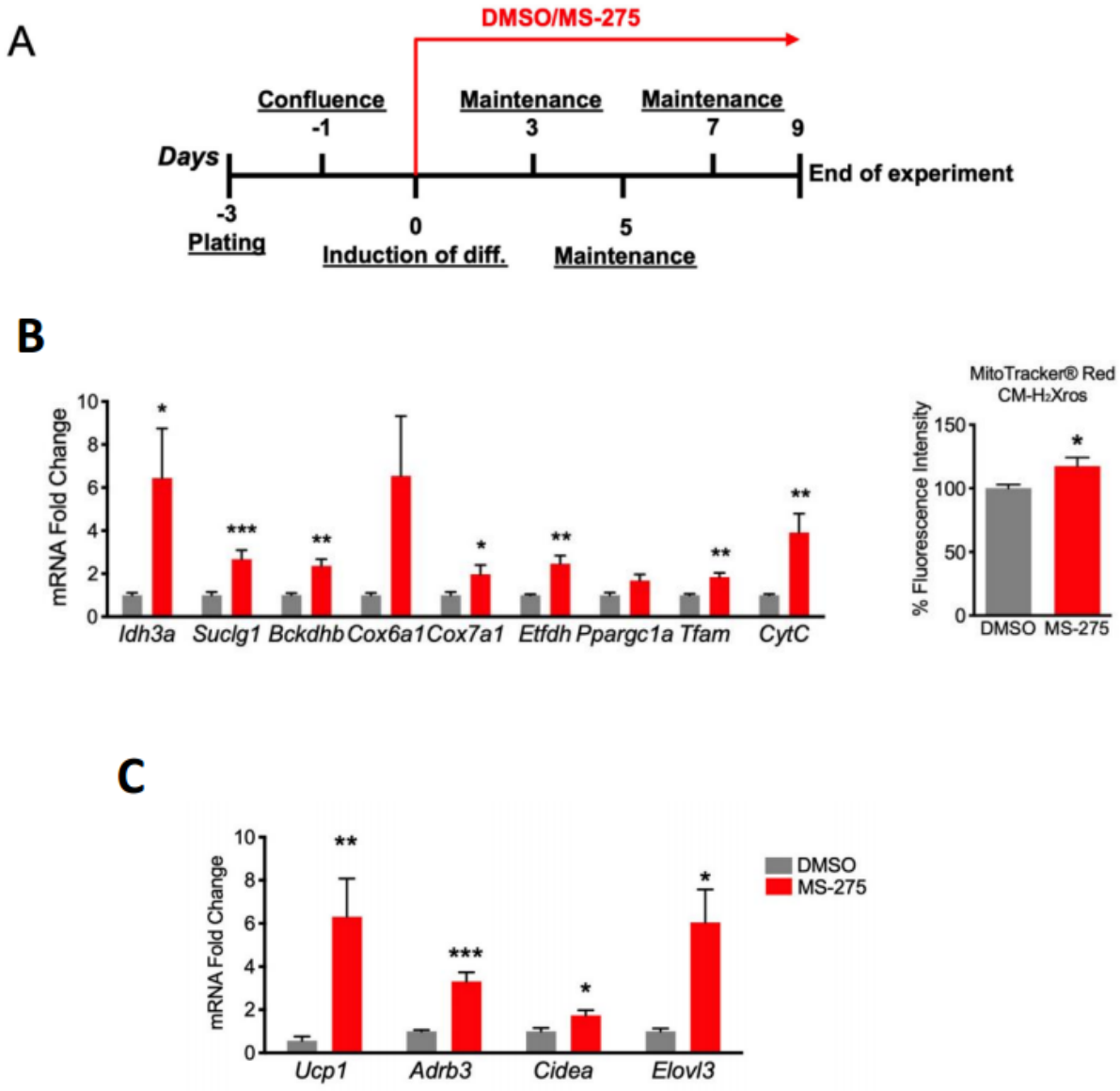

*Fig. 15 A) Differentiation scheme of C3H/10T1/2 pre-adipocytes. B) Effects of MS-275 on genes regarding mitochondrial activity at the beginning of differentiation and MitoTracker RED. C) Expression of markers of browning in cells exposed to MS-275 at the beginning of differentiation program. Data are presented as mean ± s.e.m. Student's t test; *p<0.05; **p<0.01; ****p<0.0001.Taken from* (Ferrari *et al.*, 2020).

Indeed, early treatment with MS-275 led to increased expression of genes belonging to TCA cycle (*Idh3a and Suclg1,*), branched chain amino acid catabolism (*Bckdhb* Fig. 15C) electron transport chain (*Cox6a1, Cox7a1, Etfdh, CytC* ,Fig. 15*C*) mitochondrial biogenesis (*Pgc1a, Tfam* Fig. 15*C*). High mitochondrial activity was mirrored by increased signal measured with MitoTracker Red CM-H_2Xros (Fig. 15B).

High mitochondrial activity together to increased oxidation showed in preliminary results (Fig. 11) is often correlated to phenomenon of browning of white adipocytes (Ferrari et al,2017). In fact, we found increased expression of markers of browning like *Ucp1, Adrbr3, Cidea, and Elovl3* (Fig. 15C).

On the contrary, when the class I HDACs inhibitor was used on terminally differentiated adipocytes, the outcome was different. The effects on C3H/10T1/2 cells exposed to MS-275 during the last 24 hours of differentiation were modest and only with some genes like *Ucp1* and *Elovl3* (Fig. 16). Summarizing, MS-275 promotes oxidative metabolism and the switch towards brown-like phenotype in adipocytes precursors cells but not in terminally differentiated adipocytes.

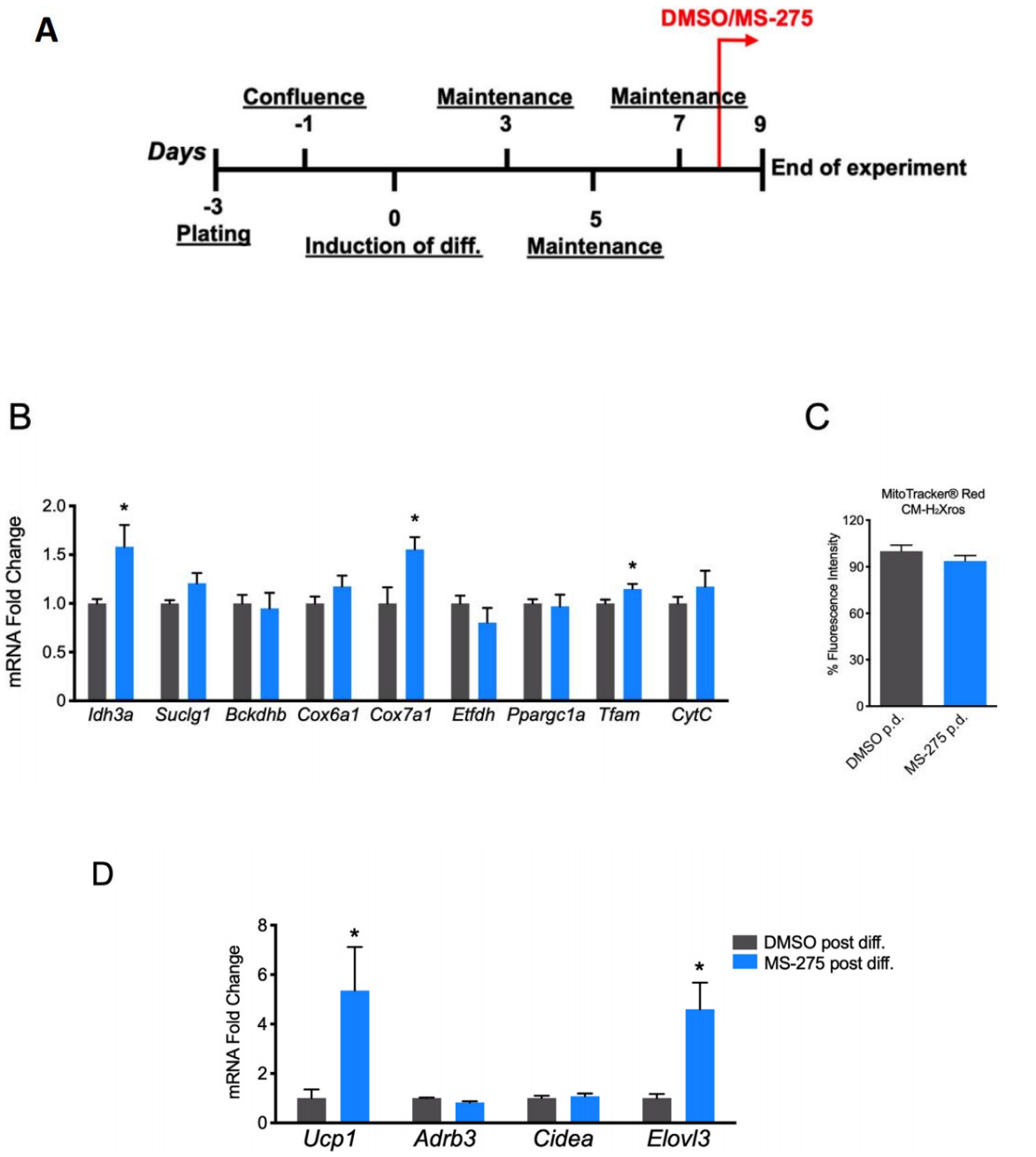

*Fig. 16 A) Differentiation scheme of C3H/10T1/2 pre-adipocytes treated at the end of differentiation. B) Effects of MS-275 on genes regarding mitochondrial activity at the end of differentiation and MitoTracker RED D) Expression of markers of browning. Data are presented as mean ± s.e.m. Student's t test; *p<0.05; **p<0.01; ****p<0.0001. Taken from* (Ferrari *et al.*, 2020).

5.1.1 Class I HDACs inhibition promotes acetylation of enhancer elements of *Pparg* and *Ucp1* genes

To understand the transcriptional effects of MS-275 we performed chromatin immunoprecipitation in C3H/10T1/2 cells: we focused on acetylation of H3K27, a histone mark of active enhancers.
After 12 hours from induction of differentiation, MS-275 was already able to increase expression and acetylation on *Pparg* and *Ucp1* genes (Fig. 17A, B, C, D). At day 9 from induction of differentiation this trend reached statistical significance, and it correlated with the observed increased expression of these genes. Therefore, increased H3K27ac of *Pparg* and *Ucp1* enhancers corresponded to higher expression of genes involved in browning and adipocyte functionality.

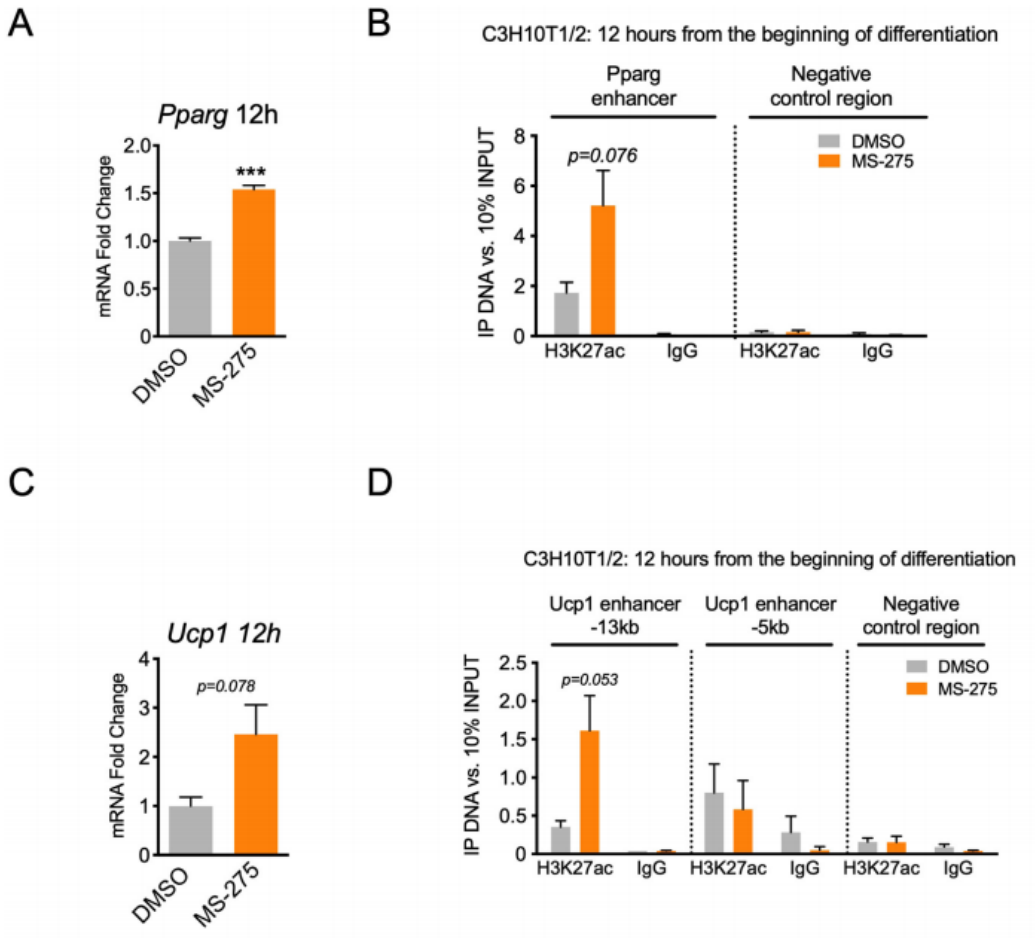

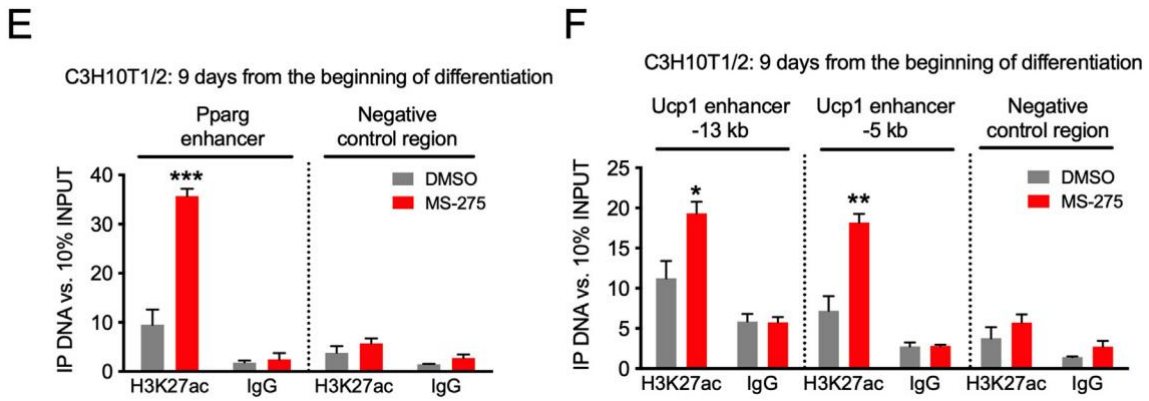

*Fig. 17: A) Expression of Pparg in cells treated with DMSO/MS-275 after 12 h from beginning of differentiation. B) H3K27ac ChIP analysis on Pparg enhancer in cells treated with DMSO/MS-275 for the first 12 h from induction of differentiation. C) Expression of Ucp1 in cells treated with DMSO/MS-275 after 12 h from beginning of differentiation. D) H3K27ac ChIP analysis on Ucp1 enhancer in cells treated with DMSO/MS-275 for the first 12 h from induction of differentiation. E) H3K27ac ChIP analysis on Pparg enhancer in cells exposed to DMSO/MS-275 for 9 days differentiation F) H3K27ac ChIP analysis on Ucp1 enhancer in cells treated with DMSO/MS-275 for 9 day of differentiation. Data are presented as mean ± s.e.m. Student's t test; *p<0.05; **p<0.01; ****p<0.0001. Taken from* (Ferrari *et al.*, 2020).

5.1.2 HAT inhibition reverses the phenotype observed with class I HDACs inhibition

To better study the counterpart of HDAC activity, i.e. histone acetyl transferase (HAT) activity, we performed experiments using garcinol, a chemical inhibitor of HATs. Since we observed that the effects of MS-275 were mainly on cells at the beginning of differentiation, we investigated the effects of HAT inhibitor in analogous conditions: we treated C3H/10T1/2 cells with 10µM garcinol or DMSO at the beginning of differentiation program until day 9. At the end of the experiments cells exposed to garcinol showed a clear reduction of adipocytes and a lot of cells resulted not even differentiated (Fig. 18B). ORO stained mirrored this trend since there was a strong reduction of lipid accumulation (Fig. 18B and C).

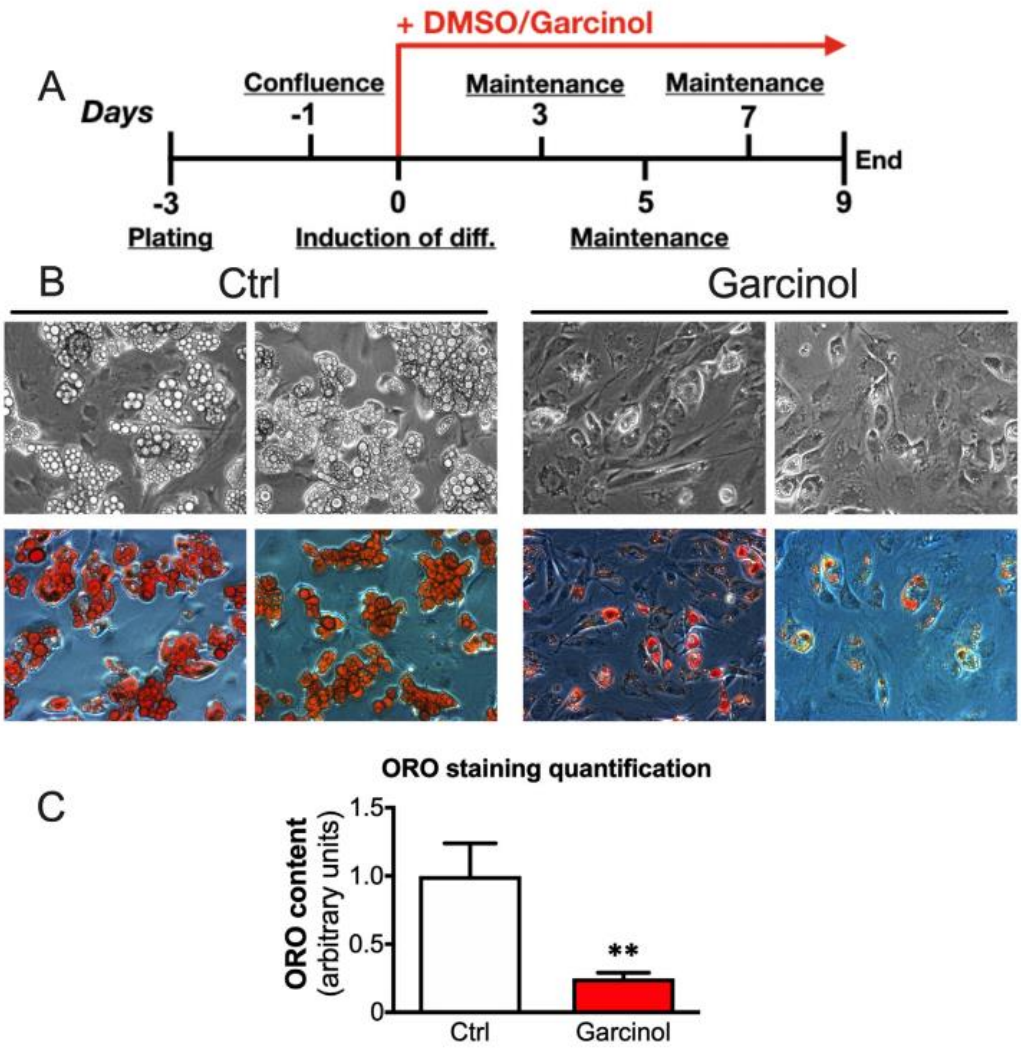

*Fig. 18: A) Experimental design of C3H/10T1/2 treatment with garcinol. B) cells morphology after exposure to DMSO/garcinol. C) ORO staining quantification. Data are presented as mean ± s.e.m. Student's t test; *p<0.05; **p<0.01; ****p<0.0001. Taken from* (Ferrari *et al.*, 2020).

Genes belonging to adipocyte functionality, lipolysis and fatty acids β-oxidation, mitochondria and markers of browning showed a significant decrease in cells treated with the HAT inhibitor garcinol. These data confirm the important role of both HATs and HDACs in determining the metabolic phenotype of preadipocytes.

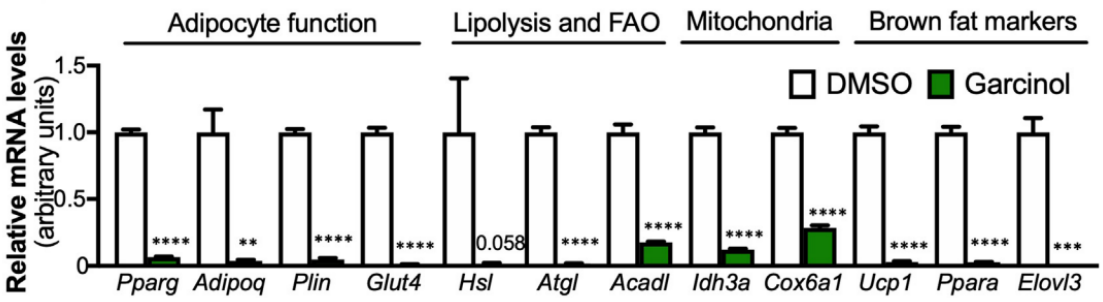

*Fig. 19: Gene expression quantification C3H/10T1/2 cells exposed to DMSO/garcinol. Data are presented as mean ± s.e.m. Student's t test; *p<0.05; **p<0.01; ****p<0.0001. Taken from* (Ferrari *et al.*, 2020).

5.2 Immune cells in adipose tissue

We previously demonstrated that HDAC3 acts as a molecular brake of the metabolic rewiring that support browning in mice WAT: in fact, *Hdac3* gene inactivation induced a futile cycle of fatty acids oxidation and synthesis that promotes browning and thermogenic capacity.

After these observations, we wanted to further explore the impact of *Hdac3* gene inactivation on the composition of immune cells in visceral fat of H3atKO mice. It is well known that immune population plays an important role in the pathophysiology of the adipose tissue and it is often related to the obesity- associated metabolic disfunctions. For this reason, we analysed the immunophenotype of H3atKO and floxed littermates after different periods (4, 9, 16 weeks respectively) of low fat or high fat diet feeding.

5.2.1 Immune remodelling in H3atKO mice after 4 weeks of diet

We first fed H3atKO mice with low fat or high fat diet for 4 weeks: the aim was to identify early changes of immune cell populations, during the beginning of an inflammatory stimulus as the HFD.

After the treatment, we collected epididymal visceral WAT (epiWAT), a fat depot more prone to develop inflammation compared to other types of adipose tissue. It is well established that visceral obesity contributes to the health risks and metabolic disfunctions connected to overweight and obesity.

We firstly noticed that epiWAT from H3atKO mice weighted less compared to controls fed LDF and, at a less extended manner, HFD (Fig. 20A); this trend did not reach statistical significance but still in line with previous results obtained in our laboratory (Ferrari *et al.*, 2017).

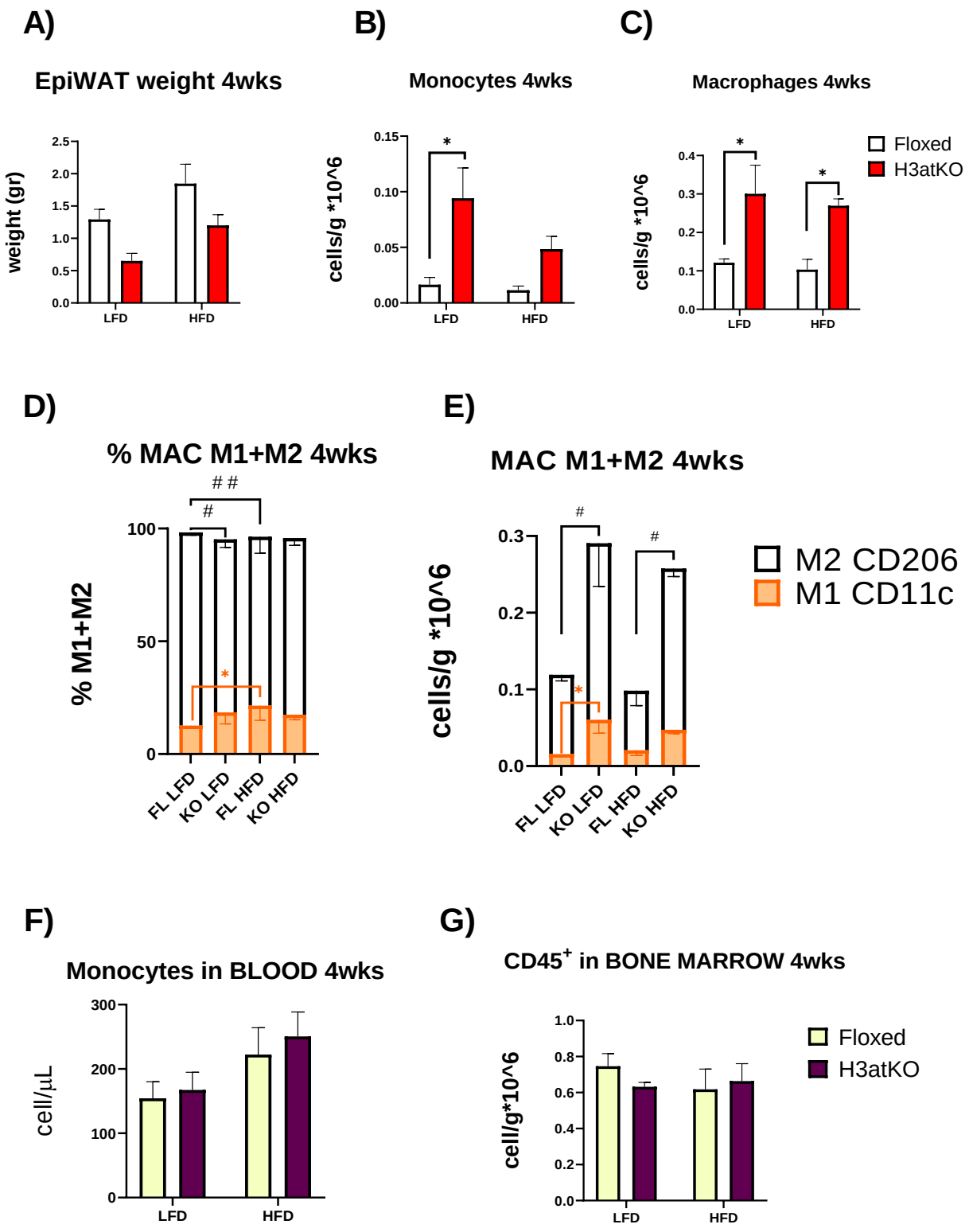

*Fig. 20: Changes in EpiWAT weight and innate immune populations after 4 weeks diet in H3atKO and Floxed mice. A) EpiWAT weight from H3atKO and Floxed mice (n=10 per group). B) Numbers of monocytes and C) macrophages in epiWAT (n=5 per group). D) Percentage of M2 and M1 macrophages in epiWAT and E) corresponding counts (n=5 per group). F) number of monocytes in H3atKO and Floxed mice in blood and G) analysis of CD45⁺ in bone marrow (n=5 per group). Data are presented as mean ± s.e.m. Two-way ANOVA, Tukey as post hoc test *p< 0.05, **p< 0.01, ***p< 0.001, ****p< 0.0001.*

FACS analysis revealed differences regarding the innate immune components: monocytes increased in H3atKO mice on LFD as well as macrophages both at low fat and high fat diet (Fig. 20B and C). Interestingly, the percentage of M1 pro-inflammatory macrophages was lower compared to M2, and this trend was mirrored by the counts of M1 macrophages (Fig. 20E). Moreover, the increased percentage of M1 macrophages in floxed HFD mice compared to controls at LFD suggests the early onset of inflammation elicited by HFD (Fig. 20).

We evaluated the immune populations in bone marrow to assess whether any differences in adipose tissue could be associated with a possible different production in bone marrow. As shown in Fig. 20G there were no changes in CD45+ leukocytes in bone marrow. The number of circulating monocytes was not different (Fig. 20F), suggesting that inflammation is limited to adipose tissue at least within the first four weeks of HFD.

Altogether, these findings showed an initial remodelling of the innate immune cell population following *Hdac3* ablation and in response to HFD.

5.2.2 Immune remodelling in H3atKO mice after 9 weeks of diet

Having assessed how the immune population changes after 4 weeks of diet, we asked whether a prolonged period of diet exacerbated the effects. In this second batch, animals were exposed to LFD or HFD for 9 weeks: we choose this interval since it is known that inflammation is more evident after 9 weeks of HFD feeding (Yamashita *et al.*, 2005) (Heydemann, 2016).

Visceral WAT weight at the end of the diet was significantly lower in H3atKO mice compared to floxed under both diet regimens (Fig. 21A) and this was in line with previous results.

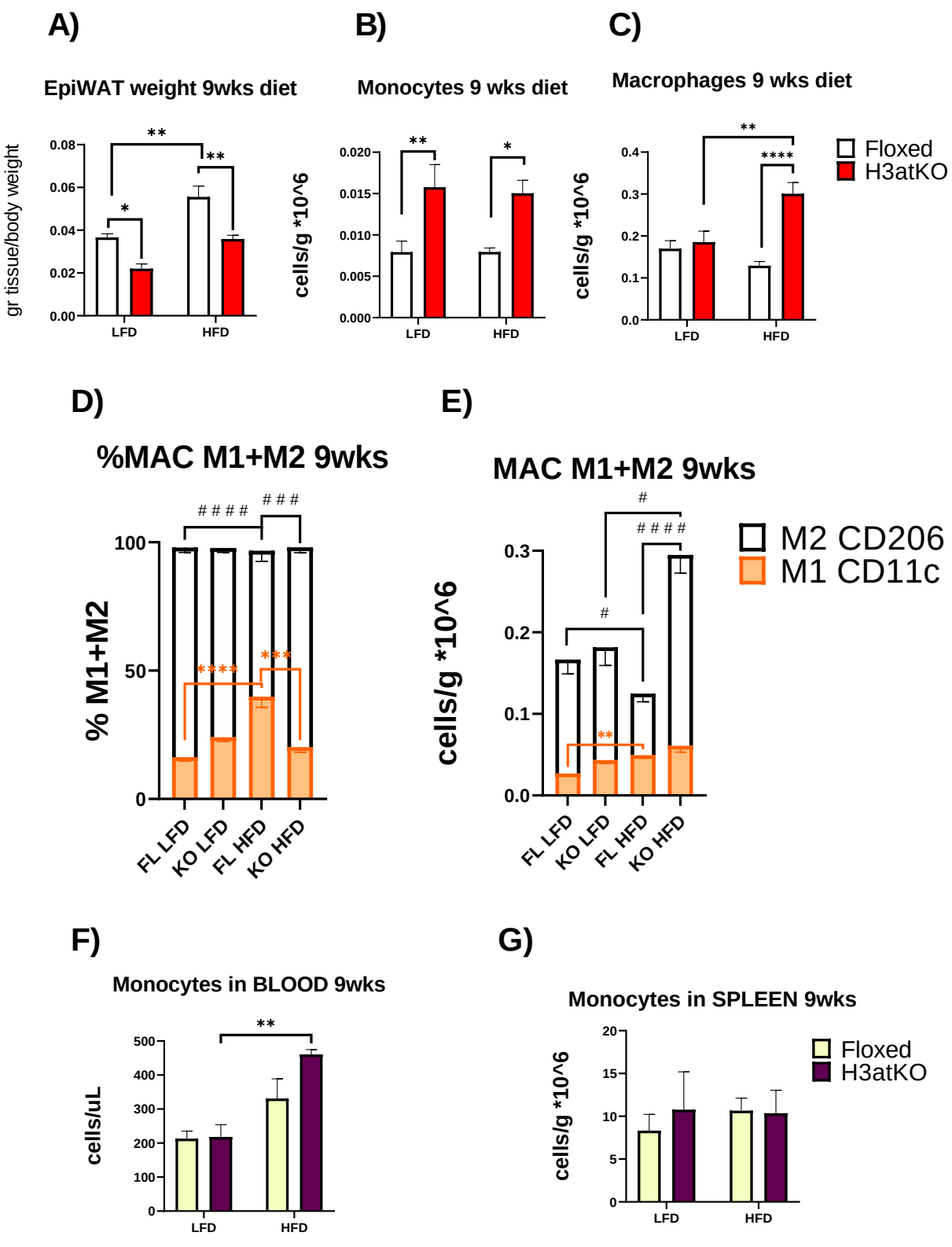

*Fig. 21 Changes in epiWAT weight and innate immune population after 9 weeks of diet. A) EpiWAT weight from H3atKO and Floxed mice (n=5-8 per group). B) Numbers of monocytes and C) macrophages in epiWAT (n=5-8 per group). D) Percentage of M2 and M1 macrophages in epiWAT and E) corresponding counts (n=5-8 per group). F) number of monocytes in H3atKO and Floxed mice in blood and G) analysis of monocytes in spleen (n=5-8 per group). Data are presented as mean ± s.e.m. Two-way ANOVA, Tukey as post hoc test *p< 0.05, **p< 0.01, ***p< 0.001, ****p< 0.0001.*

Evaluation of the innate immune population showed higher number of monocytes in epiWAT of H3atKO mice compared to floxed in both LFD and HFD (Fig. 21B).
Analysis on macrophages revealed their higher number when *Hdac3* ablation occurred, during HFD exposure (Fig. 21C): among them, M2 macrophages were the most abundant and the difference between KO and floxed mice on HFD was statistically significant (Fig. 21D and E). Concerning the percentage of M1 component, it was significantly lower in H3atKO mice when exposed to HFD (Fig. 21D). On the contrary, the increasing number of M1 in floxed HFD compared to floxed LFD confirmed the onset of inflammation and this trend was even stronger when compared to 4 weeks of treatment (Fig. 21E and Fig. 20E).
The difference in terms of percentage of M1/M2 polarization was in line with the observation at 4 weeks of treatment (Fig. 20D and Fig. 21D): the higher number of M2 pro-resolving and the concomitant lower number of M1 during HFD in H3atKO mice suggested a possible tendency of KO mice to become more tolerant to an inflammatory stimulus as diet enriched in fat.
To sum up, fat-specific *Hdac3* inactivation recruits more monocytes; once they localize in adipose tissue, monocytes polarize mostly to M2 pro-resolving phenotype rather than M1 proinflammatory macrophages. Such trend suggests that H3atKO mouse is less prone to inflammation and it might exert protective effect against inflammation in adipose tissue upon feeding HFD.

We evaluated the innate immune population in the blood and in the spleen, another hematopoietic organ. In the spleen there were no significant differences, regarding number of monocytes, between groups of mice, thus excluding a possible extramedullary haematopoiesis driven by *Hdac3* gene inactivation (Fig. 21G). Also, in the blood there were not significant differences between mice with the same diet but different genotype (Fig. 21F). Interestingly, when we compared monocytes in blood at this time point and at 4 weeks of treatment, we found a general increased of monocytes during HFD, thus suggesting an exacerbation of inflammation given by the diet stimulus.
These results are in line with observations in mice at 4 weeks of diet, thus corroborating the finding that inflammation in adipose tissue originate within the tissue: after recruitment of myeloid cells, which might be from circulation or local proliferation, adipose tissue macrophages polarize preferentially towards M2.

5.2.3 Immune remodelling in H3atKO mice after 16 weeks of diet

We then asked how a prolonged period of diet affects the immune population of the adipose tissue. To answer this question, we exposed H3atKO and control mice to 16 weeks of low fat or HFD.

EpiWAT in H3atKO mice at LFD was significantly lower than in floxed mice, while at HFD the difference was still appreciable but not statistically significant (Fig. 22A).

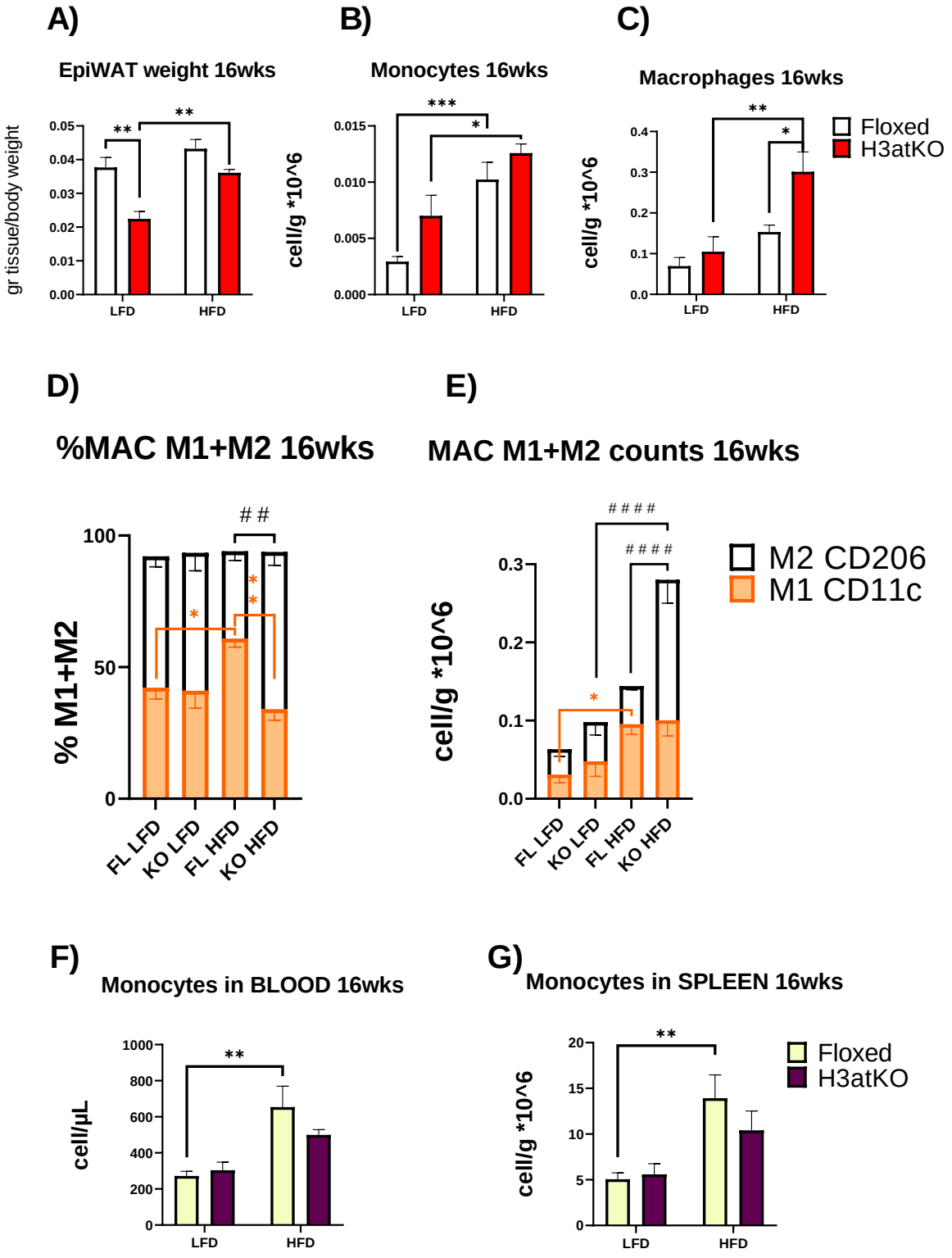

*Fig. 22 Changes in epiWAT weight and innate immune population after 16 weeks of diet. A) EpiWAT weight from H3atKO and Floxed mice (n=7-9 per group). B) Numbers of monocytes and C) macrophages in epiWAT (n=7-9 per group). D) Percentage of M2 and M1 macrophages in epiWAT and E) corresponding counts (n=7-9 per group). F) number of monocytes in H3atKO and Floxed mice in blood and G) analysis of monocytes in spleen (n=7-9 per group). Data are presented as mean ± s.e.m. Two-way ANOVA, Tukey as post hoc test *p< 0.05, **p< 0.01, ***p< 0.001, ****p< 0.0001.*

FACS analysis of immune cell populations in epiWAT revealed a trend similar to that observed at 4 and 9 weeks of diet, although with some differences. Monocytes and macrophages increased with HFD in H3atKO mice (Fig. 22B and C). Total macrophages were significantly higher in H3atKO mice compared to floxed mice, on HFD. The percentage of M2 macrophages in H3atKO mice was still higher than M1 but the difference between the two subsets was less pronounced compared to that observed at 4 and 9 weeks of diet consumption (Fig. 22D). Interestingly, the H3atKO mice were still able to maintain an higher ratio of M2/M1 when exposed to HFD, while in floxed mice fed HFD M1 macrophages were higher than M2 macrophages (Fig. 22D). These results suggest a possible protective role of *Hdac3* knock out against inflammation in visceral white adipose tissue.

FACS data from blood and spleen confirmed what previously observed in mice exposed to 4 or 9 weeks of diet. Within the same diet, there were no differences in terms of circulating monocytes between H3atKO and floxed mice (Fig. 22F). Same trend is found in the spleen (Fig. 22G). Monocytes, both in blood and spleen, showed increase in floxed mice on HFD compared to their controls on LFD Fig. 22F and G): this trend suggests inflammation because of prolonged challenge with high fat feeding. In fact, by comparing the number of circulating monocytes in floxed mice exposed to HFD through the different time point (4, 9, 16 weeks of diet) we noticed a general increase that reaches its maximum at 16 weeks of treatment (Fig. 20F, Fig. 21F, Fig. 22F).

5.2.4 Adaptive immune populations in H3atKO mice after 4, 9 and 16 weeks of diet

We also analysed the adaptive immunity during the same period of treatment. Interestingly we found no significant differences of $CD4^+$ and $CD8^+$ T lymphocytes in epididymal adipose tissue (Fig. 23A and B) and in blood either (Fig. 23C and D).

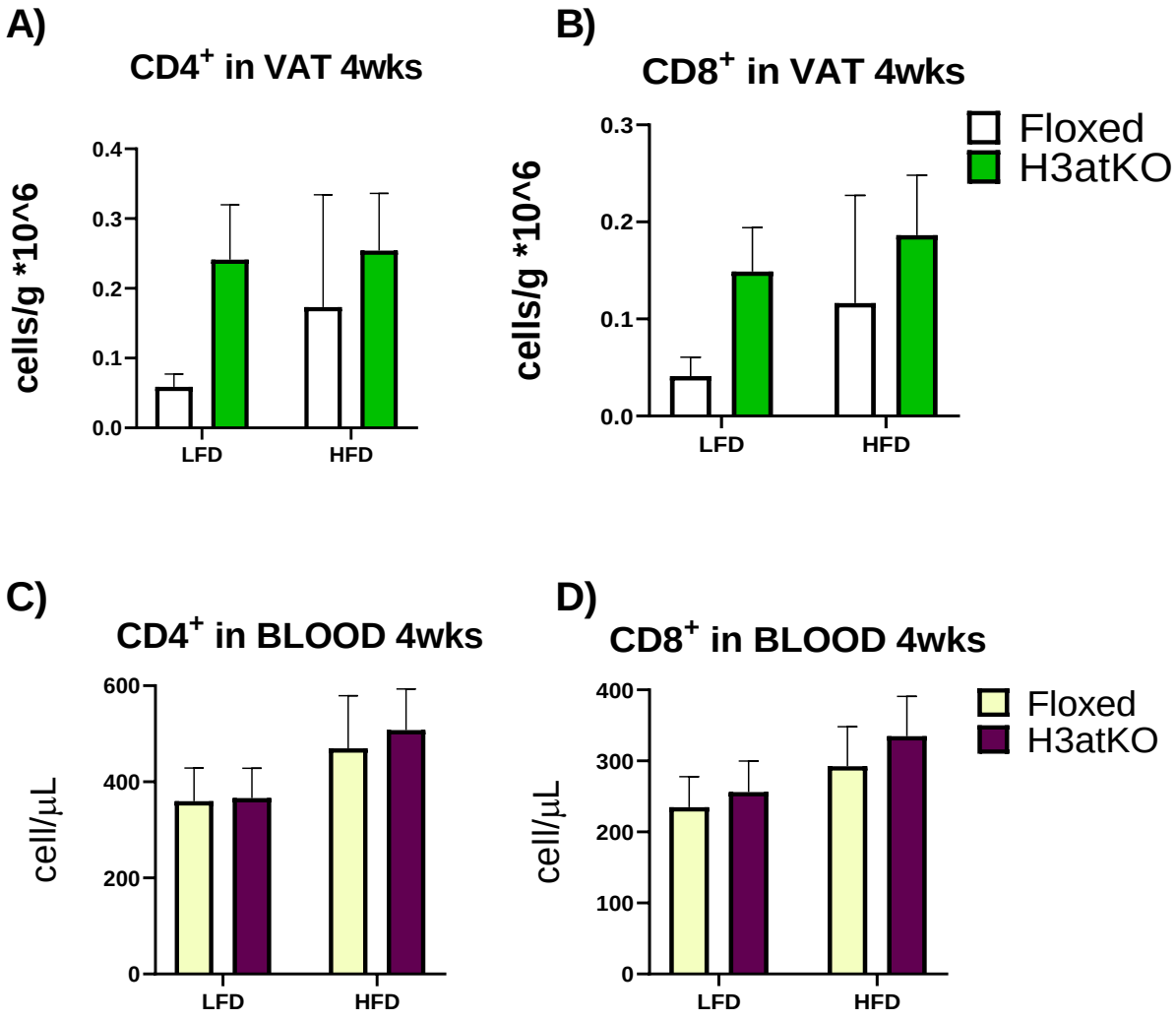

*Fig. 23 Adaptive immune population after 4 weeks of diet treatment. A) and B) represent CD4⁺ and CD8⁺ T lymphocytes counts in visceral adipose tissue. C) and D) represent CD4⁺ and CD8⁺ T lymphocytes in blood. (n=5 per group), data are presented as mean ± s.e.m. Two-way ANOVA, Tukey as post hoc test *p< 0.05, **p< 0.01, ***p< 0.001, ****p< 0.0001.*

Regarding T lymphocytes after 9 week of diet exposure, there were no differences in blood and in visceral WAT (Fig. 24), except for an increase number of $CD8^+$ T cells in epiWAT of H3atKO mice treated with high fat diet (Fig. 24B).

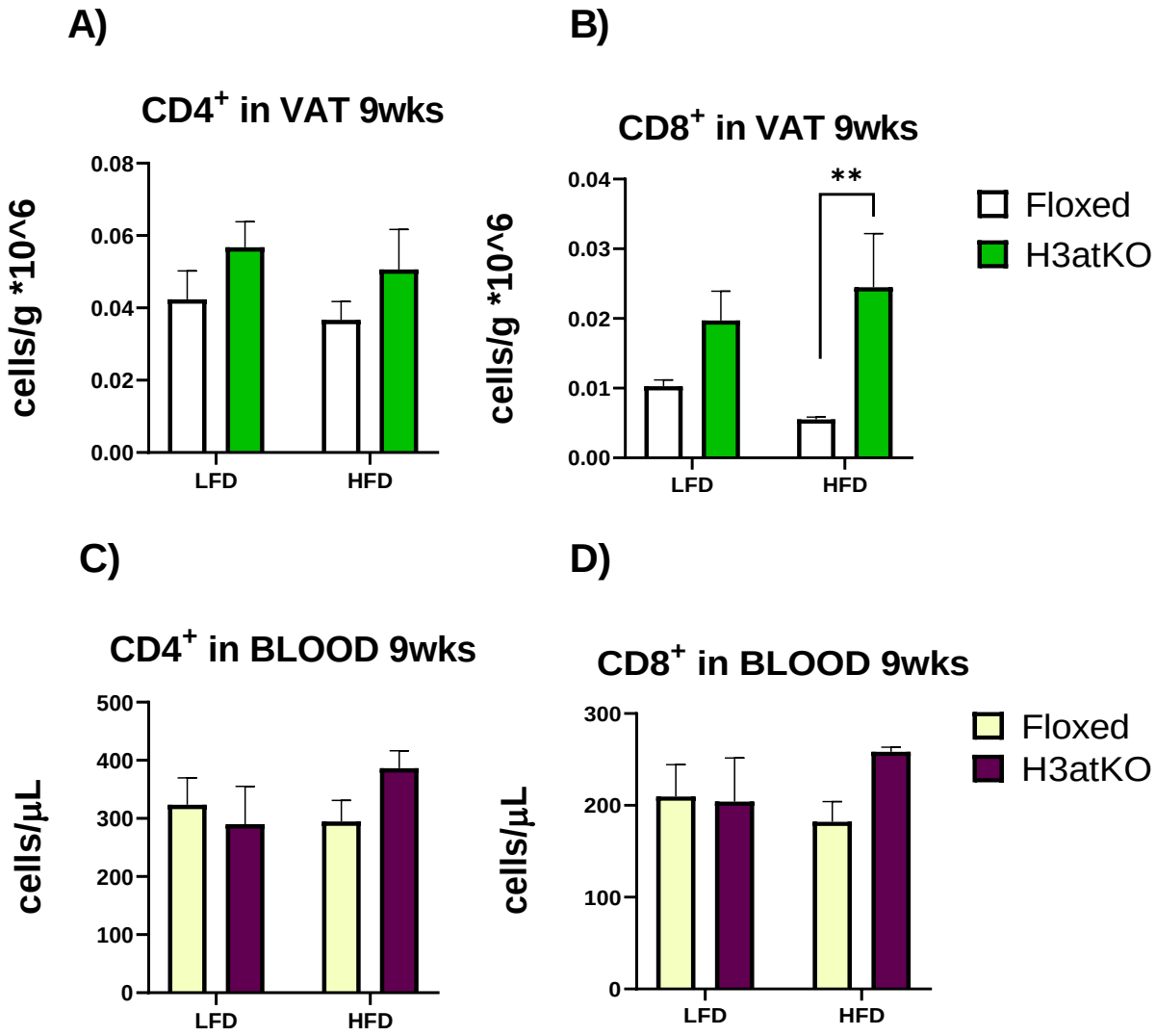

*Fig. 24 Adaptive immune population after 9 weeks of diet treatment. A) and B) represent CD4⁺ and CD8⁺ T lymphocytes counts in visceral adipose tissue. C) and D) represent CD4⁺ and CD8⁺ T lymphocytes in blood. (n=5-8 per group), data are presented as mean ± s.e.m. Two-way ANOVA, Tukey as post hoc test *p< 0.05, **p< 0.01, ***p< 0.001, ****p< 0.0001.*

Finally, adaptive immune population did not show any significant variations in different groups of mice exposed to diet for 16 weeks (Fig. 25).

Overall, our results suggest no major differences of the adaptive immune systems between the genotypes and different diet regimens.

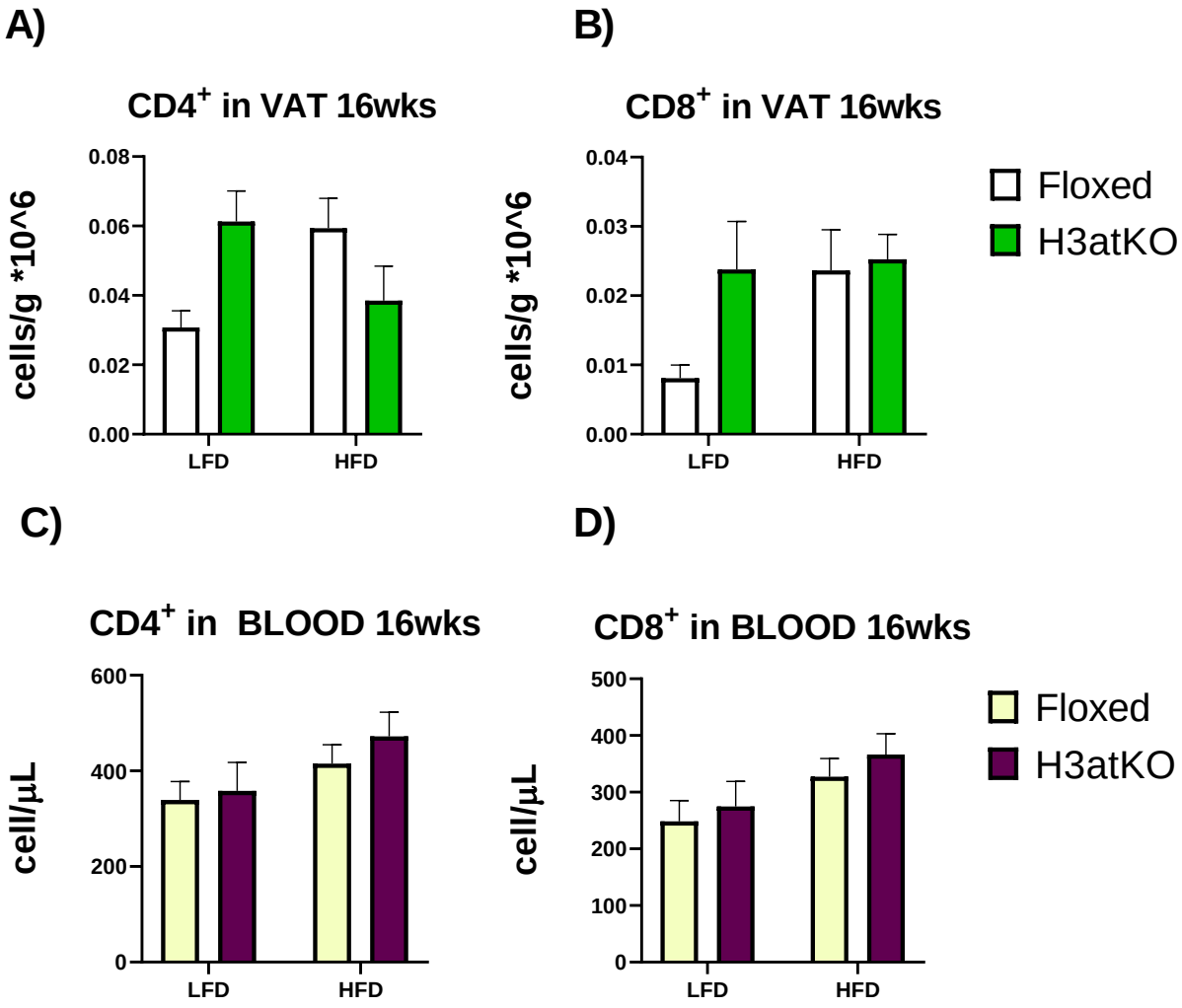

*Fig. 25 Adaptive immune population after 16 weeks of diet treatment. A) and B) represent CD4⁺ and CD8⁺ T lymphocytes counts in visceral adipose tissue. C) and D) represent CD4⁺ and CD8⁺ T lymphocytes in blood. (n=7-9 per group), data are presented as mean ± s.e.m. Two-way ANOVA, Tukey as post hoc test *p< 0.05, **p< 0.01, ***p< 0.001, ****p< 0.0001.*

5.3 Transcriptomic and Epigenomic analysis

Early events at the epigenomic level are crucial for altering the regulation of genome and determining the downstream mechanisms. In our model, the identification of early events following *Hdac3* ablation would be fundamental to understand the trigger driving subsequent effects. For this reason, we performed transcriptomic and epigenomic analysis on H3atKO mice and floxed littermates at 8 weeks age that were fed LFD or HFD for the following 4 weeks.

Since HDAC3 is an epigenomic modifier that regulates gene expression we performed RNA sequencing in subcutaneous inguinal WAT (subWAT). We chose subWAT because previous results from our group indicated that the major effects of HDAC3 KO occur in this fat depot. These analyses were paralleled

and integrated by chromatin immunoprecipitation followed by deep sequencing (ChIP-seq), to understand how HDAC3 drives transcription through epigenetic mechanism. As a read-out of HDAC3 activity we evaluated histone acetylation (H3K27ac), a marker of active enhancers and promoters. We considered hypo- and hyper-acetylated regions within a cut off of 100kb from transcription start site (TSS) of genes.

The dataset was composed of 4 experimental groups (see table below), each condition had 3 or 2 replicates made of pools of animals. The initial experimental setting included 3 pools of animals per group; however, following analysis led us to exclude pool 12 from group 4, due to quality issues.

Group 1: Floxed + LFD 4 wks			Group 2: KO + LFD 4 wks			Group 3: Floxed + HFD 4 wks			Group4: KO+HFD 4wks	
POOL NUMBER			POOL NUMBER			POOL NUMBER			POOL NUMBER	
1	2	3	4	5	6	7	8	9	10	11

The heatmap built with all analysed genes revealed a proper hierarchical clustering, thus confirming that samples were homogeneous. Moreover, we noticed a clear difference between genotype while the effect of the diet was not as strong. In fact, a slight difference was noticed when comparing floxed LFD mice vs floxed HFD. It is possible that KO model, after a short period of diet (i.e., 4 weeks), is still able to buffer the effects of HFD thus maintaining its phenotypic features (Fig. 26).

Pathway enrichment analysis was performed for the following comparisons: FL HFD vs FL LFD and KO LFD vs FL LFD, respectively (Fig. 27).

In H3atKO mice fed LFD we found upregulation of pathways regarding fatty acids metabolism, oxidative phosphorylation, citrate cycle, thermogenesis, fatty acids biosynthesis. This was in line with already published observations regarding our KO model, that is characterized by a futile cycle of simultaneous FA synthesis and β-oxidation (Alessandra Ferrari *et al.*, 2017).

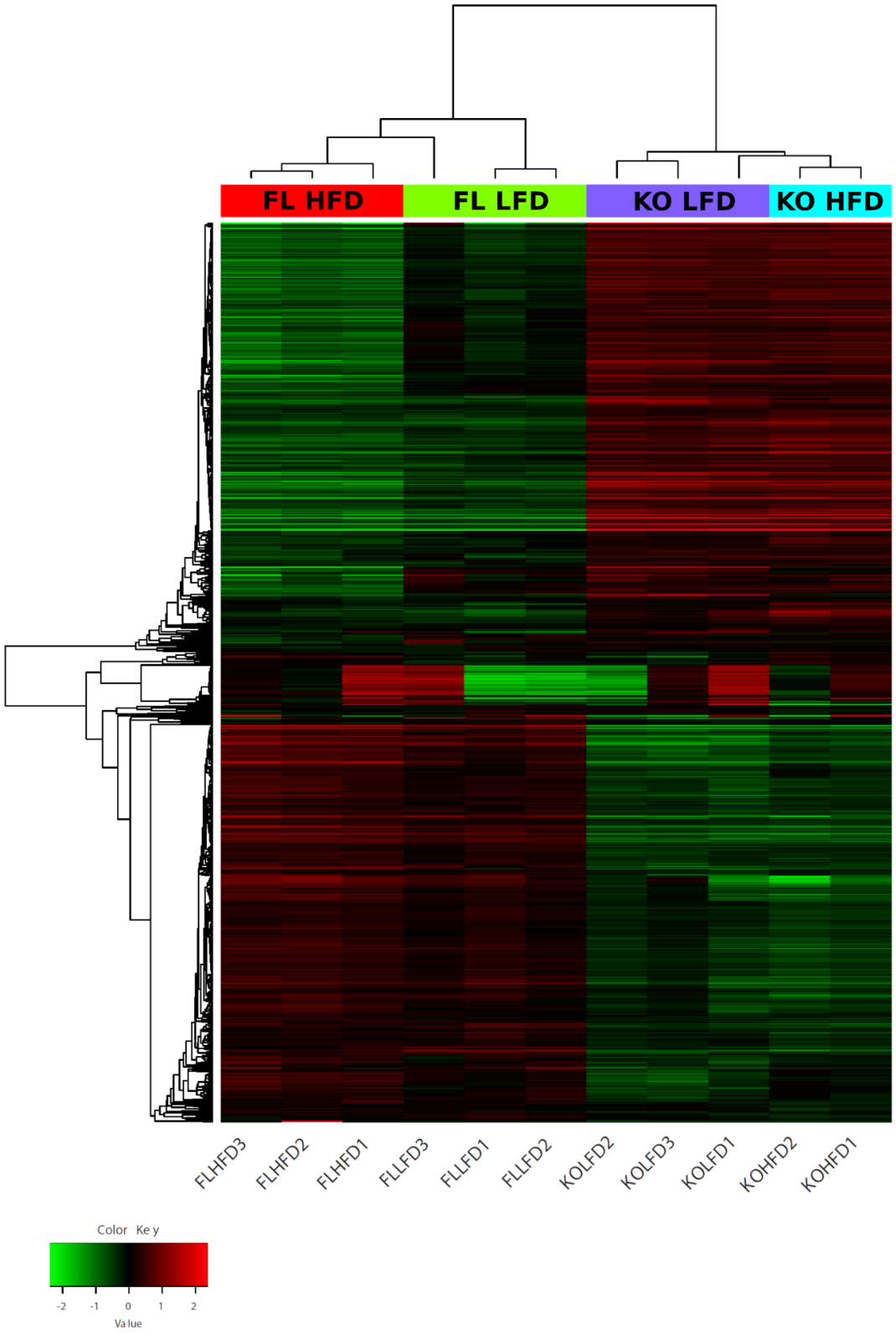

Fig. 26: Heatmap of RNA-seq analysed genes.

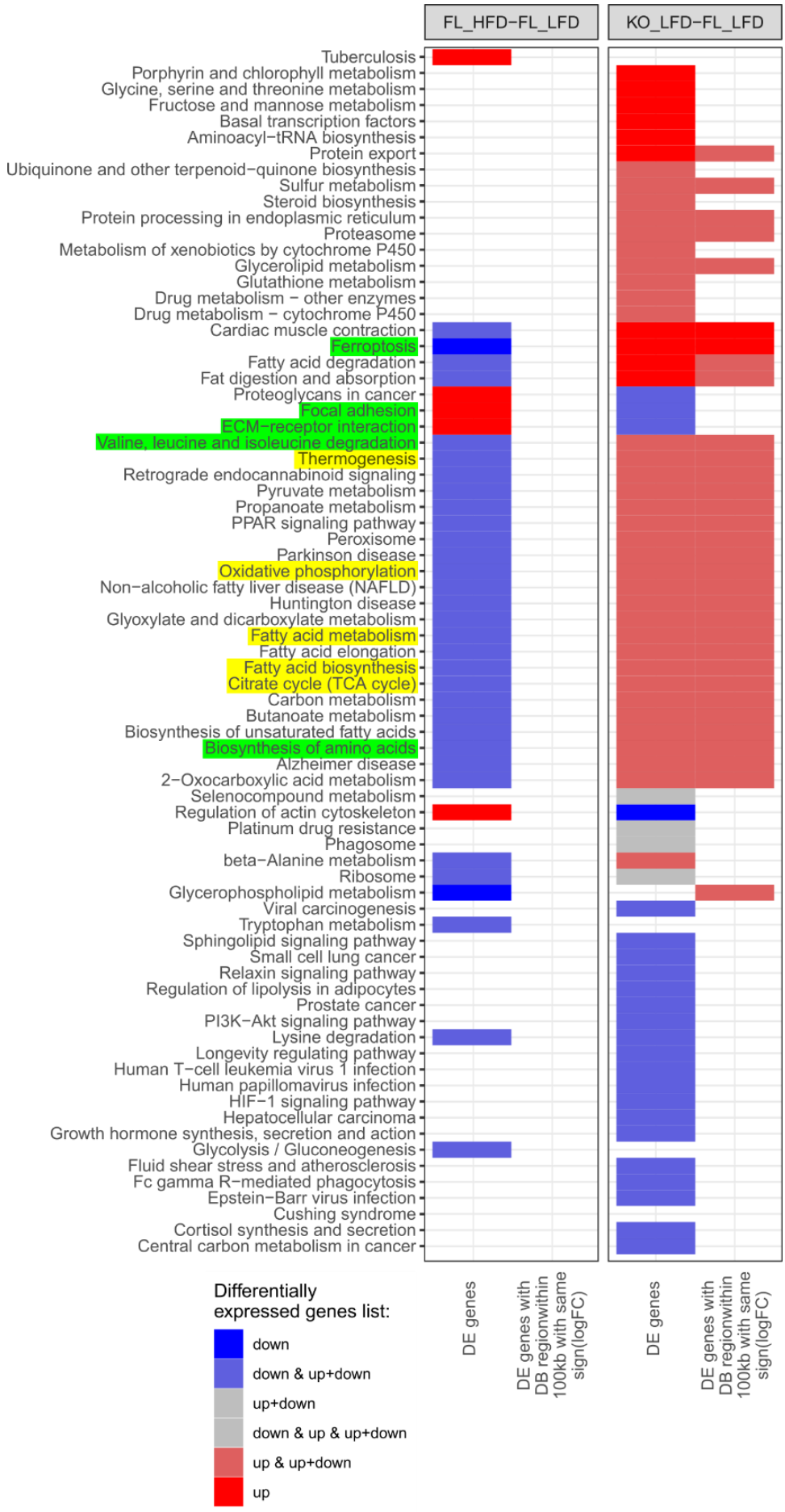
FL_HFD−FL_LFD
KO_LFD−FL_LFD
Tuberculosis
Porphyrin and chlorophyll metabolism
Glycine, serine and threonine metabolism
Fructose and mannose metabolism
Basal transcription factors
Aminoacyl−tRNA biosynthesis
Protein export
Ubiquinone and other terpenoid−quinone biosynthesis
Sulfur metabolism
Steroid biosynthesis
Protein processing in endoplasmic reticulum
Proteasome
Metabolism of xenobiotics by cytochrome P450
Glycerolipid metabolism
Glutathione metabolism
Drug metabolism − other enzymes
Drug metabolism − cytochrome P450
Cardiac muscle contraction
Ferroptosis
Fatty acid degradation
Fat digestion and absorption
Proteoglycans in cancer
Focal adhesion
ECM−receptor interaction
Valine, leucine and isoleucine degradation
Thermogenesis
Retrograde endocannabinoid signaling
Pyruvate metabolism
Propanoate metabolism
PPAR signaling pathway
Peroxisome
Parkinson disease
Oxidative phosphorylation
Non−alcoholic fatty liver disease (NAFLD)
Huntington disease
Glyoxylate and dicarboxylate metabolism
Fatty acid metabolism
Fatty acid elongation
Fatty acid biosynthesis
Citrate cycle (TCA cycle)
Carbon metabolism
Butanoate metabolism
Biosynthesis of unsaturated fatty acids
Biosynthesis of amino acids
Alzheimer disease
2−Oxocarboxylic acid metabolism
Selenocompound metabolism
Regulation of actin cytoskeleton
Platinum drug resistance
Phagosome
beta−Alanine metabolism
Ribosome
Glycerophospholipid metabolism
Viral carcinogenesis
Tryptophan metabolism
Sphingolipid signaling pathway
Small cell lung cancer
Relaxin signaling pathway
Regulation of lipolysis in adipocytes
Prostate cancer
PI3K−Akt signaling pathway
Lysine degradation
Longevity regulating pathway
Human T−cell leukemia virus 1 infection
Human papillomavirus infection
HIF−1 signaling pathway
Hepatocellular carcinoma
Growth hormone synthesis, secretion and action
Glycolysis / Gluconeogenesis
Fluid shear stress and atherosclerosis
Fc gamma R−mediated phagocytosis
Epstein−Barr virus infection
Cushing syndrome
Cortisol synthesis and secretion
Central carbon metabolism in cancer
DE genes
DE genes with DB regionwithin 100kb with same sign(logFC)
DE genes
DE genes with DB regionwithin 100kb with same sign(logFC)
Differentially expressed genes list:
down
down & up+down
up+down
down & up & up+down
up & up+down
up

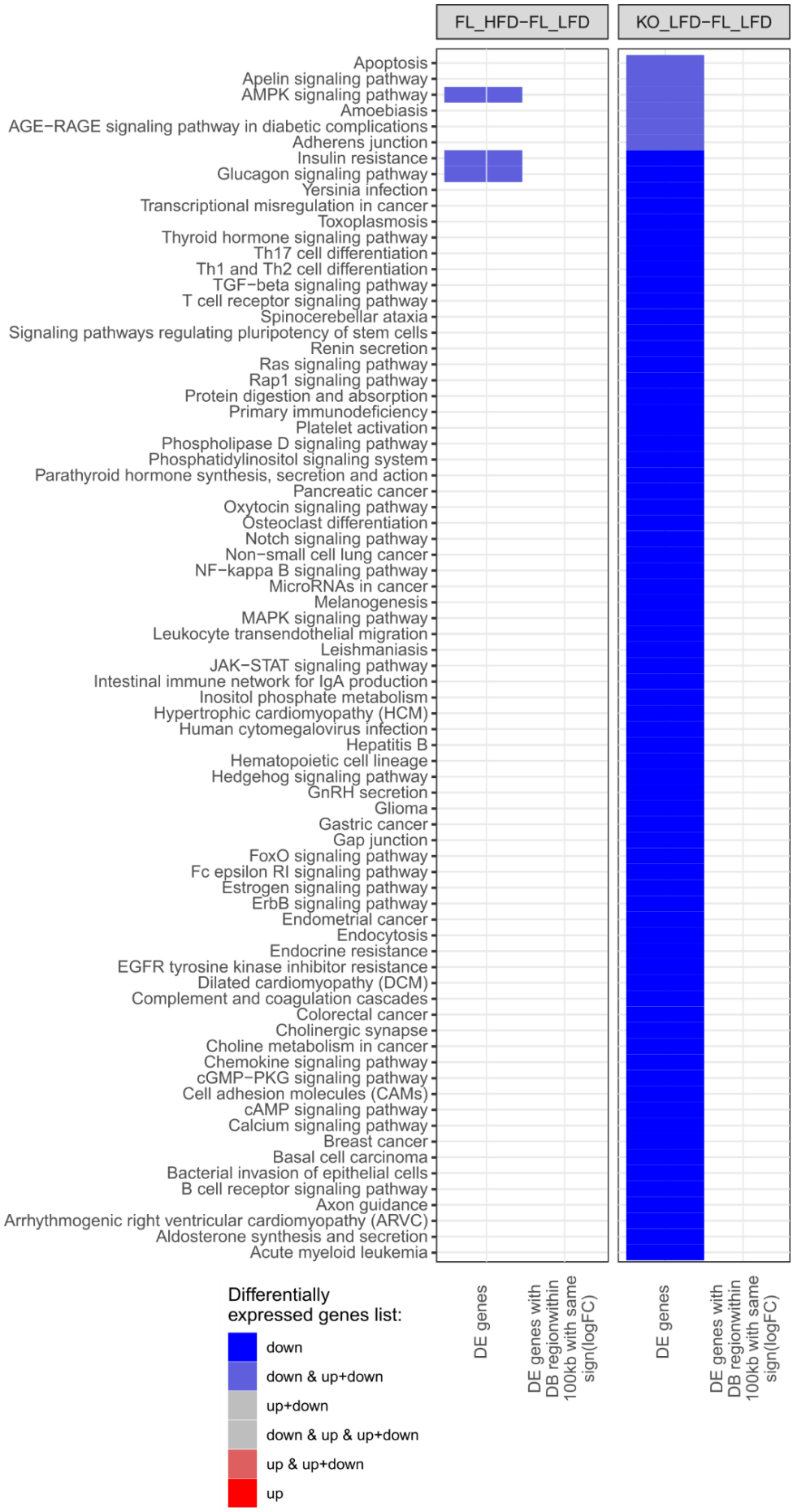
FL_HFD−FL_LFD
KO_LFD−FL_LFD
Apoptosis
Apelin signaling pathway
AMPK signaling pathway
Amoebiasis
AGE−RAGE signaling pathway in diabetic complications
Adherens junction
Insulin resistance
Glucagon signaling pathway
Yersinia infection
Transcriptional misregulation in cancer
Toxoplasmosis
Thyroid hormone signaling pathway
Th17 cell differentiation
Th1 and Th2 cell differentiation
TGF−beta signaling pathway
T cell receptor signaling pathway
Spinocerebellar ataxia
Signaling pathways regulating pluripotency of stem cells
Renin secretion
Ras signaling pathway
Rap1 signaling pathway
Protein digestion and absorption
Primary immunodeficiency
Platelet activation
Phospholipase D signaling pathway
Phosphatidylinositol signaling system
Parathyroid hormone synthesis, secretion and action
Pancreatic cancer
Oxytocin signaling pathway
Osteoclast differentiation
Notch signaling pathway
Non−small cell lung cancer
NF−kappa B signaling pathway
MicroRNAs in cancer
Melanogenesis
MAPK signaling pathway
Leukocyte transendothelial migration
Leishmaniasis
JAK−STAT signaling pathway
Intestinal immune network for IgA production
Inositol phosphate metabolism
Hypertrophic cardiomyopathy (HCM)
Human cytomegalovirus infection
Hepatitis B
Hematopoietic cell lineage
Hedgehog signaling pathway
GnRH secretion
Glioma
Gastric cancer
Gap junction
FoxO signaling pathway
Fc epsilon RI signaling pathway
Estrogen signaling pathway
ErbB signaling pathway
Endometrial cancer
Endocytosis
Endocrine resistance
EGFR tyrosine kinase inhibitor resistance
Dilated cardiomyopathy (DCM)
Complement and coagulation cascades
Colorectal cancer
Cholinergic synapse
Choline metabolism in cancer
Chemokine signaling pathway
cGMP−PKG signaling pathway
Cell adhesion molecules (CAMs)
cAMP signaling pathway
Calcium signaling pathway
Breast cancer
Basal cell carcinoma
Bacterial invasion of epithelial cells
B cell receptor signaling pathway
Axon guidance
Arrhythmogenic right ventricular cardiomyopathy (ARVC)
Aldosterone synthesis and secretion
Acute myeloid leukemia
DE genes
DE genes with DB regionwithin 100kb with same sign(logFC)
DE genes
DE genes with DB regionwithin 100kb with same sign(logFC)
Differentially expressed genes list:
down
down & up+down
up+down
down & up & up+down
up & up+down
up

Fig. 27: Summary of pathway enrichment analysis using Over Representation Analysis (ORA). Left and right panels show the results obtained with the comparison FL HFD vs FL LFD and KO LFD vs FL LFD, respectively. The first column in each panel shows results obtained with the lists of differentially expressed genes (ignoring K27ac ChIP-seq results). The second column show results obtained by considering the list of differentially expressed genes within 100kb of a differential H3K27ac binding region changing in the same direction. Blu and red denotes down or upregulated genes respectively, when expression/enrichment do not go in the same direction (i.e. the pathway is mostly upregulated, but some genes are downregulated) the colour is softened. In yellow: pathway regarding futile cycle of FAs β-oxidation and synthesis. In green: pathways debated in this thesis.

With the previous findings confirmed, we considered other enriched pathways that were altered both in KO_LFD vs FL_LFD and in FL_HFD vs FL_LFD, with the aim to fully explore the consequences of *Hdac3* ablation. We found upregulation of pathways such as ferroptosis (Fig. 28), a form of programmed cell death induced by iron (*Tal Hirschhorn and Brent R. Stockwell 2019*), while focal adhesion and extracellular receptor interaction were downregulated in KO_LFD vs FL_LFD (Fig. 29).

Interestingly, in H3atKO mice we found upregulation of biosynthesis of amino acids and valine, leucine and isoleucine degradation pathways. Their simultaneous upregulation led us to speculate a possible futile cycle of amino acids degradation and concomitant synthesis: this process might feed the already established futile cycle of *de novo* lipogenesis and fatty acid β-oxidation that occurs in H3atKO mice.

Notably, when we compared floxed mice fed HFD with floxed mice fed LFD, these pathways were regulated in the opposite manner (Fig. 27),

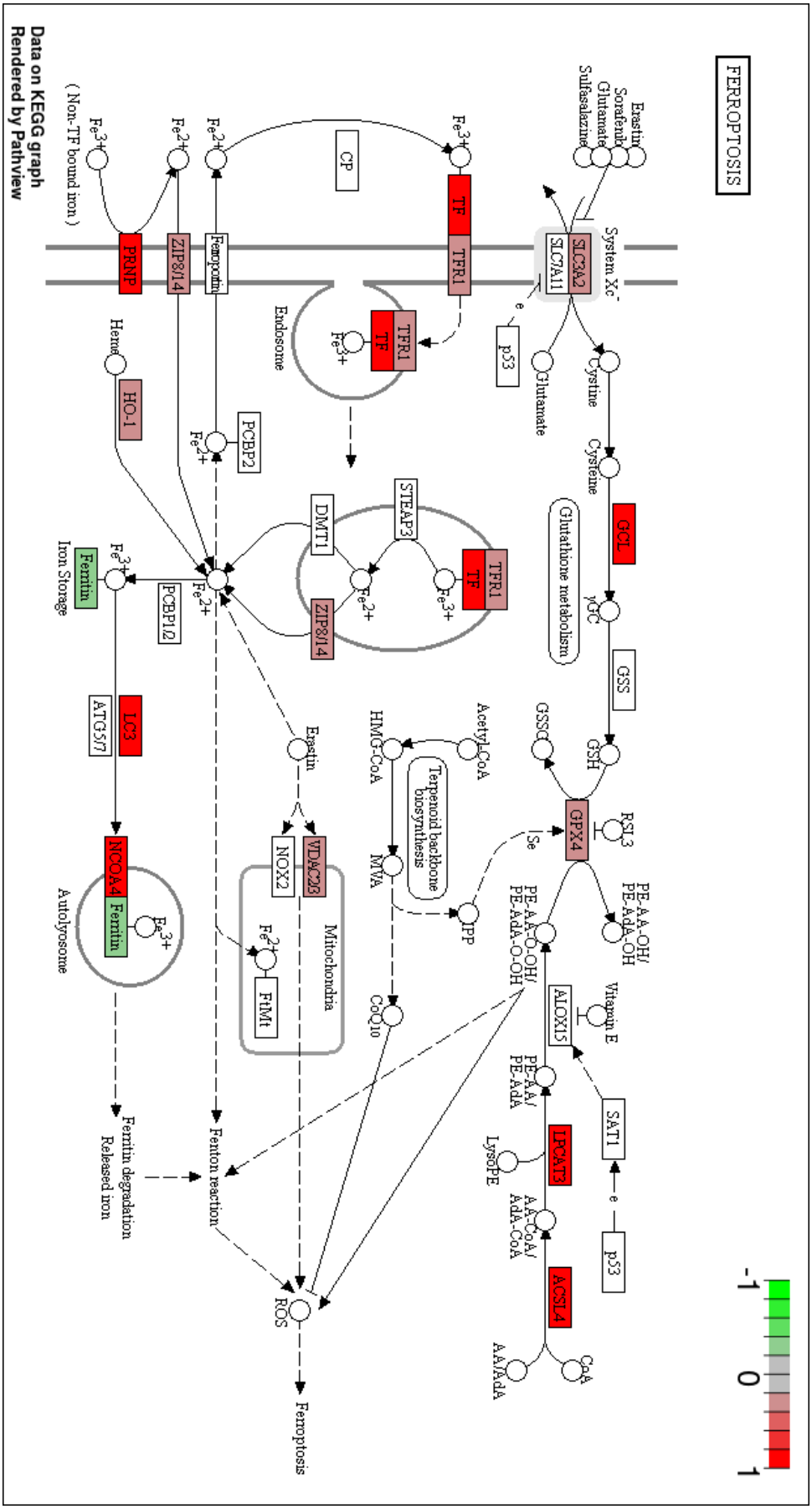

Fig. 28: KEGG Pathway of Ferroptosis

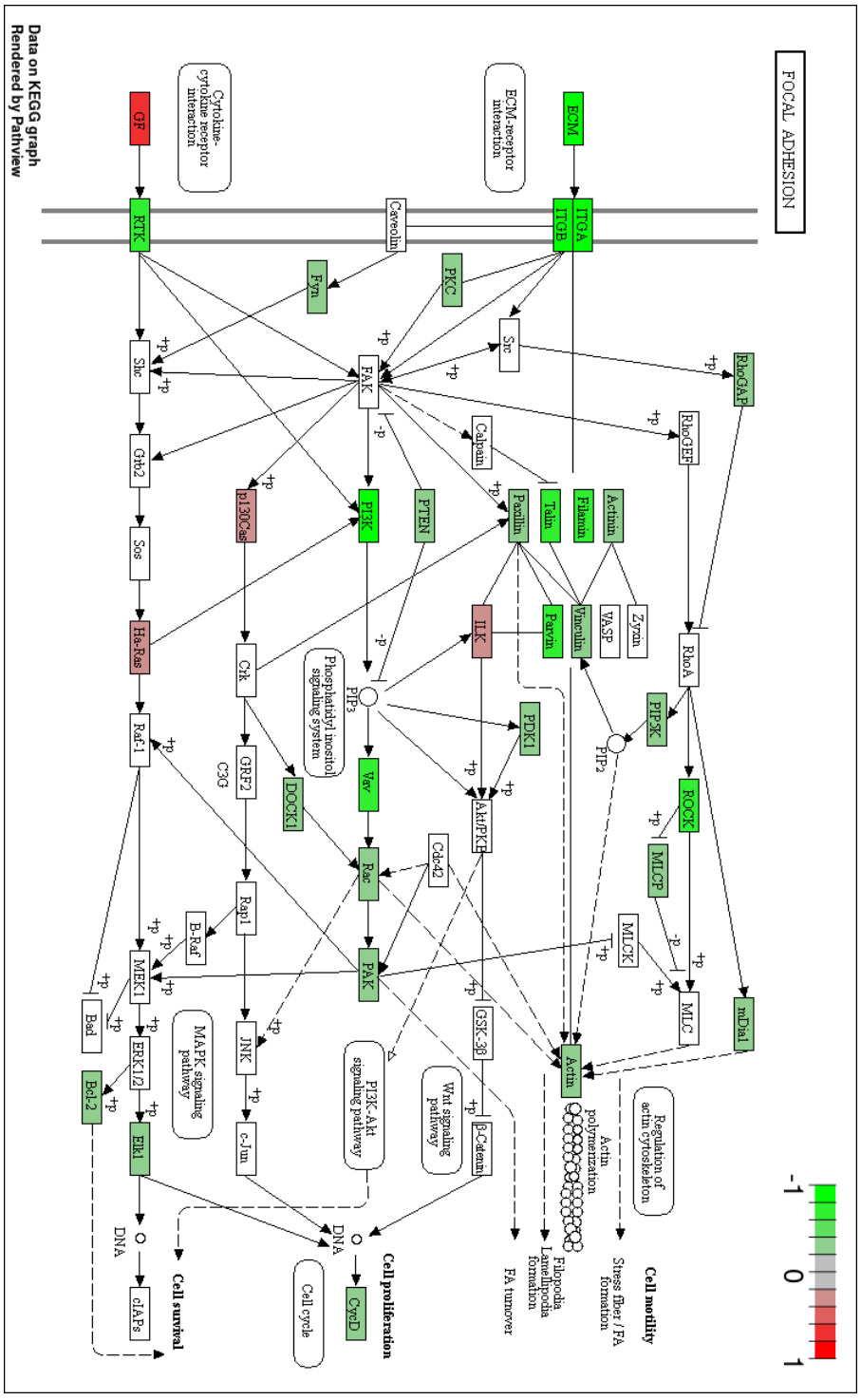

Fig. 29: KEGG Pathway of Focal adhesion

We then built Volcano plot representing all analysed genes (Fig. 30): interestingly, we found two top downregulated genes neuronatin (*Nnat*) and mesoderm specific transcript (*Mest*). Previous investigations reported that, in analogy with *H3atKO* mice, loss of *Nnat* promotes browning in primary murine adipocytes (Gburcik, Cleasby and Timmons, 2013).

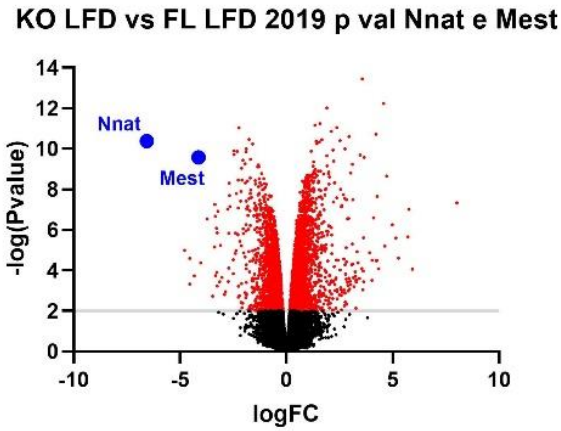

Fig. 30: Volcano Plot representing genes from RNA-seq analysis.

Analysis performed using IGV (Integrative Genomics Viewer) software revealed that, within -38,778 kb upstream *Nnat* transcription start site (TSS), there is an hypoacetylated region (around 3 kb) in KO_LFD vs. FL_LFD mice. These findings regarding changes in acetylation status in regions upstream TSS of *Nnat* gene suggest a possible involvement of *Nnat* in the phenotype of H3atKO mice. However, further analysis concerning HDAC3 and NNAT mechanism are needed.

On the other hand, comparison regarding FL_LFD vs. FL_HFD showed a hyperacetylation status just for sample FL_HDF_7, while in other mice on HFD the hyperacetylation was not substantial, probably because the diet stimulus was still attenuated. However, the significance can be appreciated looking at omic data (FDR 0,0086).

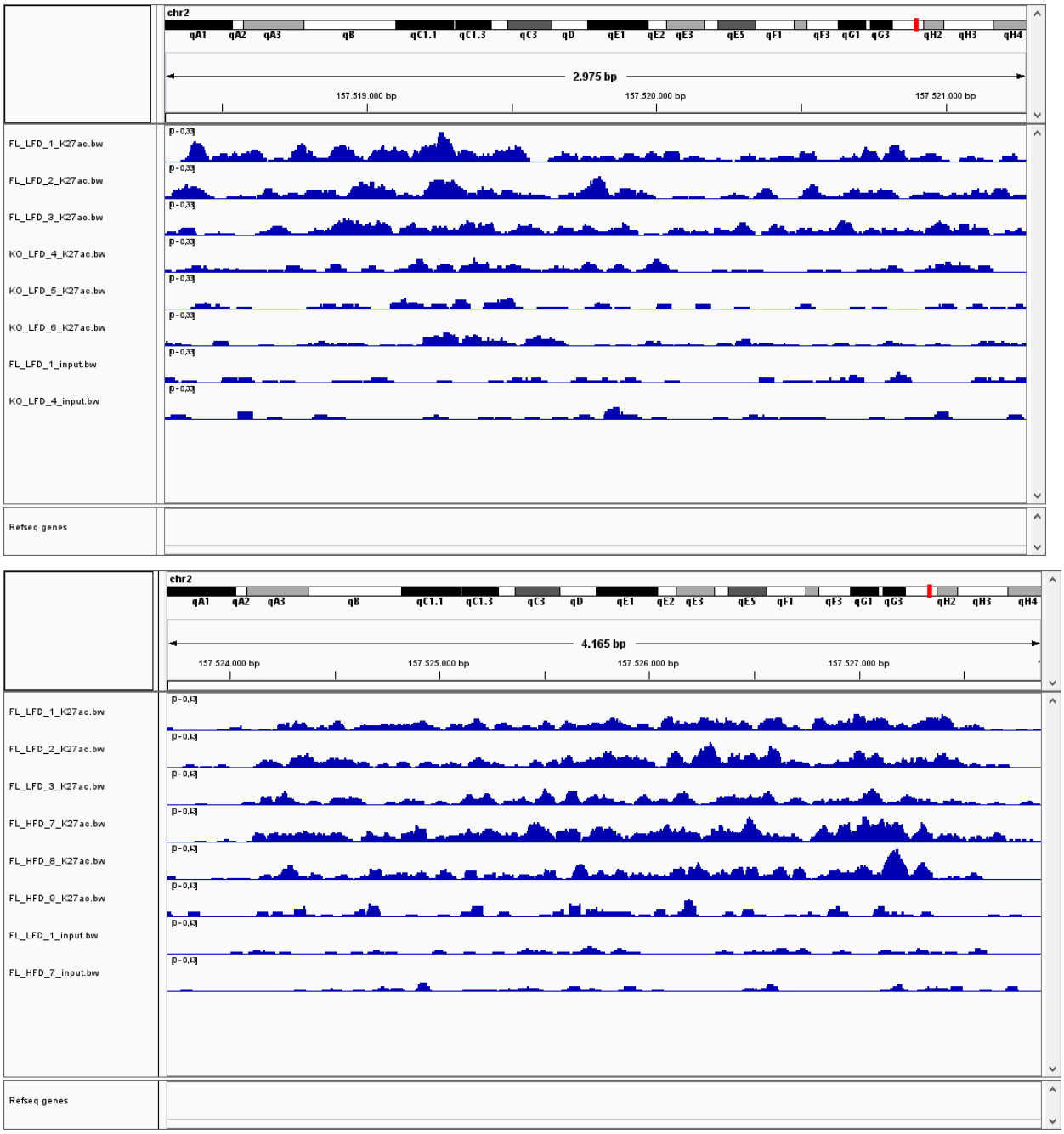

Fig. 31 From the top: figures obtained using Integrative Genomics Viewer (IGV) of the hypoacetylated and hyperacetylated region upstream Nnat TSS.

6 DISCUSSION

6.1 Class I HDACs inhibition during adipocyte differentiation promotes an imprinting towards oxidative and brown-like phenotype

The role of HDACs in adipocyte differentiation and functionality is not completely understood. In this thesis it is shown how class I HDACs is involved in the initial steps of adipocyte differentiation and in determining the achievement of brown-like phenotype.

Previous *in vitro* results obtained in our laboratory showed that inhibition of class I HDACs in the early phases of adipocyte differentiation led to changes in cell morphology and gene expression. Cells appeared multilocular, with increased expression of genes belonging to adipocyte functionality (*Pparg, Plin, Fabp4, Adipoq, Glut4, Cebpa*), lipolysis (*Cd36, Lpl, Lipe, Atgl*) and fatty acid β-oxidation (*Cpt1b, Acadl, Acadm, Hdha, Ppara*). Complementary analysis of gene expression showed in this thesis, reported high mitochondrial activity that, together with increased expression of *Ppara,* is frequently associated to a brown-like phenotype. In fact, adipocytes precursors exposed to MS-275 at the beginning of the differentiation program showed increased expression of browning markers such as *Ucp1*, *Adrbr3*, *Cidea*, *Elovl3*. Notably, changes in cell morphology were not appreciable when we treated terminally differentiated adipocytes. Moreover, the effects on oxidative genes were moderate and within BAT markers only *Ucp1* and *Elovl3* were upregulated, suggesting that class I HDACs I might directly influence these genes. However, the sole increased expression of *Ucp1* and *Elovl3* is not sufficient for the onset of browning since other markers of that pathway were not upregulated. Moreover, in fully differentiated cells, genes belonging to lipolysis such as *Lipe* and *Atgl* were decreased and it is known that UCP1 needs free fatty acids for its functioning (Fedorenko, Lishko and Kirichok, 2012) . This means that the machinery for thermogenesis is ready, however, the increase of *Ucp1* is not sufficient for the establishment of a brown phenotype. Altogether these findings emphasize the high flexibility of the epigenome during the early phases of adipocyte differentiation: we speculate that changes in these stages can strongly affect the fate of the precursors that are imprinted towards an elevated oxidative and brown-like phenotype. Conversely, when the cells have already completed the key differentiation steps, as in terminally differentiating adipocytes, HDACs inhibition and the possible epigenome modifications result less dramatic changes of adipocyte phenotype.

Moreover, by investigating the molecular mechanisms underlying the effects of MS-275, we found increased H3K27 acetylation on enhancers of *Ucp1* and of *Pparg*, mirrored by the increased expression of these two genes. It is known that hyperacetylation of *Ucp1* enhancers is found in brown adipocytes (Abe *et al.*, 2015). In addition, it can be possible that *Pparg* acts synergistically in determining high expression of *Ucp1* and in brown-like phenotype. In fact, it has been reported that ligand-activated PPARγ promotes the *Ucp1* gene expression (Petrovic *et al.*, 2010).

Based on our results, we infer that the H3K27 hyperacetylation of *Pparg* enhancer is the key event leading to the acquirement of a brown-like phenotype. At this regard, it has been shown that within the first hours of differentiation program there is a reorganization of promoter-anchored chromatin loops with concomitant reprogramming of enhancers activity, with changes in H3K27ac and gene expression (Siersbæk *et al.*, 2017). Reprogramming of chromatin is critical in determining the fate of precursor cells: here, we also showed that the inhibition of HATs, the counterparts of HDACs, with garcinol resulted in the phenotype opposite to that observed with HDACs inhibition. These findings are in line with experiments performed in 3T3-L1 cells where garcinol inhibit cell proliferation ad adipogenesis (Hsu *et al.*, 2012). Previous studies performed in our laboratory in H3atKO mice, showed increased expression of ATP-citrate lyase (*Acly),* which converts citrate into acetyl-CoA and oxaloacetate outside mitochondrial matrix: this enzyme plays an important role in epigenome modifications since it provides acetyl-CoA for histone acetylation in the nucleus (Ferrari *et al.*, 2017). In parallel, the *in vitro* inhibition of HDACs with MS-275 reported in this thesis, by increasing the expression *of Acly,* is expected to increase the amount of acetyl groups for chromatin acetylation in specific regions; this phenomenon positively correlates with adipocyte differentiation. Therefore, we speculate that inhibition of HAT with garcinol could affect the availability of acetyl groups thus leading to negative effects for differentiation. We also showed that MS-275 treatment led to an oxidative phenotype: we speculate that cells carry out an oxidative metabolism to sustain the high energy demand necessary for thermogenesis by producing the reduced coenzymes NADH and $FADH_2$ required to generate the proton gradient across the inner mitochondrial membrane. It is possible that the establishment of an oxidative metabolism is mirrored by increased acetylation of putative enhancer regions regulating the transcription of *Ppara* gene, although this should be confirmed by ChIP experiments.

Results obtained here further elucidated the role of class I HDACs in adipocyte differentiation: in fact, we demonstrated that inhibition of class I HDACs in adipocytes precursors promotes browning and oxidative metabolism. Early modifications on the epigenome determine the fate of pre-adipocytes (Fig. 32).

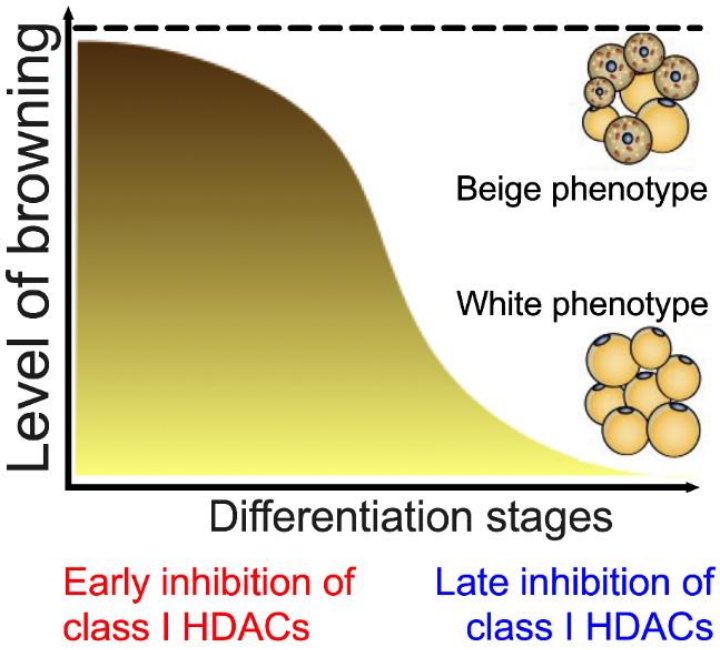

Fig. 32 Summary of the effects class I HDACs inhibition during different stages of differentiation program.

6.2 *Hdac3* ablation in white adipose tissue promotes immune populations remodeling.

Once obesity develops, adipose tissue becomes dysfunctional leading to ectopic fat accumulation in different depots such as the visceral WAT. These changes lead to inflammation and immune populations play an important role in the pathology evolution (Chait and den Hartigh, 2020). Immune cells are already present in non-pathological states, however upon onset of obesity several immune cells, like macrophages, infiltrate in WAT (Weisberg *et al.*, 2003). For this reason, understanding how immune populations change during obesity would be fundamental to gain more insights regarding obesity related disorders. In this thesis, it is reported how cells belonging to innate and adaptive immunity change after exposure to an inflammatory stimulus like the high fat diet. H3atKO and control mice were exposed to diet for three different periods. Firstly, we chose a short period as 4 weeks of treatment, to pinpoint the early changes within immune cell populations with the early onset of inflammation. Then, the second time point was settled to 9 weeks, when inflammation induced by high fat diet feeding should be more evident (Yamashita *et al.*, 2005) (Heydemann, 2016). Finally, the third period of diet was prolonged until 16 weeks of diet, when the effects of HFD should be fully established.

The number of total macrophages significantly increased in epiWAT of H3atKO mice compared to floxed mice on HFD in all three time points. At this regard, we hypothesized that adipocyte

inflammation is not a process necessarily detrimental for adipose tissue. ATMs, by surrounding dead adipocytes in crown-like structures, may promote clearance of dying-adipocytes and consequent renewal (Asterholm *et al.*, 2014). Accordingly, the increased number of total macrophages in H3atKO mice fed HFD might promote this mechanism.

Moreover, when we looked at macrophage subsets such as the canonical M1-proinflammatory and M2-pro-resolving macrophages, we found that mice lacking *Hdac3* were able to maintain a higher ratio of M2 vs M1 macrophages during HDF feeding. Such feature could support a pro-resolving inflammatory process. At longer HFD feeding, this tendency is maintained as the percentage of M2 macrophages is higher at 4 through 16 weeks of HFD feeding. However, after 16 weeks of HFD, M1 macrophages increased also in H3atKO mice, most likely because of prolonged challenge with HFD. We predict that in the long term, such increase of M1 macrophages could lead to dysfunctional adipose tissue also in H3atKO mice and may contribute to the lack of protection from insulin resistance previously reported in H3atKO mice fed HFD for longer period (Alessandra Ferrari *et al.*, 2017).

Normally, HFD feeding promotes the recruitment of classically-activated M1 macrophages, thus disadvantaging inflammation resolution (Lumeng *et al.*, 2007). Here we proposed a model whereby *Hdac3* ablation is able to maintain a higher ratio of M2/M1 macrophages until 16 weeks of treatment, thus possibly supporting a pro-resolving mechanism upon HFD in H3atKO mice.

Upon HFD administration, we also observed a trend towards increased monocytes in blood of both floxed and H3atKO mice from 4 through 16 weeks, thus demonstrating that the inflammatory response is evoked by the diet. This trend might lead to increase recruitment of monocytes/macrophages in the adipose tissue from the systemic circulation. However, we are not able to conclude whether increased number of macrophages in epiWAT belonging to H3atKO mice fed at HFD, derives from local proliferation or migration of circulating monocytes. In fact, it is known that local proliferation is responsible of ATM accumulation as well, especially at the obesity onset (Zheng *et al.*, 2016). Therefore, we speculate that initially macrophages proliferate locally: as inflammation proceeds, adipose tissue also recruits monocytes from the blood. Once in situ, they preferentially polarize towards a M2 pro-resolving phenotype rather than M1 pro-inflammatory macrophages.

Finally, it is worth to note that the most significant changes we observed were in cell populations of the innate immunity rather than the adaptive immune cells.

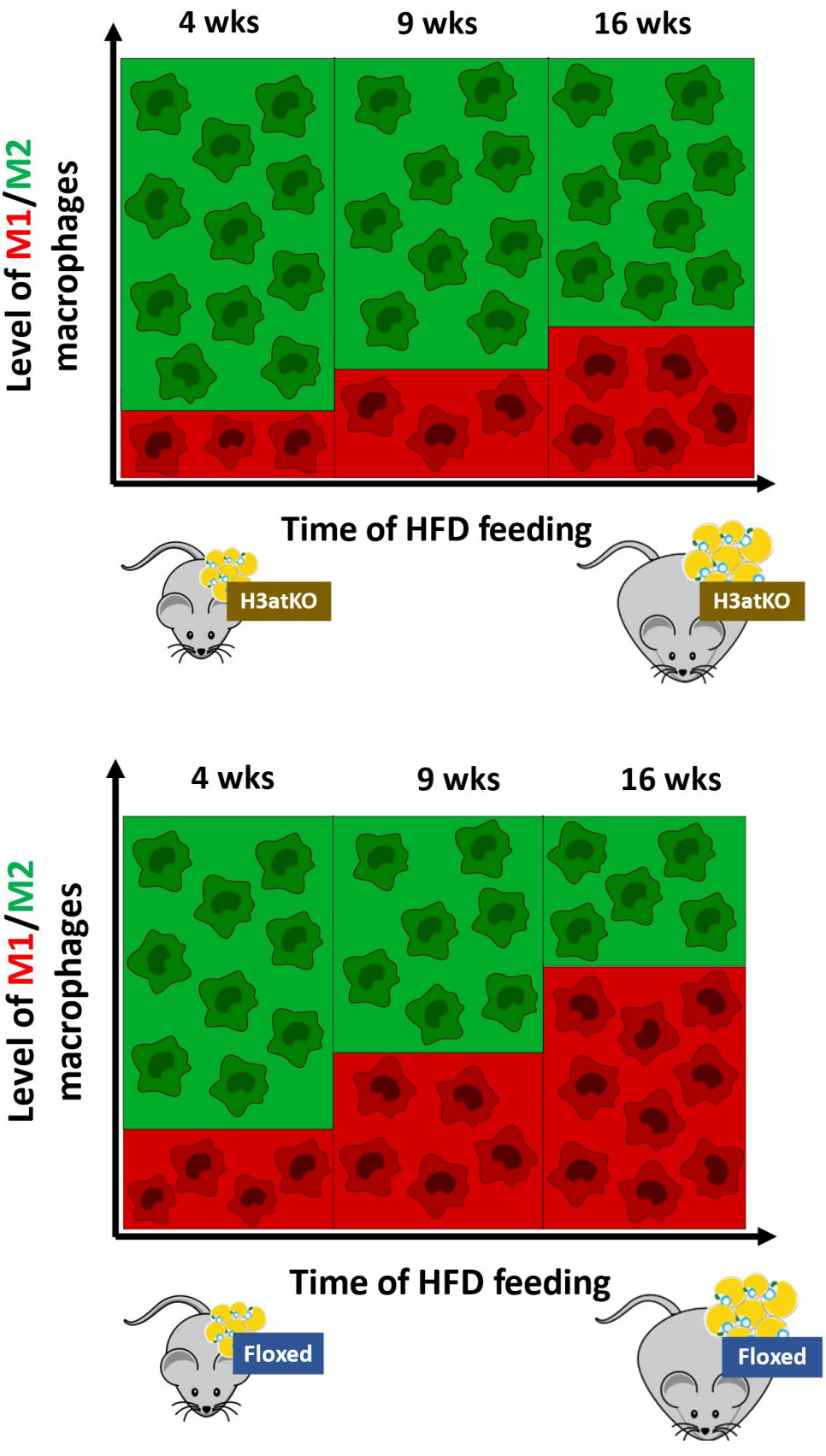

Fig. 33 Ratio of M1 (in red) and M2 (in green) macrophages during the 3 period of HFD treatment (4, 9, 16 weeks respectively), in H3atKO and floxed mice.

6.3 Transcriptomic and epigenomic analysis for a better characterization of H3atKO mouse model

Identifying early events, at the epigenomic and transcriptomic level, evoked by *Hdac3* ablation would be fundamental to understand downstream changes and mechanisms. For this reason, we performed omic analysis in H3atKO and control floxed mice after 4 weeks of LFD and HFD feeding. RNA-seq analysis revealed clear difference between mice genotypes. However, differences given by the diet were not as strong. We speculate that, since 4 weeks of diet is a short period of treatment, it might be possible that H3atKO mice are able to buffer the effects of the diet, thus maintaining their phenotype. Integrated ChIP-seq and RNA-seq analysis in H3atKO mice fed LFD showed upregulation of pathways regarding the futile cycle of simultaneous FA synthesis and β-oxidation that is characteristic of our KO model (Alessandra Ferrari *et al.*, 2017). Moreover, KO_LFD vs FL_LFD mice shown upregulation of pathways such as ferroptosis, a form of programmed cell death induced by iron (Hirschhorn and Stockwell, 2019), while focal adhesion and extracellular receptor interaction were downregulated.

Higher expression of ECM proteins leads to increased fibrosis in adipose tissue, which is detrimental for its function (Sun *et al.*, 2013): fibrosis reduces adipose tissue remodeling, metabolic rate and browning. It might be possible that in H3atKO mice, that have high metabolic rate, there is an increase of ROS (reactive oxygen species) that induce ferroptosis and adipocyte death. The observed upsurge of macrophages in visceral WAT of H3atKO mice, particularly M2 pro-resolving, might be involved in clearance of dead cells and adipocyte renewal. In fact, *Hdac3* ablation stimulates adipogenic program both *in vitro* and *in vivo* (Ferrari *et al.*, 2017), (Ferrari *et al.*, 2020).

Interestingly, in H3atKO mice we found upregulation of amino acid biosynthesis and of valine, leucine and isoleucine degradation pathways. Their simultaneous upregulation led us to speculate a possible futile cycle of amino acids degradation and synthesis: this process might feed the already established futile cycle of *de novo* lipogenesis and fatty acid β-oxidation that occurs in H3atKO mice. It would be interesting to perform experiments with stable isotopes to trace the fate of amino acids and further investigate this issue. Identification of new pathways might help discover regulatory mechanisms important for adipose tissue functionality.

Finally, one of the top downregulated gene in H3atKO mice at LFD was neuronatin (*Nnat*). Previous findings, reported that, in analogy to our KO model, loss of *Nnat* promotes browning in primary murine adipocytes (Gburcik, Cleasby and Timmons, 2013). Even though HDAC3 act as a corepressor of transcription through deacetylation of histone tails, ChIP-seq analysis showed hypoacetylation upstream *Nnat* TSS in *Hdac3* KO mice; this unconventional role of HDAC3 can be apparently misleading. However, histone deacetylases do not play a role only in the suppression but also in the activation of the transcription of some genes, through collateral mechanisms. At this regard, it has been shown that

HDAC3 activates estrogen-related receptor α (ERRα) gene through deacetylation of PGC-1α, a mechanism leading to transcription of *Ucp1* and *Pgc-1*α and of thermogenesis in BAT. Mice lacking *Hdac3* in BAT showed severe hypothermia and died after acute cold exposure (Emmett *et al.*, 2017). Another study revealed that HDAC3 acts as a coactivator of adipogenesis: the authors demonstrated that, during adipogenesis, formation of chromatin loops leads to enhancers activation correlated with recruitment of HDAC3 (Siersbæk *et al.*, 2017). A more recent study reported a dichotomous behaviour of HDAC3 in macrophages after exposure to lipopolysaccharides (LPS): HDAC3, through a non-canonical deacetylases-independent function, showed a bipartite ability both as activator or repressor of transcription. The loss of HDAC3 in macrophages protected mice from LPS but this effects do no derive from genetic or pharmacological inhibition of deacetylases activity of HDAC3 (Nguyen *et al.*, 2020). Considering these evidences, we hypothesise that HDAC3 might also activate genes that have a negative role for adipose tissue pathophysiology, through a non-canonical mechanism. Therefore, in *Hdac3* KO mice, hypoacetylation of some regions upstream *Nnat* TSS may repress *Nnat* gene transcription and, as a consequence, promotes browning of WAT. On this line, we aim to investigate more in depth the mechanism underlying the process of browning in H3atKO mice, since it is possible that HDAC3 regulates *Nnat* gene. Altogether, findings regarding omic analysis confirmed previous observations in our KO model while at the same time interesting new pathways have emerged. More in-depth investigations are needed to deepen our knowledge regarding the phenotype resulting from *Hdac3* gene inactivation and to unveil new mechanisms of regulation of adipose tissue in physiology and disease.

7 CONCLUSIONS

In vitro experiments reported in this thesis provided novel evidences regarding the role of class I HDACs in adipocyte differentiation: in fact, their early inhibition with MS-275 impacts differentiation program of pre-adipocytes imprinting cells towards oxidative and brown-like phenotype.

In vivo experiments revealed that *Hdac3* gene inactivation remodelled immune cell populations in visceral WAT of mice: the upsurge of macrophages, particularly M2 pro-resolving, during different period of HFD feeding might indicate a possible protective role exerted by H3atKO model. These novel findings help understand the visceral obesity evolution thus contributing to fighting obesity related diseases. Moreover, omic analysis corroborated previous observations regarding a futile cycle of simultaneous fatty acid β-oxidation and synthesis, and highlighted novel interesting pathways occurring in H3atKO mice. However, in the future, more in-depth studies are needed in order to validate these findings. By unravelling the underlying mechanisms, it could be possible to explore new avenues for therapeutic applications in obesity and the related comorbidities.

8 BIBLIOGRAPHY

Abe, Y. *et al.* (2015) 'JMJD1A is a signal-sensing scaffold that regulates acute chromatin dynamics via SWI/SNF association for thermogenesis', *Nature Communications*. Nature Publishing Group, 6(May). doi: 10.1038/ncomms8052.

Asterholm, I. W. *et al.* (2014) 'Adipocyte inflammation is essential for healthy adipose tissue expansion and remodeling', *Cell Metabolism*. Elsevier Inc., 20(1), pp. 103–118. doi: 10.1016/j.cmet.2014.05.005.

Bagchi, R. A. and Weeks, K. L. (2019) 'Histone deacetylases in cardiovascular and metabolic diseases', *Journal of Molecular and Cellular Cardiology*. Elsevier, 130(November 2018), pp. 151–159. doi: 10.1016/j.yjmcc.2019.04.003.

Bannister, A. J. and Kouzarides, T. (2011) 'Regulation of chromatin by histone modifications', *Cell Research*. Nature Publishing Group, 21(3), pp. 381–395. doi: 10.1038/cr.2011.22.

Cao, H. (2014) 'Adipocytokines in obesity and metabolic disease', *Journal of Endocrinology*, 220(2). doi: 10.1530/JOE-13-0339.

Chait, A. and den Hartigh, L. J. (2020) 'Adipose Tissue Distribution, Inflammation and Its Metabolic Consequences, Including Diabetes and Cardiovascular Disease', *Frontiers in Cardiovascular Medicine*, 7(February), pp. 1–41. doi: 10.3389/fcvm.2020.00022.

Chatterjee, T. K. *et al.* (2011) 'Histone deacetylase 9 is a negative regulator of adipogenic differentiation', *Journal of Biological Chemistry*, 286(31), pp. 27836–27847. doi: 10.1074/jbc.M111.262964.

Choe, S. S. *et al.* (2016) 'Adipose tissue remodeling: Its role in energy metabolism and metabolic disorders', *Frontiers in Endocrinology*, 7(APR), pp. 1–16. doi: 10.3389/fendo.2016.00030.

Chung, K. J. *et al.* (2018) 'Innate immune cells in the adipose tissue', *Reviews in Endocrine and Metabolic Disorders*. Reviews in Endocrine and Metabolic Disorders, 19(4), pp. 283–292. doi: 10.1007/s11154-018-9451-6.

Cinti, S. *et al.* (2005) 'Adipocyte death defines macrophage localization and function in adipose tissue of obese mice and humans', *Journal of Lipid Research*, 46(11), pp. 2347–2355. doi: 10.1194/jlr.M500294-JLR200.

Corrêa, Heyn and Magalhaes (2019) 'The Impact of the Adipose Organ Plasticity on Inflammation and Cancer Progression', *Cells*, 8(7), p. 662. doi: 10.3390/cells8070662.

Crichton, P. G., Lee, Y. and Kunji, E. R. S. (2017) 'The molecular features of uncoupling protein 1 support a conventional mitochondrial carrier-like mechanism', *Biochimie*, 134, pp. 35–50. doi:

10.1016/j.biochi.2016.12.016.

Dávalos-Salas, M. *et al.* (2019) 'Deletion of intestinal Hdac3 remodels the lipidome of enterocytes and protects mice from diet-induced obesity', *Nature Communications*. Springer US, 10(1), pp. 1–14. doi: 10.1038/s41467-019-13180-8.

Dijk, S. J. *et al.* (2015) 'Recent developments on the role of epigenetics in obesity and metabolic disease', *Clinical Epigenetics*. Clinical Epigenetics, 7(1). doi: 10.1186/s13148-015-0101-5.

Emmett, M., Lim, H. W., Jager, J., Richter, H., Adlanmerini, M. and Lazar, M. A. (2017) 'Histone deacetylase 3 prepares brown adipose tissue for acute thermogenic challenge', *Physiology & behavior*, 176(5), pp. 139–148. doi: 10.1016/j.physbeh.2017.03.040.

Emmett, M., Lim, H. W., Jager, J., Richter, H., Adlanmerini, M., Pedd, L., *et al.* (2017) 'Histone Deacetylase 3 Prepares Brown Adipose Tissue For Acute Thermogenic Challenge', *Nature*, 176(3), pp. 139–148. doi: 10.1016/j.physbeh.2017.03.040.

Emmett, M. and Lazar, M. A. (2019) 'Integrative regulation of physiology by histone deacetylase 3', *Physiology & behavior*, 176(1), pp. 139–148. doi: 10.1016/j.physbeh.2017.03.040.

Fedorenko, A., Lishko, P. and Kirichok, Y. (2012) 'Mechanism of Fatty-AcidDependent UCP1 Uncoupling in Brown Fat Mitochondria', *Bone*, 23(1), pp. 1–7. doi: 10.1038/jid.2014.371.

Fenzl, A. and Kiefer, F. W. (2014) 'Brown adipose tissue and thermogenesis', *Hormone Molecular Biology and Clinical Investigation*, 19(1), pp. 25–37. doi: 10.1515/hmbci-2014-0022.

Ferrari, A. *et al.* (2012) 'Linking epigenetics to lipid metabolism: Focus on histone deacetylases', *Molecular Membrane Biology*, 29(7), pp. 257–266. doi: 10.3109/09687688.2012.729094.

Ferrari, A. *et al.* (2017) 'Attenuation of diet-induced obesity and induction of white fat browning with a chemical inhibitor of histone deacetylases', *International Journal of Obesity*. Nature Publishing Group, 41(2), pp. 289–298. doi: 10.1038/ijo.2016.191.

Ferrari, Alessandra *et al.* (2017) 'HDAC3 is a molecular brake of the metabolic switch supporting white adipose tissue browning', *Nature Communications*. Springer US, 8(1). doi: 10.1038/s41467-017-00182-7.

Ferrari, A. *et al.* (2018) 'Epigenome modifiers and metabolic rewiring: New frontiers in therapeutics', *Pharmacology and Therapeutics*. Elsevier Inc., 193, pp. 178–193. doi: 10.1016/j.pharmthera.2018.08.008.

Ferrari, A. *et al.* (2020) 'Inhibition of class I HDACs imprints adipogenesis toward oxidative and

brown-like phenotype', *Biochimica et Biophysica Acta - Molecular and Cell Biology of Lipids*, 1865(4). doi: 10.1016/j.bbalip.2019.158594.

Feuerer, M. *et al.* (2009) 'Lean, but not obese, fat is enriched for a unique population of regulatory T cells that affect metabolic parameters', *Nature Medicine*. Nature Publishing Group, 15(8), pp. 930–939. doi: 10.1038/nm.2002.

Galmozzi, A. *et al.* (2013) 'Inhibition of class i histone deacetylases unveils a mitochondrial signature and enhances oxidative metabolism in skeletal muscle and adipose tissue', *Diabetes*, 62(3), pp. 732–742. doi: 10.2337/db12-0548.

Gaur, V. *et al.* (2017) 'Scriptaid enhances skeletal muscle insulin action and cardiac function in obese mice', *Diabetes, Obesity and Metabolism*, 19(7), pp. 936–943. doi: 10.1111/dom.12896.

Gburcik, V., Cleasby, M. E. and Timmons, J. A. (2013) 'Loss of neuronatin promotes "browning" of primary mouse adipocytes while reducing Glut1-mediated glucose disposal', *American Journal of Physiology - Endocrinology and Metabolism*, 304(8), pp. 885–894. doi: 10.1152/ajpendo.00463.2012.

Haberland, M., Montgomery, R. L. and Olson, E. N. (2009) 'The many roles of histone deacetylases in development and physiology: implications for disease and therapy', *Nature Reviews. Genetics*, 10(1), pp. 32–42. doi: 10.1038/nrg2485.The.

Harms, M. and Seale, P. (2013) 'Brown and beige fat: Development, function and therapeutic potential', *Nature Medicine*. Nature Publishing Group, 19(10), pp. 1252–1263. doi: 10.1038/nm.3361.

Haslam, D. W. and James, W. P. T. (2005) 'Obesity', *Lancet*, pp. 1197–1209.

Heijmans, B. T. *et al.* (2008) 'Persistent epigenetic differences associated with prenatal exposure to famine in humans', *PNAS*, 105(44), pp. 17046–17049. doi: 10.1073/pnas.0806560105.

Herrera, B. M., Keildson, S. and Lindgren, C. M. (2011) 'Genetics and epigenetics of obesity', *Maturitas*. Elsevier Ireland Ltd, 69(1), pp. 41–49. doi: 10.1016/j.maturitas.2011.02.018.

Heydemann, A. (2016) 'An Overview of Murine High Fat Diet as a Model for Type 2 Diabetes Mellitus', *Journal of Diabetes Research*, 2016. doi: 10.1155/2016/2902351.

Hill, D. A. *et al.* (2018) 'Distinct macrophage populations direct inflammatory versus physiological changes in adipose tissue', *Proceedings of the National Academy of Sciences of the United States of America*, 115(22), pp. E5096–E5105. doi: 10.1073/pnas.1802611115.

Hirschhorn, T. and Stockwell, B. R. (2019) 'The development of the concept of ferroptosis', *Free Radical Biology and Medicine*, 133, pp. 130–143. doi: 10.1016/j.freeradbiomed.2018.09.043.

Hsu, C. L. *et al.* (2012) 'Inhibitory effects of garcinol and pterostilbene on cell proliferation and adipogenesis in 3T3-L1 cells', *Food and Function*, 3(1), pp. 49–57. doi: 10.1039/c1fo10209e.

Ikeda, K. *et al.* (2018) 'UCP1-independent signaling involving SERCA2b-mediated calcium cycling regulates beige fat thermogenesis and systemic glucose homeostasis', *Nature Medicine*, 23(12), pp. 1454–1465. doi: 10.1038/nm.4429.UCP1-independent.

Ikeda, K. and Yamada, T. (2020) 'UCP1 Dependent and Independent Thermogenesis in Brown and Beige Adipocytes', *Frontiers in Endocrinology*, 11(July), pp. 1–6. doi: 10.3389/fendo.2020.00498.

Kaushik, P. and Anderson, J. T. (2016) 'Obesity: Epigenetic aspects', *Biomolecular Concepts*, 7(3), pp. 145–155. doi: 10.1515/bmc-2016-0010.

Keating, S. T. and El-Osta, A. (2015) 'Epigenetics and metabolism', *Circulation Research*, 116(4), pp. 715–736. doi: 10.1161/CIRCRESAHA.116.303936.

Kim, C. H. (2016) 'Measurements of Adiposity and Body Composition', *The Korean Journal of Obesity*, 25(3), pp. 115–120. doi: 10.7570/kjo.2016.25.3.115.

Kimbrough, D. *et al.* (2018) 'HDAC inhibition helps post-MI healing by modulating macrophage polarization', *Journal of Molecular and Cellular Cardiology*. Elsevier, 119(April), pp. 51–63. doi: 10.1016/j.yjmcc.2018.04.011.

Knutson, S. K. *et al.* (2008) 'Liver-specific deletion of histone deacetylase 3 disrupts metabolic transcriptional networks', *EMBO Journal*, 27(7), pp. 1017–1028. doi: 10.1038/emboj.2008.51.

Kopelman, P. G. (2000) 'Obesity as a medical problem', *Nature*, 404(6778), pp. 635–643. doi: 10.1038/35007508.

Lee, B.-C. (2014) 'Cellular and Molecular Players in Adipose Tissue Inflammation in the Development of Obesity-induced Insulin Resistance', *Biochim Biophys Acta*, 1842(3), pp. 446–462. doi: 10.1016/j.bbadis.2013.05.017.Cellular.

Li, Y., Yun, K. and Mu, R. (2020) 'A review on the biology and properties of adipose tissue macrophages involved in adipose tissue physiological and pathophysiological processes', *Lipids in Health and Disease*. Lipids in Health and Disease, 19(1), pp. 1–9. doi: 10.1186/s12944-020-01342-3.

Longo, M. *et al.* (2019) 'Adipose tissue dysfunction as determinant of obesity-associated metabolic complications', *International Journal of Molecular Sciences*, 20(9). doi: 10.3390/ijms20092358.

Longo, R. *et al.* (2017) 'Of mice and humans through the looking glass: "reflections" on epigenetics of lipid metabolism', *Molecular Aspects of Medicine*. Elsevier Ltd, 54, pp. 16–27. doi:

10.1016/j.mam.2017.01.005.

Lumeng, C. N. *et al.* (2007) 'Obesity induces a phenotypic switch in adipose tissue macrophage polarization Find the latest version : Obesity induces a phenotypic switch in adipose tissue macrophage polarization', *J Clin Invest*, 117(1), pp. 175–184. doi: 10.1172/JCI29881.both.

Macdougall, C. E. and Longhi, M. P. (2019) 'Adipose tissue dendritic cells in steady-state', *Immunology*, 156(3), pp. 228–234. doi: 10.1111/imm.13034.

Mclaughlin, T. *et al.* (2017) 'Role of innate and adaptive immunity in obesity-associated metabolic disease', *Journal of Clinical Investigation*, 127(1), pp. 5–13. doi: 10.1172/JCI88876.

Mitro, N. *et al.* (2007) 'Insights in the regulation of cholesterol 7α-hydroxylase gene reveal a target for modulating bile acid synthesis', *Hepatology*, 46(3), pp. 885–897. doi: 10.1002/hep.21819.

Mullican, S. E. *et al.* (2011) 'Histone deacetylase 3 is an epigenomic brake in macrophage alternative activation', *Genes and Development*, 25(23), pp. 2480–2488. doi: 10.1101/gad.175950.111.

Murano, I. *et al.* (2008) 'Dead adipocytes, detected as crown-like structures, are prevalent in visceral fat depots of genetically obese mice', *Journal of Lipid Research*, 49(7), pp. 1562–1568. doi: 10.1194/jlr.M800019-JLR200.

Nguyen, H. C. B. *et al.* (2020) 'Dichotomous engagement of HDAC3 activity governs inflammatory responses', *Nature*. Springer US, 584(7820), pp. 286–290. doi: 10.1038/s41586-020-2576-2.

Nishimura, S. *et al.* (2009) 'CD8+ effector T cells contribute to macrophage recruitment and adipose tissue inflammation in obesity', *Nature Medicine*. Nature Publishing Group, 15(8), pp. 914–920. doi: 10.1038/nm.1964.

Park, A., Won, K. K. and Bae, K.-H. (2014) 'Distinction of white, beige and brown adipocytes derived from mesenchymal stem cells', *World Journal of Stem Cells*, 6(1), p. 33. doi: 10.4252/wjsc.v6.i1.33.

Patsouris, D. *et al.* (2009) 'Ablation of CD11c-positive cells normalizes insulin sensitivity in obese insulin resistant animals', *Cell Metabolism*, 8(4), pp. 301–309. doi: 10.1016/j.cmet.2008.08.015.Ablation.

Petrovic, N. *et al.* (2010) 'Chronic peroxisome proliferator-activated receptor γ (PPARγ) activation of epididymally derived white adipocyte cultures reveals a population of thermogenically competent, UCP1-containing adipocytes molecularly distinct from classic brown adipocytes', *Journal of Biological Chemistry*, 285(10), pp. 7153–7164. doi: 10.1074/jbc.M109.053942.

Rosen, E. D. and Spiegelman, B. M. (2014) 'What we talk about when we talk about fat', *Cell*. Elsevier

Inc., 156(1–2), pp. 20–44. doi: 10.1016/j.cell.2013.12.012.

Sadakierska-Chudy, A., Kostrzewa, R. M. and Filip, M. (2015) 'A Comprehensive View of the Epigenetic Landscape Part I: DNA Methylation, Passive and Active DNA Demethylation Pathways and Histone Variants', *Neurotoxicity Research*, 27(1), pp. 84–97. doi: 10.1007/s12640-014-9497-5.

Seto, E. and Yoshida, M. (2014) 'Erasers of histone acetylation: The histone deacetylase enzymes', *Cold Spring Harbor Perspectives in Biology*, 6(4), pp. 1–26. doi: 10.1101/cshperspect.a018713.

Shapira, S. and Seale, P. (2016) 'Transcriptional control of brown and beige fat development and function', *Physiology & behavior*, 176(1), pp. 139–148. doi: 10.1016/j.physbeh.2017.03.040.

Sidossis, L. and Kajimura, S. (2015) 'Brown and beige fat in humans: Thermogenic adipocytes that control energy and glucose homeostasis', *Journal of Clinical Investigation*, 125(2), pp. 478–486. doi: 10.1172/JCI78362.

Siersbæk, R. *et al.* (2017) 'Dynamic Rewiring of Promoter-Anchored Chromatin Loops during Adipocyte Differentiation', *Molecular Cell*. Elsevier Inc., 66(3), pp. 420-435.e5. doi: 10.1016/j.molcel.2017.04.010.

Siersbæk, R., Nielsen, R. and Mandrup, S. (2012) 'Transcriptional networks and chromatin remodeling controlling adipogenesis', *Trends in Endocrinology and Metabolism*. Elsevier Ltd, 23(2), pp. 56–64. doi: 10.1016/j.tem.2011.10.001.

Spalding, K. L. *et al.* (2008) 'Dynamics of fat cell turnover in humans', *Nature*, 453(7196), pp. 783–787. doi: 10.1038/nature06902.

Stein, A. D. *et al.* (2007) 'Anthropometric measures in middle age after exposure to famine during gestation: Evidence from the Dutch famine', *American Journal of Clinical Nutrition*, 85(3), pp. 869–876. doi: 10.1093/ajcn/85.3.869.

Strahl, B. D. and Allis, C. D. (2000) 'The language of covalent histone modifications', *Nature*, 403(6765), pp. 41–45. doi: 10.1038/47412.

Sun, K. *et al.* (2013) 'Fibrosis and adipose tissue dysfunction', *Cell Metabolism*, 18(4), pp. 470–477. doi: 10.1016/j.cmet.2013.06.016.

Sun, Z. *et al.* (2011) 'Diet-induced lethality due to deletion of the Hdac3 gene in heart and skeletal muscle', *Journal of Biological Chemistry*, 286(38), pp. 33301–33309. doi: 10.1074/jbc.M111.277707.

Sun, Z. *et al.* (2012) 'Hepatic Hdac3 promotes gluconeogenesis by repressing lipid synthesis and sequestration', *Nature Medicine*, 18(6), pp. 934–942. doi: 10.1038/nm.2744.Hepatic.

Tajima, K. *et al.* (2020) 'Wireless optogenetics protects against obesity via stimulation of non-canonical fat thermogenesis', *Nature Communications*. Springer US, 11(1), pp. 1–5. doi: 10.1038/s41467-020-15589-y.

Talukdar, S. *et al.* (2012) 'Neutrophils mediate insulin resistance in high fat diet fed mice via secreted elastase', *Nature Medicine*, 18(9), pp. 1407–1412. doi: 10.1038/nm.2885.Neutrophils.

Weisberg, S. P. *et al.* (2003) 'Obesity is associated with macrophage accumulation in adipose tissue Find the latest version : Obesity is associated with', *J Clin Invest.*, 112(12), pp. 1796–1808. doi: 10.1172/JCI200319246.Introduction.

Winer, D. *et al.* (2011) 'B Lymphocytes Promote Insulin Resistance through Modulation of T Lymphocytes and Production of Pathogenic IgG Antibody', *Reproduction*, 17(5), pp. 3–6. doi: 10.1038/nm.2353.B.

Wright, S. M. and Aronne, L. J. (2012) 'Causes of obesity', *Abdominal Imaging*, 37(5), pp. 730–732. doi: 10.1007/s00261-012-9862-x.

Yamashita, K. *et al.* (2005) 'The High-Fat Diet–Fed Mouse', *Journal of Critical Care*, 20, pp. 172–175. doi: 10.2337/diabetes.53.suppl_3.S215.

Zentner, G. E. and Henikoff, S. (2013) 'Regulation of nucleosome dynamics by histone modifications', *Nature Structural and Molecular Biology*. Nature Publishing Group, 20(3), pp. 259–266. doi: 10.1038/nsmb.2470.

Zheng, C. *et al.* (2016) 'Local proliferation initiates macrophage accumulation in adipose tissue during obesity', *Cell Death and Disease*. Nature Publishing Group, 7(3), pp. 1–9. doi: 10.1038/cddis.2016.54.

Zhu, Q. *et al.* (2020) 'Suppressing adipocyte inflammation promotes insulin resistance in mice', *Molecular Metabolism*, 39(May), pp. 1–11. doi: 10.1016/j.molmet.2020.101010.